ESTIMATION OF EVAPOTRANSPIRATION OF CHICKPEA USING VEGETATION INDICES BASED CROP COEFFICIENTS

THESIS

Submitted to
Dr. Panjabrao Deshmukh Krishi Vidyapeeth, Akola
in partial fulfilment of the requirements
for the Degree of

MASTER OF TECHNOLOGY
IN
AGRICULTURAL ENGINEERING
(IRRIGATION AND DRAINAGE ENGINEERING)

By

MONCY S AKKARA

DEPARTMENT OF IRRIGATION AND DRAINAGE ENGINEERING
POST GRADUATE INSTITUTE, AKOLA

DR. PANJABRAO DESHMUKH KRISHI VIDYAPEETH,
KRISHINAGAR PO, AKOLA (MS) 444104

Enrolment Number - SS-3117 **2022**

DECLARATION OF STUDENT

I hereby declare that the experimental work and its interpretation of the Thesis entitled "**ESTIMATION OF EVAPOTRANSPIRATION OF CHICKPEA USING VEGETATION INDICES BASED CROP COEFFICIENTS**" or part thereof has neither been submitted for any other degree or diploma of any University, nor the data have been derived from any thesis / publication of any University or scientific organization. The source of materials used and all assistance received during the course of investigation have been duly acknowledged.

Place: Akola (Moncy S Akkara)

Date: / / 2022 Enrolment No. SS-3117

CERTIFICATE

This is to certify that thesis entitled **"ESTIMATION OF EVAPOTRANSPIRATION OF CHICKPEA USING VEGETATION INDICES BASED CROP COEFFICIENTS"** submitted in partial fulfilment of the requirement for the degree of **'Master of Technology in Agricultural Engineering (Irrigation and Drainage Engineering)'** of Dr. Panjabrao Deshmukh Krishi Vidyapeeth, Akola is a record of bonafide research work carried out by **Moncy S Akkara** under my guidance and supervision.

The subject of thesis has been approved by the Student's Advisory Committee.

Place : Akola
Date :

Chairman
Advisory Committee

Countersigned

Associate Dean,
Post Graduate Institute
Dr. Panjabrao Deshmukh Krishi Vidyapeeth, Akola

THESIS APPROVED BY THE STUDENT'S ADVISORY COMMITTEE
INCLUDING EXTERNAL EXAMINER (AFTER VIVA–VOCE)

1. Chairman	Dr. A. R. Pimpale	_____
2. Member	Dr. S. B. Wadatkar	_____
3. Member	Dr. P. B. Rajankar	_____
4. Member	Dr. I. K. Ramteke	_____
5. External member	Dr. M. U. Kale	_____

ACKNOWLEDGEMENT

First and foremost, praises and thanks to my God, the almighty, for all the love and blessings throughout my life, especially for the resilience during my course period.

I would like to express my most sincere gratitude to the Chairman of my Advisory Committee, Dr. A.R. Pimpale, Assistant Professor (Agricultural Engineering), College of Agriculture, Nagpur, Dr. Panjabrao Deshmukh Krishi Vidyapeeth, Akola for his invaluable guidance and cooperation throughout the research. I am deeply inspired by his commitment and dynamism toward the profession and the optimism he has in general. I would also like to thank him for his empathy, friendship and constant motivation. I am extremely grateful for the opportunity to work and learn under his guidance.

I am deeply indebted to Dr. S.B. Wadatkar, member of my Advisory Committee and Associate Dean & Head of IDE, Dr. Panjabrao Deshmukh Krishi Vidyapeeth, Akola for his constant support and guidance, scientific excellence, valuable and constructive feedback and encouragement during the entire period of study. I would like to express my heartfelt gratitude and respect to him for being my constant support pillar with utmost empathy.

I would like to express my deepest appreciation to my advisory committee members, Dr. P.B. Rajankar, Associate Scientist, Maharashtra Remote Sensing Centre, Nagpur and Dr. I. K. Ramteke, Scientific Associate, Maharashtra Remote Sensing Centre, Nagpur, for their invaluable suggestions in all the topics related to Remote Sensing and GIS and continuous encouragement and cooperation endowed during the course of my research work. Working and learning under their excellence was a great privilege and honor.

I am grateful to Dr. D.B. Undirwade, Ex. Associate Dean and Dr. Y.B.Taide, Associate Dean, Post Graduate Institue, Dr. PDKV, Akola for providing necessary facilities for carrying out the present investigation and rendering valuable guidance from time to time.

I am extremely grateful to Dr. M.U. Kale, Education-in-charge and Assistant Professor, Department of IDE, Dr. PDKV, Akola for his valuable suggestions and continuous support during the course of study.

I would like to extend my sincere thanks to Dr. A.N. Mankar, Assistant Professor (IDE) and Dr. M.M. Deshmukh, Associate Professor (IDE) for the valuable feedback and support endowed during my course of study.

I would also like to extend my deepest gratitude to Dr. Archana Thorat, Associate professor, Dr. M.D Giri, Assistant Professor and Dr. E R Vaidya, Senior Research Scientist, Pulses Research Unit, Dr. PDKV, Akola along with Dr. Anil Karunakar, Agrometeorological Observatory, Dr. PDKV, Akola for their expert guidance and kind help in the moments of need.

Many thanks to Shri. Sanjay Chinchghare (MRSAC), Er. Mahesh Londhe, Senior Research Fellow (IDE) and Er. Mayur Adawadkar, Ph.D. Scholar (IDE) who extended timely help in various stages of my work.

Special thanks to Shri. Avinash More and Shri. Arun, staff members (IDE) along with my friends and seniors for their love, support and timely help.

The completion of my dissertation would not have been possible without the constant support, love and nurturing of my mother Darly Santhosh and sisters, Dr. Thanksy S Akkara, Dr.Shelcy S Akkara and Francy S Akkara. I express my deepest sense of love and admiration to my deceased father, Shri. Santhosh F Akkara. I am forever indebted to my family for their selfless love and support through thick and thin.

Many thanks to all the authors and researchers, whose articles helped me organize my research work in proper line and utilize the proper tools for interpreting the results. Finally, I am thankful to all who helped me directly or indirectly in the completion of this research work.

Place: Akola (Moncy S Akkara)

Date: / / 2022 Enrolment No. SS-3117

Table of Contents

A) List of Tables

B) List of Figures

C) List of Plates

D) Abbreviations

Abbreviation		Description
%	-	Per cent
º	-	Degree
ºC	-	Degree centigrade
'	-	Minute
"	-	Second
Agric.	-	Agriculture
AOI	-	Area of Interest
ASAE	-	American Society of Agricultural Engineering
ASCE	-	American Society of Civil engineering
AWiFS	-	Advanced Wide Field Sensor
cm	-	Centimeter
Conf.	-	Conference
Conser.	-	Conservation
Div.	-	Division
Drain.	-	Drainage
Eng.	-	Engineering
Environ.	-	Environmental
et al.	-	Et alibi (and other)
etc.	-	Etcetera
ET	-	Evapotranspiration
ETo	-	Reference Evapotranspiration
FAO	-	Food and Agriculture Organization
fAPAR	-	Fraction of Photosynthetically Active Radiation
FASAL	-	Forecasting Agricultural Outputs using Space, Agrometeorology and Land based observations
Fig.	-	Figure
GIS	-	Geographical Information System
Govt.	-	Government
GT	-	Ground Truth
Ha	-	Hectare
Hr	-	Hour

Hydrol.	-	Hydrology
i.e.	-	that is
Int.	-	International
IRS	-	Indian Remote Sensing Satellites
ISRO	-	Indian Space Research Organization
Irrig.	-	Irrigation
J.	-	Journal
Kc	-	Crop Coefficients
Kg	-	Kilogram
Km	-	Kilometre
LAI	-	Leaf Area Index
M	-	Meter
Manage.	-	Management
Mha	-	Million hectare
Mm^3	-	Million cubic meter
MRSAC	-	Maharashtra Remote Sensing And Application Center
MSI	-	Multispectral Imager
MSL	-	Mean Sea Level
MSAVI	-	Modified Soil Adjusted Vegetation Index
MXL	-	Maximum Likelihood
NDVI	-	Normalized Difference Vegetation Index
NDWI	-	Normalized Difference Water Index
No.	-	Number
OSM	-	Open Series Map
PDKV	-	Panjabrao Deshmukh Krishi Vidyapeeth
PGI	-	Post Graduate Institute
Plann.	-	Planning
Proc.	-	Proceeding
Res.	-	Research
Rev	-	Review
Resour.	-	Resource
RI	-	Reference Image
RS	-	Remote Sensing

RVI	-	Ratio Vegetation Index
s	-	Second
SAVI	-	Soil Adjusted Vegetation Index
Sci.	-	Science
SCS	-	Soil Conservation Service
SEBAL	-	Surface Energy Balance Algorithm for Land
Soc.	-	Social
SOI	-	Survey of India
Symp.	-	Symposium
TNDVI	-	Transformed Normalized Difference Vegetation Index
Trans.	-	Transactions
Univ.	-	University
Unpub.	-	Unpublished
USDA	-	United State Department of Agriculture
VIs	-	Vegetation Indices

E) THESIS ABSTRACT

a)	**Title of thesis**	**: Estimation of Evapotranspiration of Chickpea using Vegetation Indices Based Crop Coefficients**
b)	**Full name of student**	**:** Moncy S Akkara
c)	**Name and address of Major Advisor**	**:** Dr. A. R. Pimpale Assistant Professor (Agriculture Engineering), College of Agriculture, Nagpur
d)	**Degree to be awarded**	**:** M.Tech. (Agril. Engg.) Irrigation and Drainage Engineering
e)	**Year of award of degree**	**:** 2022
f)	**Major subject**	**:** Irrigation and Drainage Engineering
g)	**Total number of pages in thesis**	**:** 105
h)	**Number of words in the abstract**	**:** 558
i)	**Signature of the student**	**:**
j)	**Signature, name and address of forwarding authority**	**:**

Head

Department of Irrigation and Drainage Engineering, Dr. PDKV, Akola

---

ABSTRACT

Ever growing water demand of world along with the severe reduction in water availability- quantitatively and qualitatively, necessitates monitoring and management of existing water resources in the best possible way. Agriculture being major shareholder of fresh water consumption calls for an immediate action to adopt proper irrigation methods and develop technology to make judicious use of water. Better estimation of irrigation water requirements is essential for water conservation aspects as well as better yield and economic aspects. Evapotranspiration being the major consumptive use of irrigation water, crop evapotranspiration represents crop water requirement and is

calculated by FAO-56 procedures based on literature derived crop coefficients. Irrigation scheduling based on literature derived crop coefficients often leads to over irrigation due to the non optimal actual field conditions and spatial and temporal variations in Kc. Remotely sensed multispectral vegetation indices (VIs) have similar pattern as that of crop coefficients (Kc). Hence, Kc can be modelled using VIs. The Kc derived from VI responds to actual field conditions and captures spatial variability. Thus, VI based approach can be used for crop identification, acreage estimation and precision irrigation management. Furthermore, yield and quality of moisture sensitive chickpea crop can be considerably increased by applying precise irrigation in critical stages though it is a *rabi* crop. The present investigation entitled 'Estimation of Evapotranspiration of Chickpea using Vegetation Indices Based Crop Coefficients' was undertaken with major objective of identifying the most appropriate VI having highest correlation with crop coefficients of *rabi* chickpea crop in order to estimate the water demand.

The study was conducted in Akola district located in Maharashtra. Multidate Sentinel 2 A (MSI sensor) satellite images were used to extract most commonly used vegetation indices RVI, NDVI, NDWI and SAVI. The spectral behaviour of the chickpea crop suggested that the VIs follow a similar pattern to crop coefficients. The two stage hybrid classification technique of remote sensing was employed to compute the crop acreage. The results showed an overestimation of 3.12% than the crop statistics published by the Department of Agriculture, Government of Maharashtra.

The values of multi-date vegetation indices RVI, NDVI, NDWI and SAVI were distributed according to the age of the crop on each day of satellite data acquisition. Simple linear regression analysis was applied to derive the relationship between the mean weekly VI values and the week-wise crop coefficients (Kc) recommended by MPKV Rahuri and the relationships were established in the form of prediction models. All the vegetation indices exhibited good correlation with crop coefficients (Kc) with high R^2 values. However, NDWI-Kc model outperformed all other regression models. NDWI-Kc model showed highest R^2 and D values of 0.9550 and 0.9884 respectively with lowest values of SE, RMSE and PD of 0.0743, 0.0698 and 4.1016

respectively. Hence, NDWI was identified as the most superior remote sensing indicator for estimation of chickpea crop coefficients.

The weekly crop coefficients were derived from the best performing NDWI-Kc model and the crop water requirement was estimated as 248.23 mm for chickpea crop. Crop water demand of *rabi* chickpea in Akola district was determined as 213.4138 Mm^3.

The outcomes of this study show the potential of multispectral vegetation indices for estimating spatial crop coefficients, leading to the determination of site-specific crop water demand and thus ultimately helping in precise irrigation water management, by providing irrigation with high water use efficiency and saving significant amount of water.

Keywords: Vegetation indices, Evapotranspiration, Crop coefficients, Remote sensing, GIS, Sentinel 2A, Chickpea.

CHAPTER I

INTRODUCTION

1.1 Background Information

Water is essential for all known forms of life, despite not providing food, energy, or organic micronutrients and hence regarded as the elixir of life. Besides, water plays a crucial role in the socioeconomic development of the world. Though almost 70% of the surface of the earth is covered by water, freshwater contributes to less than 3.5% of it. Furthermore, only 1.7% of the freshwater resources are available to humans. Freshwater is a resource that is constantly replenished as a result of the hydrologic cycle but access to it is under stress due to its inherently asymmetrical spatial and temporal distribution, increasing populations and expanding economic demands from industry and agriculture. Ever-growing water challenges of the world due to climactic, demographic and economic pressures along with the severe reduction in water availability- both quantitatively and qualitatively, necessitate monitoring and management of existing water resources in the best possible way. The situation gains huge gravity in arid and semiarid regions which were already water-sensitive challenging global food security.

The agricultural sector is the major shareholder of freshwater consumption across the globe, accounting for 70% and is primarily utilized for irrigation. The arising global water crisis can be tackled only by efficient use of water while increasing agricultural productivity to meet the rising food demands. The context calls for immediate action to adopt proper irrigation methods and develop technology to make judicious use of water. Per drop more crop concept aims to maximize the agricultural production per unit of water which is an important step towards this goal. In the pursuit of higher yields, farmers frequently over-irrigate their crops. Low yield, poor quality and inefficient nutrient use can result from under or overwatering. Thus, apart from conservational aspects, the precise application of irrigation water to crops has got better plant health resulting in better yield and economic aspects. Therefore, proper knowledge of the water requirement for each crop is essential for precision agriculture.

Evapotranspiration is the combination of evaporation from soil surfaces and transpiration from vegetation. The water requirement of a crop is the amount of water required to meet the evapotranspiration losses. Crop water requirement for each crop and at every growth stage varies. Local conditions also play an important role in crop water requirement (FAO, 2005). Crop evapotranspiration (ETc) represents the water requirement of a crop at a given stage of the crop, at a specific location, accounting for the major consumptive use of irrigation water. Hence, water consumption can be approximated by quantifying evapotranspiration and thus is of great help in irrigation water management. Once the ETc is determined, irrigation can be done with regard to the crop area and the irrigation efficiency.

Though there are various methods for the estimation of crop evapotranspiration (ETc), the FAO Penman-Monteith method (Allen *et al.*, 1998) has been considered the sole standard method. In this method, location-specific daily reference evapotranspiration (ETo) is estimated by using meteorological data and crop evapotranspiration (ETc) is then calculated by multiplication with crop coefficient (Kc).

$$ETc = Kc \times ETo \qquad \text{----------1}$$

Crop coefficients corresponding to major growth stages are usually calculated from field studies using lysimeters for crops grown under optimum agronomic and water management conditions. Doorenbos and Pruitt (1977) tabulated Kc values for different crops using lysimeters for the major crop development stages in the FAO-24 paper. These Kc values correspond to optimum agronomic conditions and are generally limited to three values only (Kc ini, Kc mid and Kc end). Due to variations in the crop characteristics throughout its growing season, Kc for a given crop changes from the very beginning process of sowing to the end of harvesting. Furthermore, actual field conditions usually are non-optimal in nature such as the presence of pests and diseases, water shortage, water logging, soil salinity, soil fertility, etc and result in stunted plant growth, low plant density leading to the decline of evapotranspiration rate below ETc. In such conditions, Kc should be adjusted to account for all kinds of stress and environmental constraints. Crop coefficient values taken from the literature may provide a practical guideline

for scheduling irrigation, but a considerable error in estimating crop water requirement can occur due to their empirical nature (Jagtap and Jones, 1989). Thus, the calculated values are only useful approximations of the actual ET and water requirements for a given crop. Therefore, it becomes necessary to make corrections in crop coefficient values as per local conditions.

Determination of ETc under variable climate and field conditions is required for precision irrigation management. The crop coefficients also lack spatial variability due to variation in crop variety and growth stage from field to field. Hence, determination of the water requirement of a region for a specific period is difficult since the sowing dates of the same crop might vary within a shorter distance. It is very difficult to identify spatial and temporal variations in water use with present crop coefficient procedures. Actual water demand in field conditions is lower than that obtained under agronomic optimal conditions resulting in over-irrigation of crops ultimately causing adverse effects at the field, district and regional levels, during irrigation water shortages (Santos *et al.*, 2007).

For effective and timely agricultural development as well as making critical decisions on procurement, storage, public distribution, export, import and other associated issues, planners and policymakers must have accurate and timely estimates of the crop area. Currently, the estimates of crop acreage are obtained by revenue authorities through enumeration, sample surveys and personal evaluations by village officer. Hence the method is labor intensive as well as time-consuming and results are not free from errors either.

For acreage estimation and precise irrigation water management, the use of remote sensing and GIS tools can introduce a new paradigm.

1.2 Importance

Satellite remote sensing enables to monitor land surface conditions and the status of water resources on different spatial and temporal resolutions. Utilizing remote sensing for estimating crop water requirements in irrigation commands is the most accurate, time-efficient approach for irrigation water management. The crop coefficient generated from remote sensing responds

to actual crop conditions in a field and captures the variability among different fields, which occurs due to different dates of sowing of the crop, crop variety, soil and field condition. Evapotranspiration (ET) over wider areas has been evaluated during the past few decades, particularly using data from remote sensing. The main benefit of using remote sensing is that water consumption by the soil-water-vegetation system may be determined directly without the need to quantify other intricate hydrological processes.

Multispectral vegetation indices (VIs) computed as differences, ratios, or linear combinations of reflected light in the visible (blue, green, or red) and near-infrared (NIR) bands have been proved to be closely related to several crop growth parameters (Moran *et al.*, 1995). Many researchers have found similarities in the temporal patterns of Kc and VI. Therefore, Kc can be modeled in terms of VI and can be further used for estimating crop water requirement. Weekly or biweekly extracted VIs can provide more accurate Kc enabling near real-time irrigation scheduling.

Acreage estimation based on remote sensing is time efficient and accurate. Besides, remote sensing makes the whole process effortless which is otherwise laborious. The accuracy can be further increased by utilizing remotely sensed data from advanced satellites with improved spectral and spatial resolution.

The chickpea *(Cicer arietinum L.)* is an annual legume of the family Fabaceae, subfamily Faboideae. Its different types are variously known as gram or Bengal gram, garbanzo or garbanzo bean, or Egyptian pea. Chickpeas are a type of pulse, with one seedpod containing two or three peas. The plant grows to 20–50 cm (8–20 inches) high and has small, feathery leaves on either side of the stem. It has white flowers with blue, violet, or pink veins. Dozens of varieties of chickpea are cultivated throughout the world. The larger light tan Kabuli and variously colored Desi are the two main types of chickpea. They are green when picked early and vary from tan or beige, speckled, dark brown to black. 75% of world production is of the smaller desi type. Desi chana as called in north India or called Boot in Eastern India (Assam, parts of Bihar) has small, darker seeds and a rough coat. They are grown mostly in India and other parts of the Indian subcontinent.

Garbanzo beans or 'Kabuli' chana are lighter-colored, larger and with a smoother coat.

Chickpeas are a nutrient-dense food, providing rich content (20% or higher of the Daily Value, DV) of protein(38%), dietary fiber(68%), vitamin B6(25%) and certain dietary minerals, such as iron(34%), magnesium(28%) potassium(25%) in a 100-gram reference amount. Chickpea is important in Indian cuisine, used in salads, soups and stews, curry, chana masala and in other meal products. In 2019, world production of chickpeas was 14 million tonnes, led by India with 70% of the global total and Turkey as a secondary producer. Maharashtra contributes 16% of the national production of chickpea under an area of 1.44 million ha.

Chickpea being a major rabi crop is grown under rainfed conditions where drought is the main constraint, limiting their production. It can be regarded as a moisture-sensitive crop since excess water causes fungal growth and water stress causes stunted growth, resulting in reduced grain yield. However, optimum yield can be obtained by irrigation at the branching, flowering and pod formation stages. Thus, irrigation plays an important role in getting higher yields. Chickpea is well suited to well-drained, nonacidic soils with medium to heavy clay texture. Hence, the precise application of water on a spatial basis is important. The mean daily water requirement of chickpea increases along the initial, developmental and mid stages and then decreases along the maturation (late) stage. Pandey *et al.* (2008) reported crop water requirement of chickpea at various locations across the command area of Narmada Canal in India in the range of 194 -246 mm and concluded that with varying soil type, response of chickpea to moisture varies. The mean crop water requirement of chickpea during the rabi season was estimated to be 470.2 mm in arid and semi-arid conditions in the middle Gujrat with a peak mean value of 5.9 mm/day during midseason. Large variations were reported in daily water requirements across the locations in the range of 1.4 to 7.4 mm/day along the crop period whereas total crop water requirement varied from 334.1 mm to 564.9 mm across the Gujrat (Mehta *et al.,* 2016).

Considering all the aforementioned advantages of remotely sensed data in precise irrigation management, this research was focused on

implementing the VI-based Kc within the framework of FAO procedures for predicting real-time spatial water use patterns for determining appropriate irrigation scheduling. Hence, the investigation was undertaken for the chickpea crop in the Akola district of Maharashtra state where this rabi crop is dominant, as limited work has been attempted so far on this methodology.

1.3 Objectives

The objectives of the investigation were:

1. To develop temporal spectral profile of chickpea
2. To identify chickpea crop and estimate its acreage using remote sensing
3. To establish the relationships between vegetation indices and crop coefficients
4. To utilize the established best relationship for near real time irrigation water management

1.4 Scope and Limitations

The research will help us to test a strategy for implementing the VI-based Kc within the framework of FAO procedures for predicting real-time spatial water use patterns for determining appropriate irrigation scheduling. The temporal VI spectral profile can be used to identify crops, estimate acreage and determine evapotranspiration with high accuracy in real-time. The identification of crops and their acreage estimation enables addressing spatial water requirements.

This research established the relationship between VIs and crop coefficients (Kc) for chickpea crop. VI having the closest relation with Kc was identified and the Kc developed from the VI was used in place of crop coefficients from lysimeter studies for accurately determining near real time irrigation water requirement. This approach proved to be a scientific and simple tool for both planners and stakeholders. This approach will be useful for developing an expert system for irrigation scheduling of a large area by combining the near real-time agrometeorological data from automatic weather stations and near real-time VI data from the satellites.

However, there are a few limitations associated with using such a novel technology, including:

1. During the rainy season, when the majority of rainfed crops are grown, cloud cover frequently hinders the use of imagery.
2. In the case of mixed cropping, crop type must be precisely identified which is challenging when cultivated plots are smaller than an image pixel.
3. Accurate identification is hampered by large field-to-field variations in sowing and harvesting dates and cultural and crop management practices.
4. Crop evapotranspiration estimates are limited for the period covered by the available satellite imagery. These constraints restrict the use of satellite-based remote sensing for determining the probability distributions and long-term variability of soil moisture stress in rainfed crops.

However, these constraints can be overcome by utilizing high spatial and spectral resolution data with greater repeatability, which is possible with advanced remote sensing satellites having onboard fine-resolution sensors.

1.5 Hypothesis

Remote sensing plays a significant role in precise irrigation water management. One of the most popular ways to regulate irrigation water usage is the FA0-56, crop coefficient (Kc)-based calculation of crop evapotranspiration. Meanwhile, the crop evapotranspiration estimations may, however, deviate significantly from the real crop evapotranspiration at the particular site due to uncertainties in the approach. Remotely sensed vegetation indices exhibit a similar behavior as that of crop coefficients throughout the entire life cycle of the crop and reach a peak value in the midseason stage when the crop attains full effective green cover coinciding with the maximum value of crop coefficient. The crop coefficients can be modeled as a function of VIs based on the similarities between the crop coefficient curve and the temporal pattern of VIs. The best-performing VI model can be identified after testing various VI models. The site-specific evapotranspiration and water requirement can be estimated with Kc derived from the selected VI. The temporal VI spectral profile can be utilized for crop identification, acreage estimation and ultimately, the total water demand of a specific crop in the area.

CHAPTER II

REVIEW OF LITERATURE

One of the key initiatives to promote water conservation in the agricultural sector is improving the water productivity of various crops. Better water management in various agricultural crops can be achieved by providing adequate amount of water to meet the actual crop water requirement. About 99 percent of the water that plants take up from the soil is lost through evapotranspiration (ET), so calculating crop evapotranspiration (ETc) from the daily reference evapotranspiration and crop coefficients is equivalent to determining the daily crop water requirement. Crop water requirement fluctuate throughout the growing season, primarily due to changes in crop canopy and meteorological conditions and are also influenced by cropping practices and irrigation techniques. In this study, a vegetation indices-based crop coefficient approach is used to precisely calculate crop evapotranspiration and, ultimately, agricultural water demand. The prior research conducted at various sites related to the subject of this study is reviewed and elaborated in this chapter under the following headings:

2.1 Evapotranspiration and Crop Coefficient

2.2 Vegetation Indices (VIs): Concepts and Applications

2.3 Identification and Acreage Estimation of Crops using Remote Sensing

2.4 Relationships between Vegetation Indices and Crop Coefficients

2.5 Utilization of Remote Sensing Techniques for Irrigation Water Management

2.1 Evapotranspiration and Crop Coefficient

A thorough understanding of the evapotranspiration mechanism is necessary to calculate the actual water requirement of crops.

Thornthwaite (1948) was the first to have concern over evapotranspiration. He described evapotranspiration as the combined process of evaporation from the soil and transpiration from the plants. He introduced the concept of potential evapotranspiration. According to him, potential evapotranspiration is the maximum evapotranspiration from a vegetation

completely covering the ground surface that has an unlimited water supply to its roots. He also put forth a temperature-based empirical equation to estimate evapotranspiration.

Penman (1948) introduced another method to estimate evapotranspiration which was based on the energy balance of the surface. This method, popularly known as the Penman method, is one of the most discussed methods to measure evapotranspiration. Small differences were found in the evapotranspiration computed by the Penman method when compared with actual measurements.

Blaney and Criddle (1950) observed that the amount of water consumptively used by the crops during their growing season was closely correlated with mean monthly temperatures and daylight hours. He computed monthly consumptive use as a product of the consumptive use coefficient and consumptive use factor of the corresponding month.

Monteith (1965) incorporated the principles of energy balance and resistance to water vapor movement and modified the Penman equation. He incorporated an additional surface (vegetation) resistance term. This modified Penman equation is also known as the combination equation. When this equation is applied to a plant canopy, it assumes the evaporating surface as a single big leaf.

Doorenbos and Pruitt (1977) published the details of estimating crop evapotranspiration and crop coefficients based on the Penman equation in the publication FAO-24. Researchers found that the methodology published in FAO-24 tended to overestimate the reference evapotranspiration and suggested the use of the Penman-Monteith equation in place of the Penman equation (Allen *et al.* 1994).

Allen *et al.* (1989) found that the Penman-Monteith method produced more accurate estimates of evapotranspiration when compared with other forms of Penman's equation. The Penman-Monteith equation is widely used by researchers to estimate crop evapotranspiration. For estimation of crop evapotranspiration, the potential evapotranspiration was considered to measure the evapotranspiration from a reference crop surface such as short

grass or alfalfa and multiplied by a factor called the crop coefficient (Doorenbos and Pruitt, 1977, Wright, 1982).

The FAO irrigation and drainage paper 56 (Allen *et al.* 1998) included the revised procedures for estimating reference evapotranspiration. The reference crop was redefined as a hypothetical grass surface growing under ideal conditions with a height of 0.12 m, a fixed surface resistance of 70 ds m·' and an albedo of 0.23. This publication also introduces two types of crop coefficients: a single crop coefficient for use when the soil surface is dry and a dual crop coefficient (a basal crop coefficients and a soil evaporation factor) when the soil surface is wet as proposed by Wright (1982).

Hunsaker (1999) developed crop coefficients for a short season cotton variety in Arizona and found that these crop coefficients were larger than the published FAO-56 crop coefficients for cotton.

Allen *et al.* (2000) expressed that the crop coefficient is the ratio of reference evapotranspiration to crop evapotranspiration. The crop coefficient incorporates the effects due to the difference between the hypothetical reference crop and various field crops in terms of crop height, surface resistance and albedo. They compared the crop evapotranspiration of three agricultural crops, snap beans (*Pisum sativum* L.) and sugarbeets (*Beta vulgaris* L.), grown in 10 lysimeters in Kimberly, Idaho, with the crop evapotranspiration calculated by the FAO-56 method. They found that both methods produced similar results.

Brown *et al.* (2001) developed crop coefficients for turf grass growing in a desert climate. They observed that the crop coefficients varied during the cloudy condition in winter and suggested that irrigation scheduling based on weather data may be less reliable under those environmental conditions.

Ray *et al*. (2001) evaluated the use of satellite-based remote sensing (RS) data and geographic information system (GIS) tools for estimating seasonal crop evapotranspiration in the Mahi Right Bank Canal (MRBC) command area of Gujarat, India. Crop coefficients (Kc) for various major crops grown in MRBC were estimated, empirically, from the RS derived soil adjusted vegetation index (SAVI) values. A reference crop evapotranspiration

(ETo) map was generated from point meteorological observations. The Kc and ETo maps were combined to generate seasonal crop evapotranspiration (ETcrop) map which highlighted spatial variation in ETcrop ranging from more than 600 mm for healthy tobacco crops to less than 150 mm for very poor wheat crops.

Howell *et al.* (2004) applied the FAO-56 method to estimate the evapotranspiration for well-watered, deficit-irrigated and dryland cotton on the Northern Texas High Plains. They found that the FAO-56 method performed better for the fully irrigated cotton than for the deficit-irrigated and dryland cotton.

Howell *et al.* (2006) developed crop coefficients for major irrigated crops in the Texas High Plains by measuring evapotranspiration with large precision weighing lysimeters. The crops were corn (*Zea mays* L.), wheat (*Triticum aestivum* L.), sorghum (*Sorghum bicolor* L.), soybean (*Glycine max* L.), cotton (*Gossypium hirsutum* l.) and alfalfa *(Medicago sativa* L.). These crop coefficients, known as the Bushland crop coefficients, were used in the evapotranspiration networks in Texas and surrounding states.

Marek *et al.* (2006) compared the evapotranspiration of cotton, grain sorghum and soybeans by the FAO-56 and Bushland crop coefficient methods. They used the ASCE/EWRI reference evapotranspiration equation (Allen 2005) to calculate the reference evapotranspiration. They found major differences in crop evapotranspiration estimated by these methods in the late growing season for corn and grain sorghum.

Suleiman *et al.* (2007) found that in humid areas the FAO-56 method worked accurately for estimating the cotton evapotranspiration under deficit irrigation conditions.

Anonymous (2012) after lysimeter studies at Mahatma Phule Krishi Vidyapeeth, Rahuri, Maharashtra recommended week-wise crop coefficients of wheat and chickpea for local conditions.

Anonymous (2013) after lysimeter studies at Mahatma Phule Krishi Vidyapeeth, Rahuri, Maharashtra recommended week-wise crop coefficients of *kharif* and *rabi* sorghum considering local conditions.

Silva *et al.* (2021) determined the water requirements and Kc for three chickpea cultivars viz. Cícero, BRS Aleppo and BRS Cristalino inside the greenhouse which artificially generated Brazilian Savannah Biome. Mini lysimeters and soil moisture sensors were used for ETc determination whereas Kc was given by ETc/ETo ratio. Average ETc was found to be 4.5, 4.1 and 4.5 $mmday^{-1}$ and Kc values in the range of 0.38 to 1.00, 0.39 to 0.80 and 0.38 to 0.95 for Cícero, BRS Aleppo and BRS Cristalino cultivars respectively. Variations in Kc were observed with the changes in leaf number and crop phase patterns. Similarly, water requirements varied based on weather, crop growth and phenology. For better irrigation management and water relations estimation, ETc estimation for each cultivar was suggested to be a more efficient method.

Several scientists and researchers have observed that the FAO-56 method has problems in accurately predicting crop evapotranspiration. Allen (1999) concluded that these differences in crop evapotranspiration may be due to the fact that the crop growing conditions in other studies are not representative of the conditions used to develop the crop coefficients in FAO-56.

2.2 Vegetation Indices (VIs): Concepts and Applications

With the launch of the first satellite in the early 1970s, several VIs have been developed by linear combination or ratios of different spectral bands and are used for vegetation monitoring. Plant canopy reflectance factors and derived multispectral VIs are receiving increased attention in agricultural research as robust surrogates for traditional agronomic parameters e.g. leaf area index (LAI), fraction of green cover, fraction of absorbed photosynthetically active radiation (fAPAR), crop coefficients etc.

Jordan (1969) first presented the ratio vegetation index (RVI). It is based on the principle that leaves absorb relatively more red than infrared light and therefore, the more leaves that are present in the canopy, the greater will be the ratio.

Rouse *et al.* (1973) further suggested the most widely used Normalized Difference Vegetation Index (NDVI) to improve identifying the vegetated areas and their condition.

Huete (1988) proposed a Soil Adjusted Vegetation Index (SAVI) to reduce the impact to the NDVI from the soil variations in lower vegetation cover areas, by introducing a correction factor L.

Nemani and Running (1989) found that in different studies, vegetation indices have been related to radiometric surface temperature to predict transpiration and soil evaporation. In general, a negative correlation between NDVI and radiometric surface temperature was found. However, besides vegetation cover, surface temperature is strongly related to surface soil moisture, so that the consideration of this parameter is required for estimations of ET.

Wiegand *et al.* (1990) expressed view that often viewed simply as measures of plant biomass or green leaf area index, VIs have been designed to find a functional relationship between crop characteristics and remote spatial observation.

Jackson and Huete (1991) stated that while VIs were developed to extract only the plant signal, other factors such as soil background, canopy architecture, moisture condition, solar zenith angle, view angle and atmospheric constraints alter the index values in a complex way. Thus, for the effective use and interpretation of VIs, all these factors require to be simultaneously considered.

Qi *et al.* (1993) observed that VIs are more sensitive than individual bands to vegetation parameters.

Moran *et al.* (1994) derived a vegetation index temperature trapezoid, which combines satellite vegetation indices with radiometric surface temperature and extended crop water stress index theory. The method is based on the hypothesis that a trapezoidal shape results from a plot of the difference between radiometric surface temperature and air temperature (Trad-Ta) against vegetation cover. In addition, the method considers that, for

a given Rn, vapor pressure deficit of the air and aerodynamic resistance are linearly related with ET.

Gao (1996) introduced Normalized Difference Water Index (NDWI) to monitor moisture content in plants and soil. This index is resistant to atmospheric effects, distinguishing it from NDVI.

Sandholt *et al.* (2002) proposed the Temperature-Vegetation Dryness Index (TVDI), which is obtained from space LST-NDVI and can be used as an indicator of soil moisture and hence the vegetation water stress.

Barnes *et al.* (2003) stated that VIs can be used as a mapping device. They used in image classification, to separate vegetated areas from non-vegetated areas, to distinguish between different types and densities of vegetation, to monitor seasonal variations in vegetative vigor, abundance and distribution.

Robertson *et al.* (2013) monitored the reflectance of soybean and maize crop continuously with four band radiometer and studied diurnal and seasonal temporal behaviour of reflectance and advocated that the temporal profile of vegetation indices (NDVI and EVI2) can indicate the crop phenology, water stress, early and late sowing, disease and pest attacks very clearly.

Kadam *et al.* (2017) indicated that it is possible to quantify water stress by NDVI and to use remotely sensed data to develop maps of water stress conditions of soybean.

Zolfagharnejad *et al.* (2017) estimated vegetation index-Deduced Crop Coefficient of Wheat (*Triticum aestivum*) using Remote Sensing. They investigated and determined the monthly Kc of winter wheat (*Triticum aestivum* L.) using five vegetation indices (VIs): Normalized Difference Vegetation Index (NDVI), Difference Vegetation Index (DVI), Soil Adjusted Vegetation Index (SAVI), Infrared Percentage Vegetation Index (IPVI) and Ratio Vegetation Index (RVI) of four basins in Golestan province, Iran. Landsat-8 images according to crop growth stage were used to estimate monthly Kc of wheat. VIs were calculated based on infrared and near infrared bands of Landsat 8 images using Geographical Information System (GIS) software.

Deoli and Kumar (2019) conducted the spatiotemporal mapping of the Ramganga reservoir from 2013 to 2018 on the QGIS platform. The reservoir was mapped and the water spread area was found using Landsat-8 derived NDVI. The study suggested that NDVI can accurately extract water features and their spread area and hence can be used for the spatiotemporal mapping of water bodies.

Akkara *et al.* (2022) reviewed that vegetation indices can be used for crop monitoring as a surrogate for agronomic parameters and the inferences derived can be further utilized for precision agricultural practices leading to better agricultural management.

2.3 Identification and Acreage Estimation of Crops using Remote Sensing

There have been many investigations on various aspects of crop identification and area estimation using air-borne to space borne sensors for different crops and agricultural regions in India and abroad.

Ayyangar *et al.* (1980) used the spectral-temporal profiles with red and near infrared bands for crop identification and condition assessment of rice and sugarcane crops. They have used near real time satellite imageries to derive the VIs.

Munshi (1982) in his study used space borne data and employed visual mapping for wheat crop.

Dadhwal and Parihar (1985) stated that first attempt in the country towards the use of satellite data in crop acreage estimation was made in the Karnal district of Haryana using Landsat MSS data. The work emphasized the use of single date data and supervised Maximum Likelihood (MXL) classification approach.

Sharma (1995) delineated four vigour classes of coconut crop in the Allepy district of Kerala using digital analysis and complete enumeration method.

Panigrahy and Chakraborty (1996) reported mapping of potato crop using multi-date RS data.

Guruge (1996) monitored the development of sugarcane in Buttala area of Monaragala district, Sri Lanka from 1983 to 1994 using aerial photographs and IRS images. Sugarcane areas were computed using digital images for four years (1983, 1988, 1992 and 1994).

Kimothi *et al.* (1997) carried out a study to identify and map apple and almond plantations in Shimla district of Himachal Pardesh using IRS-1A & 1B, LISS-1 and LISS-II data. Overall accuracy for identification was 87% for 90 % confidence interval.

Narsico *et al.* (1999) investigated the use of satellite imagery for identifying and classifying sugarcane and providing timely and acceptably accurate information on the area under sugarcane production. The procedure was tested in the Eston district using a Landsat Thematic Mapper image acquired on April 22 1996. Digital maps of farms and a database of actual area under cane were used to assess the accuracy of the classification procedures.

Gears *et al.* (2001) investigated on the use of Spot 4 satellite imagery to monitor sugarcane areas harvested by small holder growers in a selected area within the Umfolozi mill supply area. This was achieved by manipulation of the four satellite-measured spectral bands and subsequent classification of sugarcane into harvested and non-harvested areas. Results indicate that the satellite imagery classifications are able to clearly distinguish between standing sugarcane and harvested plots.

Coppa (2006) designed a concept for an operational crop monitoring system using SPOT remote sensing data of the five agricultural crop types: barley, canola, chickpeas, lentils and wheat in Gooroc, Southeast Australia. Crop type classification was done using discriminant function analysis. An early phase prototype crop monitoring system, Agricultural Land Management Information System (ALMIS) was trialed with 25 farmers and critical parameters for an improved version of crop monitoring were suggested.

Dheeravath *et al.* (2010) mentioned VIs as the best approach to provide normalized information in the study to map land classes by removing clouds, reducing data volume and enriching data.

Mukherji *et al.* (2010) compared IRS LISS-III and AWiFS sensors data for wheat yield and acreage prediction in the Rupnager district of Punjab. Maximum Likelihood Classification is done for crop classification through the district boundary mask approach. Wheat acreage was estimated through complete enumeration. Results showed that wheat acreage was better estimated from LIS-III data compared to AWiFS. The yield was estimated from wheat yield models developed through regression analysis between yield and various VIs like RVI, NDVI, DVI, TVI, SAVI and IPVI. Among VIs, RVI had the highest and DVI had the lowest correlation coefficient with wheat yield for both sensors. Though a similar relationship of VIs was obtained for both sensors, correlation coefficients corresponding to AWiFS were higher than LISS-III. Overall, the prediction equation developed by stepwise regression techniques revealed yield can be estimated with an accountability up to 90% from the remote sensing approach.

Vaidyanathan Committee (2011) in its final report on agricultural statistics informed that the Ministry of Agriculture has been working with ISRO since 1987 leading to the launch of the FASAL project, in 2002, (Forecasting Agricultural Output Using Space, Agro- meteorology and Land based observations). FASAL has developed and used methodology for estimating area under different land uses and crops. It provides the Ministry advance estimates of area of major crops at the national, state and in some cases, district levels. The report highlights the fact that the feasible level of crop and spatial detail, as well accuracy of estimates, is limited by the capability of satellites and sensors currently in use.

Pimpale *et al.* (2015) classified *rabi* wheat crop using multidate IRS P6 AWiFS data derived NDVI time series. A hybrid classification technique based on two-stage ISODATA clustering and visual analysis was adopted to produce a final classified image having pure-class pixels (93-98%) and mixed-class pixels (2-7%). An overestimated wheat acreage by 9.78% more than the official records was observed during the accuracy assessment. This might be due to either the coexisting crops with similar spectral profiles or the effect of soil moisture on crop reflectance. Besides, it was pointed out that analysis

based on multidate spectral data is more reliable than that of single-date spectral data.

Chen *et. al.* (2016) utilized multi-temporal Sentinel-1 A data for the crop acreage estimation of rice in Mekong River Delta (MRD) in Vietnam. For rice crop mapping, they utilized normalized difference in value between sowing and heading dates index (NDSH). They applied receiver operating characteristic (ROC) curve using ground reference data to get threshold for mapping rice growing area with regard to two rice and non-rice classes. They analyse the classified map with ground data and found overall accuracy 86.2% and Kappa coefficient 0.72.

Csillik and Belgiu (2016) report the study of cropland mapping from Sentinel-2 time-series data using object as spatial analysis units. For cropland mapping and monitoring of south-eastern part Romania, the image objects were classified using the Time-Weighted Dynamic Time Warping (TWDTW) method. The implemented cropland mapping framework yielded an overall precision of 93.43% and a kappa index of 92%.

Campos-Taberner *et. al.* (2017) investigated multi-temporal LAI information from sentinel-2A, with time series of sentinel-1A pictures over the primary European rice districts for the 2016 harvest season, rice grown region was recognized. Inverting the PROSAIL radiative transfer model with Gaussian process regression and detecting Rice cultivation using an integrated multi temporal rule-based algorithm was used to obtain LAI information. Their research reveals the elevated consistency between surface readings and estimates, elevated correlation value ($R^2 > 0.93$) and excellent accuracy (RMSE < 0.83, rRMSEm < 23.6% and rRMSEr < 16.6%).

Gomez (2017) found the 98% overall classification precision using polygon-based approach and found 84% precision using pixel-based approach, in to investigate the classification accuracies of specific land covers obtained after a random forest classification of multi-temporal Sentinel data over an agricultural area. Four scenarios have been tested for the classification: (1) Sentinel-1, (2) Sentinel-2, (3) Sentinel-2 and vegetation indices, (4) Sentinel-1, Sentinel-2 and vegetation indices.

Torbick *et. al.* (2017) used Sentinel-1A wide interferometric images to map rice crops throughout Myanmar. They have integrated and classified land use land cover map fusing Sentinel-1, Landsat-8 OLI and PALSAR-2 using a random forest algorithm. An assessment of a phenological time series refined the cropland class to generate a rice mask by extrapolating distinctive rice crop stages indices from the dense Sentinel-1 time series to map rice paddy features in an automated strategy. Their assessment shows that the rice region harvested was 6652111 ha with overall precision (R^2=0.78) with statistics from the state census.

Bhatt and Nain (2018) studied the potentiality of SAR application for measuring rice acreage during cloud cover condition using Sentinel-1A data of European Space Agency in Udham Singh Nagar, it is one of major rice producing area of Uttarakhand state. The SAR dataset classified with a Support Vector Machine (SVM) algorithm provided in ENVI- 5.1 produced the accurate LULC map, which shows, Udham Singh Nagar covers rice area (108,095 ha) with an overall classification precision of 92.88% and a Kappa coefficient of 0.89.

Chai *et al.* (2018) collected total 30 dual-polarizing images across two provenances (Nueva Ecija and Tarlac) in the Philippines using high spatial resolution Sentinel-1 multi temporal imagery to detect rice-based cropping pattern in the majority of rice-growing area in Philippines. Overall precision of 83% is obtained using rule-based classifier to delineate rice cropping patterns compared to the decision tree classifier 76% method.

Lasko *et al.* (2018) researched rice classification Sentinel-1 SAR graphics in Hanoi capital region, Vietnam using Random Forest Algorithm and 10 and 20 m resolution time series using VV-only, VH-only and both polarizations. They compare spatial variability and quantify the significance of input bands, estimate plant development phases, evaluate rice field / collective metrics using frag statistics with image segmentation and emphasize the significance of the consequence for land use and land cover (LULC). They found that 10 m data for VV / VH had the highest overall accuracy in the accuracy assessment (93.5 percent, ±1.33 percent), whereas

VV had the lowest overall accuracy at 10 and 20 m (93.5 percent, ±1.57; 91.0 percent, ±2.75).

Mohite *et al.* (2018) studied the four district Krishan, Guntur, west Godavari and East Godavari of Andhra Pradesh during the *kharif* 2017 for the rice area mapping. They used multi-date images of Sentinel-1 (SAR sensor) with frequency of 12 days and 10-meter spatial resolution. Initially their model was being trained considering two images available from mid-June 2017, further various model has been trained by adding one successive image till end of August 2017. The classification of agriculture, non-agriculture and aquaculture layer has been masked out, which are derived from global land cover obtained from ESA. The overall classification precision was found between 78.11 to 87.00 %.

Subbarao *et al*. (2021) found that acreage estimation can be successfully performed by multi-temporal Sentinel-1 SAR data with RF classifier. The study estimated the area of *rabi* rice in Bhandara district of Maharashtra as 1760 km^2 with an overall accuracy of 91% at a Kappa coefficient value of 0.80.

Hudait and Patel (2022) identified the major summer crop acreage in the Purba Medinipur district of West Bengal using multi-spectral NDVI derived from Sentinel-2 images and two ML algorithms namely, KNN and RF. Though both methods resulted in overall accuracy of above 90%, the Random Forest (RF) method turned out to be more accurate with an overall accuracy of 97.22% at a Kappa index value of 96.08%. The method found to be capable of extracting both larger and smaller fields satisfactorily.

2.4 Relationships between Vegetation Indices and Crop Coefficients

Jackson *et al.* (1980) proposed to use multispectral VIs as near real time surrogates for crop coefficients. They pointed out the similarity between the seasonal pattern of a VI for wheat and that of the wheat crop coefficient

Bausch and Neale (1987) used a hand-held radiometer, which measured radiance in three bands similar to Landsat TM bands 3,4 and 5 to demonstrate the similarity of a seasonal NDVI curve and a basal crop coefficient curve for corn. They concluded that NDVI-derived crop coefficients

represent real-time crop coefficients. Later work by Neale *et al*. (1989) correlated the spectral crop coefficients to corn ET measured by lysimeters. They also stated that reflectance-based coefficients are sensitive to variable growth rates caused by variable weather conditions.

Bausch (1993) used the reflectance-based crop coefficient for corn by using the soil adjusted vegetation index (SAVI) to represent the Kc. Consequently, soil background effects were minimized which eliminates additional calibration for different soils.

Hunsaker *et al.* (2003) developed regression equations to estimate the seasonal distribution of Kcb with NDVI for a full-season cotton cultivar grown in the southwestern USA. An initial evaluation of the model indicated that the NDVI-based Kcb provided ETc estimations that closely described the observed ETc attained for another cotton cultivar grown under different conditions than those under which the model was developed. The NDVI-based Kcb functions can be easily incorporated within the FAO-56 dual crop coefficient procedures and thereby, provide means to apply remotely sensed observations for real-time cotton irrigation scheduling.

Salah *et al.* (2010) expressed that vegetation index methods replace (or supplement) crop coefficients with VI that reflects the actual growth stage of the crop at the time of measurement. VI based crop coefficients have been developed for individual and mixed crops in many agricultural regions since many years. In this context, several relationships between Kc and VIs have been established. However, there is no agreement on the nature and generality of these relationships. Some studies have shown that these relationships are linear, but others have found non linearity relationships. Therefore, establishing a unique relationship between crop coefficient and spectral vegetation indices is an ongoing research topic.

Kamble *et al.* (2013) developed a simple linear regression model to establish a general relationship between a (NDVI) from a moderate resolution satellite data (MODIS) and the crop coefficient (Kc) calculated from the flux data measured for different crops and cropping practices using AmeriFlux towers and found a strong linear correlation between the NDVI-estimated Kc and the measured Kc with an R^2 value of 0.91 and 0.90.

El-Shirbeny *et al*. (2014) assessed wheat crop coefficient using satellite-derived NDVI and established a linear relationship between Kc_{sat} and Kc calculated from FAO 56 paper with a high value of R^2 equals 0.96.

Mohammed *et al.* (2014) conducted a study in which Normalized Deference Vegetation Index (NDVI) was used to estimate wheat crop coefficient according to satellite data (Kc_{sat}) through simple model (Kc_{sat} = 2NDVI - 0.2). Linear relationship between Kc_{FAO} and Kc_{sat} was established and R^2 was 0.96.

Pimpale *et al*. (2014) carried out a study on the determination of the spatial crop coefficient of chickpea. A regression model was developed to find Kc and found that the NDVI is highly correlated with Kc linearly.

Parmar and Gontia (2016) established the relationship between remote sensing-based vegetation indices viz. NDVI and SAVI and temporal crop coefficients of summer groundnut to estimate crop evapotranspiration in the command area of Ozat-II canal. Landsat-8 OLI satellite images were corrected and processed using Geomatica V10.0 and GRASS GIS7.1 softwares. SAVI outperformed NDVI with a high R^2 value of 0.9594.

Pimpale *et al.* (2019) compared the different vegetation indices viz. RVI, SAVI, NDVI, TNDVI and MSAVI2 on their ability to surrogate crop coefficient of *khar* sorghum. This study was carried out in five districts of Maharashtra using multidate satellite images from the AWiFS sensor during the crop duration. Amongst all vegetation indices studied, the strongest correlation with crop coefficients was observed for MSAVI2 on the subsequent linear regression analysis with an R^2 value of 0.805 and a D value of 0.943. Furthermore, it was suggested to use the combination of near real-time MSAVI2 data and automatic weather data for automated irrigated systems.

Spiliotopoulos *et al.* (2019) carried out research for the investigation of specific relationships between crop coefficients and vegetation indices (VI) computed at the water- limited environment of Lake Karla Watershed, Thessaly, in central Greece. Cotton, sugar beets and corn fields were utilized for the study and NDVI, SAVI and EVI were tested separately for each crop. The resulting equations explained those relationships with a very high R^2

value (>0.86). These relationships have been validated against independent data.

Zhang *et al.* (2019) aimed to map the maize crop coefficient (Kc) with improved accuracy under different levels of deficit irrigation. The results showed that the NDVI values under different levels of deficit irrigation had no significant difference in the reproductive stage but changed significantly in the maturation stage, with a decrease of 0.09 with 72% water applied difference. They reported that overall, use of the UAV-measured multispectral vegetation index approach could improve water management at the farm scale.

French *et al*. (2020) used remotely sensed NDVI to model basal crop coefficient of wheat and found that it accurately estimated Kc and crop evapotranspiration during midseason and late season stages.

Gonzalez *et al.* (2020) conducted study to monitor the height and NDVI vegetation index of safflower during two cultivation cycles, developed a new Kc based on the NDVI and calculate the crop evapotranspiration (ETc) taking into account the Kc values. The results indicated similar NDVI field curves in both cycles. High coefficients of determination (R^2 = 0.93 and 0.89) were obtained between the NDVI field and the Kc of FAO-56

Rawat and Mishra (2020) studied the spatial crop coefficient (Kc) estimated from the surface energy balance algorithms for land (SEBAL) model was compared to simulated spatial Kc based on the normalized difference vegetation index (NDVI) and leaf area index (LAI). Statistical analyses showed that the LAI-Kc model outperforms the NDVI-Kc model in terms of spatial Kc as opposed to SEBAL-Kc. Furthermore, the LAI-based simulated spatial Kc has a strong coefficient of determination of 0.976 (at 95 percent) with SEBAL-Kc rather than NDVI-Kc, according to the data.

Dingre *et al.* (2021) conducted a study, in which, the possibility of correlating crop coefficient (Kc) and ground based normalized difference vegetation index (NDVI) of a sugarcane crop was investigated. The results found that the Kc was 16.6% less than that suggested by FAO-56. Unlike other crops, sugarcane NDVI at the maturity stage did not reduce from 0.85 even at harvest due to the continued production of fresh green leaves at the

top of the plant. The relationship between crop Kc and NDVI was characterized with 2nd order polynomial regression but correlation was moderately strong (R^2 = 0.75, n = 315). Stronger correlations between Kc and NDVI were obtained by splitting growth period into the growth phase (R^2 = 0.98, n = 245) and decline phase (R^2 = 0.99, n = 70).

Mariana *et al.* (2021) analysed the estimation of the crop coefficient (Kc) as a spectral function of the product of two variables: VIs and green vegetation cover fraction (fv). Multispectral images from experimental maize plots were classified to separate pixels into three classes (vegetation, shade and soil) using the OBIA (Object based image analysis) approach. Only vegetation pixels were used to estimate the VIs and fv variables. The spectral Kc_{fv}:VI models were compared with Kc based on cumulative growing degree days (CGDD) (Kc_{CGDD}). They indicated that three spectral-based Kc models showed good performance (R^2>0.80). The model that best fit the Kc values was fv:NDVI (R^2=0.91 to 0.94), fv:EVI2 and fv:WDRVI models showed lower performance, indicating that UAV images when vegetation is isolated from soil in high spatial resolution overcome the weaknesses of the NDVI index.

Shao *et al.* (2021) aimed to explore the potential of leaf area index (LAI) and multispectral vegetation indices (VIs) obtained by an unmanned aerial vehicle (UAV) for estimating the Kc value for a maize crop on a field scale and to obtain a high-resolution spatial-temporal map of Kc values. The results showed that the RFR algorithm effectively (R^2=0.65) estimated maize Kc values based on ground-based LAI and UAV-based VIs. Furthermore, the results indicated that the combination of UAV multispectral remote sensing technology and the RFR algorithm provides a potential solution for the distribution of water use and precision irrigation on a field scale.

Hassan *et al*. (2022) developed Kc prediction equations for the wheat crop using simple linear regression analysis on field Kc and LandSAT-8 derived NDVI. The linear prediction equation, Kc= 2.0114 NDVI – 0.147 showed a high R^2 value of 0.96 and was further utilized for calculating crop evapotranspiration.

2.5 Utilization of Remote Sensing Techniques for Irrigation Water Management

Many researchers have applied remote sensing techniques for accurate assessment of water requirement and water demand of crop.

Hafeez *et al*. (2002) used a surface energy balance algorithm for land (SEBAL) to compute ETa for paddy crops from Landsat 7 ETM+ images. All essential pre-processing parameters required for SEBAL such as the NDVI, emissivity, broadband surface albedo and surface temperature were calculated from the spectral data. The calculated ETa values were 6% lower than potential rice evapotranspiration values calculated with the modified Penman Monteith method using meteorological data. Hence, concluded that SEBAL provides realistic estimates of actual evapotranspiration of irrigated rice over spatially extended areas in the tropics.

Tasumi *et al.* (2006) compared the application of LandSAT and MODIS (Moderate Resolution Imaging Spectroradiometer) satellite images in ET mapping and water resources management in New Mexico using the METRIC (Mapping Evapotranspiration at high Resolution and with Internalized Calibration) model.

Gontia and Tiwari (2010) used WiFS sensor data and applied GIS techniques to estimate the evapotranspiration of wheat crop grown in Tarafeni South Main Canal (TSMC) irrigation command of West Bengal, India. Pixel wise crop coefficients were found by applying SAVI-Kc relationship and Kc maps were generated. Reference evapotraspiration was computed by FAO Penman-Monteith method. The spatially distributed actual crop evapotranspiration of wheat crop was estimated using the Kc maps and the reference evapotranspiration for irrigation command area. The attribute tables were prepared to determine the number of pixels and area under them for each group of ETc values in maps. Monthly crop water demand was computed by multiplying the area with ETc.

Pakhale *et al.* (2010) determined monthly crop water demand of wheat for the growing seasons of 1999-2003. They used Hargreaves equation to get PET and used locally developed Kc to get evapotranspiration. The ETc for

wheat crop was obtained by the product of Kc and PET. The crop water demand was estimated by multiplying ETc of each month of the season by crop area obtained by ANN technique. The crop water requirement varied from 78.63 mm/month to 201.14 mm/month. The maximum CWR was observed in the month of December while the minimum was observed in the month of March. They estimated irrigation water requirement assuming conveyance and field losses nearly 35%.

Farg *et al.* (2012) calculated wheat crop actual evapotranspiration in south Nile delta of Egypt by using integrated FAO-56 approach and remote sensing data. They estimated monthly reference evapotranspiration (ETo) by FAO-Penman Monteith equation and used wheat crop coefficients (Kc) derived from multi linear regression equation based on NDVI and SAVI and obtained monthly evapotranspiration of wheat crop. They observed that water requirement was higher in vegetative and midseason stage and showed decreasing trend towards maturity stage.

Palacios *et al.* (2012) studied the development wheat NDVI obtained from Landsat 5 Landsat 7 images of wheat in 13 plots in the 2008 agricultural year in Irrigation District 038, Mayo River, Sonora. Mexico. They computed the per plot average of the normalized difference vegetation index (NDVI). The basal crop coefficient (Kc) was computed from a linear relationship with NDVI. This Kc was then multiplied by the accumulated value of reference evapotranspiration in the period of influence of each image, measured in a representative weather station. Crop evapotranspiration was computed using data from reference evapotranspiration and Kc values estimated from NDVI values for 15 Landsat 5 and 7 images covering the entire wheat growing cycle. To help the producers to improve their efficiency in water use, a program was also developed.

Mamta Kumari *et al.* (2013) conducted a study to develop a relationship of crop coefficient (Kc) and vegetation indices obtained from AWiFs data and found Kc for rice and wheat. Crop coefficient maps were generated for each month of rice -wheat crop season by applying regression equation over the image in Model Maker tool of ERDAS Imagine. Monthly reference crop evapotranspiration (ETo) was estimated based on FAO-56,

Penman Monteith method. ETo was combined with spatially distributed Kc maps of different months of wheat crop season to generate crop evapotranspiration (ETc) maps of each month. The crop water demand (CWR) for different months of the crop growing period was computed by multiplying Kc values for the rice and wheat crop with the potential evapotranspiration. The estimated crop water requirement was 241.66, 531.34, 440.86 and 192.63 Mha.m for rice and 127.43, 135.77, 305.55, 262.84 and 204.5 Mha.m for wheat at various growth stages.

Ozcan *et al.* (2014) in their study in Hilvan and Akcakale districts of Turkey on wheat crop, estimated ETc values using Kc based on MSAVI values and ETo values obtained using FAD Penman-Monteith formula. Crop water demand based on actual crop evapotranspiration was obtained with product of average ETc value and corresponding area. They observed that water demands may vary for cultivated wheat fields on different soil types having different land use capability classes. It can be summarized that combination of spatially distributed vegetation indices based crop coefficients (Kc) and reference evapotranspiration (ETo) can be utilized for precise estimation of crop water requirements.

Desta *et al.* (2015) determined the crop water requirement of the crop for this particular growing area of Ethiopia is therefore paramount importance for proper planning of chickpea production using supplemental irrigation. In view of this, the crop water requirement of chickpea was estimated using the FAO CROPWAT 8.1 Software and long term weather data record where the planning date is simulated to be 24 December. The assessment has showed that the net irrigation requirement of the crop is 37.2, 114.4, 205.2 and 79.8 mm during seedling, vegetation, late (maturity) growth stages of the crop, respectively. The irrigation requirement of the crop for a single growing season as revealed by the program is estimated to be 436.7 mm.

Pimpale *et al.* (2015) estimated the water requirement of wheat crop using multispectral multi-temporal vegetation indices viz. SAVI, RVI, NDVI, TNDVI and MSAVI2. Linear models were generated correlating weekly crop coefficients and weekly vegetation indices. Amongst all models, NDVI – Kc model was found more accurate with the highest R^2 and D values while

having the lowest SE, RMSE and PD values. Crop water requirement of wheat (ETc) was computed in the range of 378.34 mm to 439.10 mm as the product of NDVI-Kc model derived crop coefficients (Kc) and Penman-Monteith equation derived reference evapotranspiration (ETo). Multispectral vegetation indices with their ability to predict spatial and temporal crop coefficients of the wheat crop are considered to be very suitable to estimate temporal and spatial crop water requirements of wheat leading to proper planning resulting in water saving.

Mehta *et al.* (2016) studied to estimate the crop water requirement (ETc). The study was therefore carried out to estimate crop evapotranspiration (ETc) for winter crops (mustard and chickpea) at eighteen stations of Gujarat, India using crop coefficient (Kc) and reference evapotranspiration (ETo). The reference evapotranspiration (ETo) was determined by Penman-Monteith method. The Kc values for winter chickpea and mustard as given in FAO- 56 were corrected for climatic condition of stations. The results revealed that during winter season (November to February) the mean daily reference evapotranspiration (ETo) varies from 4.4 to 7.4 mm/day. However total crop water requirement of mustard (515.0 mm) was more than that of chickpea (470.2 mm). The results are useful for planning the irrigation scheduling in winter season at different locations of Gujarat.

Singh *et al.* (2016) carried out a study on cotton crop in Sirsa district of Haryana. Spectral index such SAVI (Soil Adjusted Vegetation Index) was used to estimate Kcb value adopting the empirical equation. High spatial resolution Landsat TM5 images were used. Reference Crop Evapotranspiration (ETo) was estimated using Blaney-Criddle Method, taking weather data from observatory. The crop coefficients derived from remote sensing data were used along with ET o values to estimate crop evapotranspiration (ETc). Seasonal crop water requirement was estimated by aggregation of monthly water requirement during June-November.

Arshad *et al.* (2018) conducted a study with the aim to compute the real time spatially distributed crop coefficient (Kc) and water demand of wheat crop grown in Faisalabad Irrigation District, Pakistan. In this study monthly

crop evapotranspiration for command area was computed using MODIS 13Q1 satellite imagery. Kc maps were generated from MODIS 13Q1 satellite imagery while reference evapotranspiration (ETo) was estimation using CROPWAT model which compute ETo based FAO-24 modified Blaney-Criddle method using multi variables. It was found that average ETc value for wheat was increased gradually from Dec to Feb as 0.59 to 1.16 mm/days and then decreased to 1.05 mm/days in March. Seasonal crop water requirement of wheat was varied from 265 mm to 665 mm with an average of 465 mm.

Reyes-González *et al*. (2018) generated Kc maps using a linear regression equation obtained between NDVI and Kc values and created ETc maps with high spatial resolution at regional and field scales for silage corn. It was found that using ETc maps developed from remotely sensed multispectral vegetation indices at field scale, farmers can supply appropriate amounts of irrigation water corresponding to each growth stage and hence, a useful tool to quantify crop water consumption at regional and field scales.

Sutariya *et al.* (2021) compared MOD16 remote sensing data to the Landsat 8 data in determining crop evapotranspiration of chickpea crop in the Panam canal command in the semi-arid middle Gujrat region. Landsat 8 was found to outperform MOD16 in estimating actual evapotranspiration owing to the better spatial resolution. The daily peak crop water requirement of chickpea was found to be 2.5 mm and 2.1 mm corresponding to Landsat 8 and MOD16 respectively.

Gamal *et al*. (2022) developed a remote sensing based ET model by integrating MODIS Terra and Sentinel-2 data and found that it gives acceptable daily and seasonal ET values on testing it with Energy Balance flux tower ET measurements. However, models shown overestimation during winter season.

CHAPTER III

MATERIAL AND METHODS

The present investigation has been conducted at the Department of Irrigation and Drainage Engineering, Dr. PDKV, Akola and Maharashtra Remote Sensing Application Centre (MRSAC), Nagpur. This chapter broadly encompasses the location of the study area, materials and methods used for the research work. The extensive material collected and used for the present study includes meteorological data, remote sensing satellite data, ancillary data, crop data, phenological information, sowing details and crop evapotranspiration.

3.1 Study Area

The research area has been chosen to be the Akola district in middle east Maharashtra, which has a total size of 5428 square kilometers and is situated between latitudes 20.17º N and 21.16º N and longitudes 76.7º E and 77.4º E. It contributes 1.76% of the total area of the state and is at an average altitude of 285 m from the mean sea level. It shares an eastern border with Anjangaon, Daryapur and Nandgaon, Khandeshwar tehsils of Amravati district and Karanja tehsil of Washim while the southern and western sides of the district are bordered by Washim and Buldhana districts. It comprises seven tehsils namely Akola, Akot, Balapur, Barshitakli, Murtizapur, Patur and Telhara.

The climate of the Akola district varies a little from north to south. It is primarily tropical savannah. However, the northern regions of the district, which are made up of hills and mountains that rise to a height of around 950 to 1000 meters, exhibit a subtropical climate with chilly winters. The winters are dry and mild to cold whereas the summers are very scorching. From June through September, there is an average of 90% rainfall (SW monsoon). Annual rainfall averages between 750 and 1000 mm. The majority of soils are dark, clayey soils. Irrigated area is 22504 hectares. Cropping intensity is 120%. The two main agricultural products of the district are cotton and sorghum. Also prevalent are oil and Dal mills. Agriculture is the main sector of the economy. Due to the development of large soybean plants in the region,

the soybean crop is now significant. The main rabi crops grown in the area are safflower, wheat and chickpea. Hence, chickpea has been chosen as the study crop.

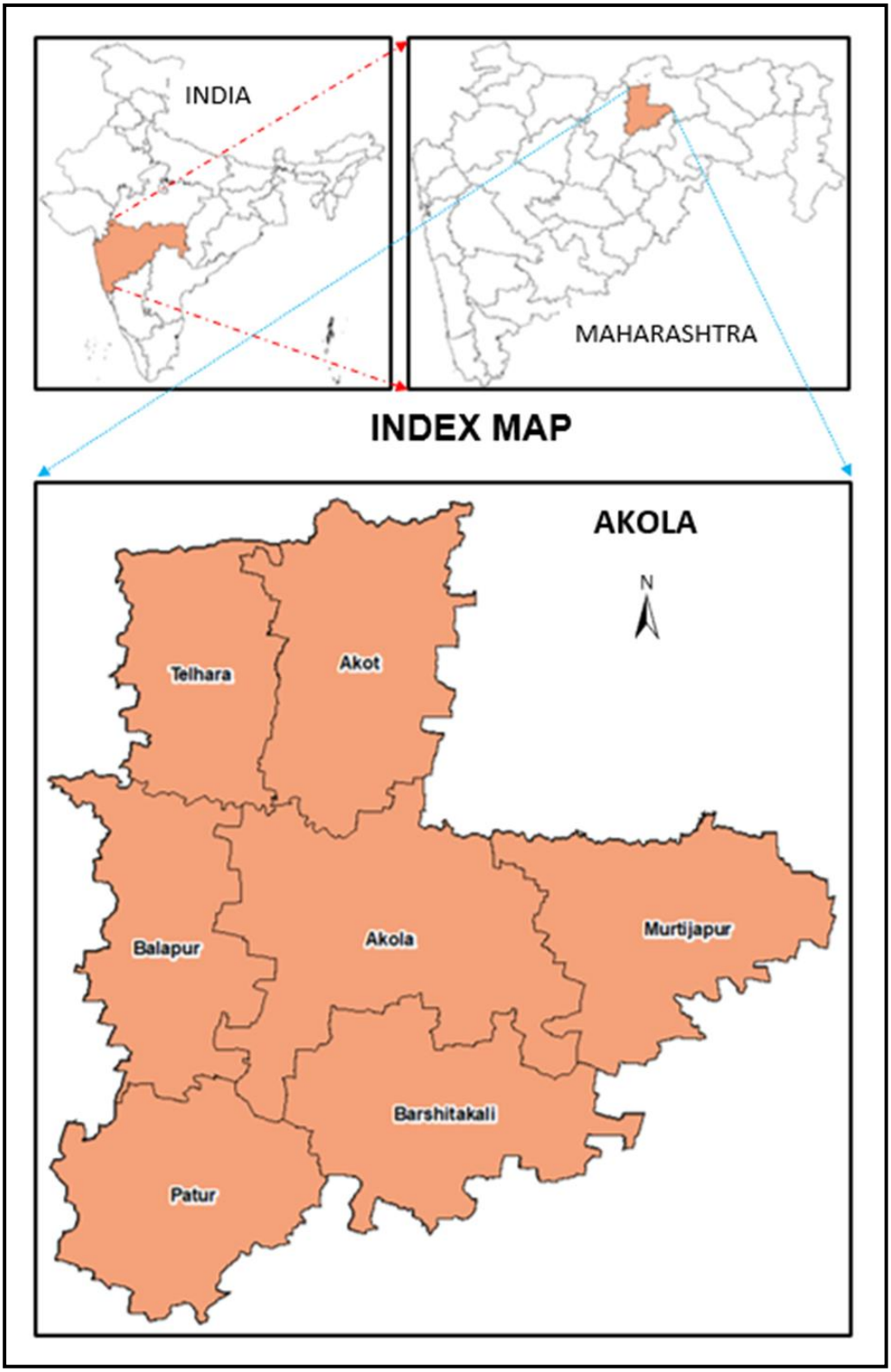

Fig. 1 Location of Study Area

3.2 Remote Sensing Satellite Data

Multi-date, multispectral Sentinel-2A satellite images were downloaded from the USGS Earth Explorer website for a period of six months from November 2021 to April 2022. Satellite images corresponding to two dates were obtained for each month except April. Six months were given to accommodate early or late sowing of chickpea at various places. Proper care is taken to select satellite images with lesser cloud cover and with an almost uniform time gap between the consecutive ones, say, one from the first half and the other from the second half of the month. Table 1 provides information about the satellite data that was used. The European Space Agency developed and maintains the remote sensing satellite Sentinel-2. It contains thirteen spectral bands (443-2190 nm), a 290 km wide swath and spatial resolutions of 10 m (four visible and near-infrared bands), 20 m (six red edge and shortwave infrared bands) and 60 m (three atmospheric correction bands).

The study area is spread across four tiles (T43QFC, T43QFD, T43QGC and T43QGD) and hence, four tile images were obtained corresponding to each date. Resampling of the 11^{th} band was done for changing its spatial resolution to 10 m from the actual 20 m using ERDAS Imagine. Once all the bands were in the same spatial resolution, here 10 m, layer stacking is carried out and composite images for each tile are obtained. All four composites from the same date were merged to form the mosaic. Subsets of each date were prepared using the district boundary as an area of interest (AOI) in the raster subset module of ERDAS Imagine software. The remote sensing and GIS part of the investigation is analyzed using ERDAS Imagine 2014 and ArcGIS version 10.2 software. The 11 subsets obtained altogether during the study are shown in Plate 1 and Plate 2.

Table 1. Multi-date, Multispectral Sentinel 2 A satellite data used for the study

Sr. No	Satellite	Sensor	Tile No.	Date of Pass
1	Sentinel 2 A	MSI	L1C_T43QFC_A024398_20211107T052551 L1C_T43QFD_A024398_20211107T052551 L1C_T43QGC_A024398_20211107T052551 L1C_T43QGD_A024398_20211107T052551	07-11-2021
2	Sentinel 2 A	MSI	L1C_T43QFC_A024684_20211127T053053 L1C_T43QFD_A024684_20211127T053053 L1C_T43QGC_A024684_20211127T053053 L1C_T43QGD_A024684_20211127T053053	27-11-2021
3	Sentinel 2 A	MSI	L1C_T43QFC_A033807_20211212T052221 L1C_T43QFD_A033807_20211212T052221 L1C_T43QGC_A033807_20211212T052221 L1C_T43QGD_A033807_20211212T052221	12-12-2021
4	Sentinel 2 A	MSI	L1C_T43QFC_A025113_20211227T053237 L1C_T43QFD_A025113_20211227T053237 L1C_T43QGC_A025113_20211227T053237 L1C_T43QGD_A025113_20211227T053237	27-12-2021
5	Sentinel 2 A	MSI	L1C_T43QFC_A025256_20220106T053234 L1C_T43QFD_A025256_20220106T053234 L1C_T43QGC_A025256_20220106T053234 L1C_T43QGD_A025256_20220106T053234	06-01-2022
6	Sentinel 2 A	MSI	L1C_T43QFC_A025542_20220126T053113 L1C_T43QFD_A025542_20220126T053113 L1C_T43QGC_A025542_20220126T053113 L1C_T43QGD_A025542_20220126T053113	26-01-2022
7	Sentinel 2 A	MSI	L1C_T43QFC_A034665_20220210T052038 L1C_T43QFD_A034665_20220210T052038 L1C_T43QGC_A034665_20220210T052038 L1C_T43QGD_A034665_20220210T052038	10-02-2022
8	Sentinel 2 A	MSI	L1C_T43QFC_A025971_20220225T052828 L1C_T43QFD_A025971_20220225T052828 L1C_T43QGC_A025971_20220225T052828 L1C_T43QGD_A025971_20220225T052828	25-02-2022
9	Sentinel 2 A	MSI	L1C_T43QFC_A035094_20220312T052910 L1C_T43QFD_A035094_20220312T052910 L1C_T43QGC_A035094_20220312T052910 L1C_T43QGD_A035094_20220312T052910	12-03-2022
10	Sentinel 2 A	MSI	L1C_T43QFC_A026400_20220327T052411 L1C_T43QFD_A026400_20220327T052411 L1C_T43QGC_A026400_20220327T052411 L1C_T43QGD_A026400_20220327T052411	27-03-2022
11	Sentinel 2 A	MSI	L1C_T43QFC_A026543_20220406T052823 L1C_T43QFD_A026543_20220406T052823 L1C_T43QGC_A026543_20220406T052823 L1C_T43QGD_A026543_20220406T052823	06-04-2022

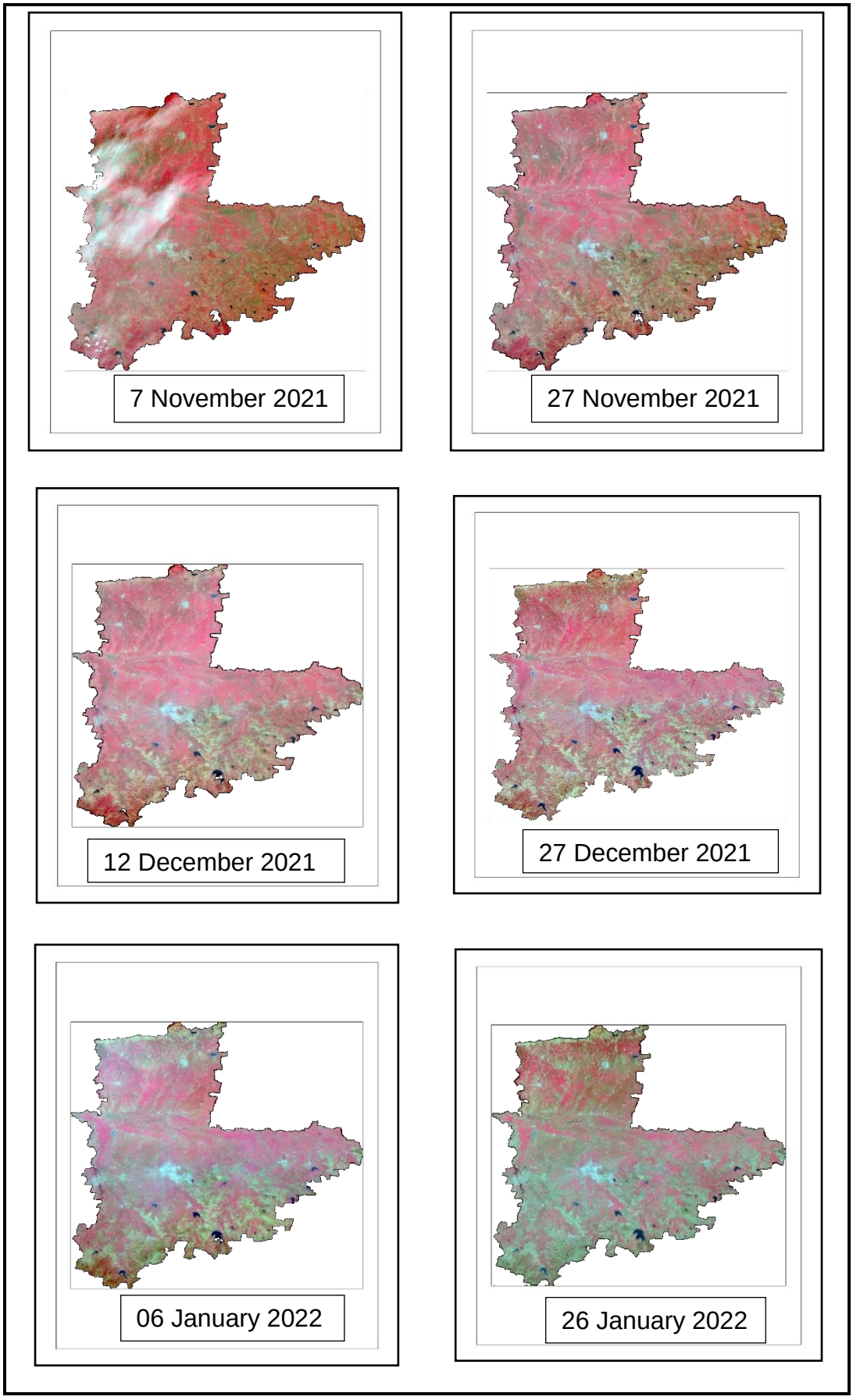

Plate 1. Sentinel 2 A subset images used for the study (November 2021 - January 2022)

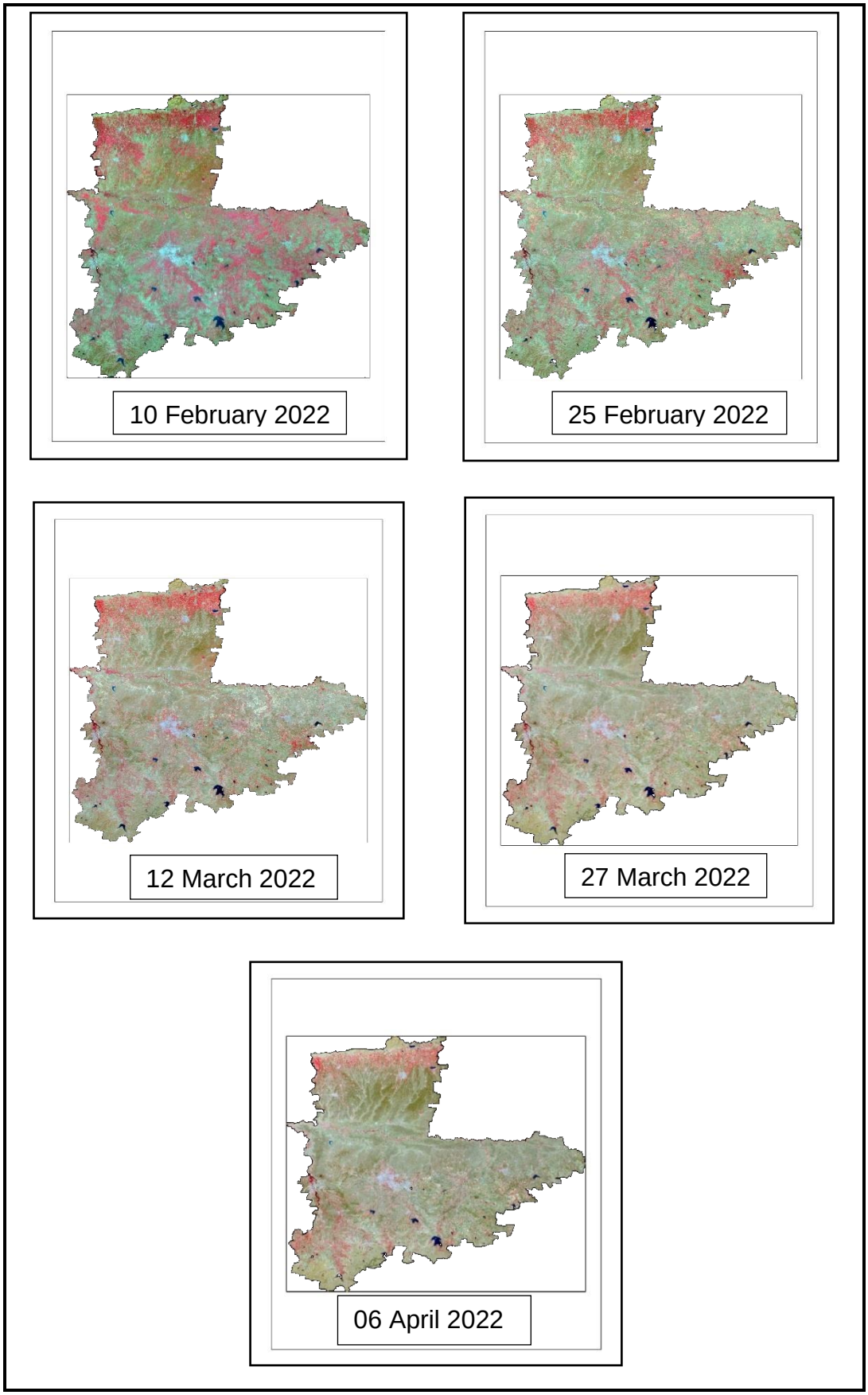

Plate 2. Sentinel 2 A subset images used for the study (February 2022 - April 2022)

3.3 Ancillary Data

The 1:50000 scale topographical maps (toposheets) of the study area from the Survey of India (SOI) were acquired and used as a guide in the current investigation. The Survey of India toposheets were used to digitize the administrative borders of the district under investigation.

The non crop mask (NCM) of the research area was created using information about water bodies, urban sprawl, woods, wastelands and other non-crop features. A vector layer representing basic features in the study area such as roads, railways, dams, canals and so on was prepared.

To examine the outcomes of acreage estimation, the district crop statistics (Area, Production and Yield data) of the Department of Agriculture, Government of Maharashtra released on the website www.maharashtra.gov.in was used as a reference.

3.4 Meteorological data

The Agrometeorological observatory, Dr. PDKV, Akola provided the necessary daily meteorological information, including the maximum air temperature, minimum air temperature, maximum relative humidity, minimum relative humidity, bright sunshine hours, wind speed and rainfall of the station Akola for the period under study (Annexure-I).

3.5 The Digital Analysis

ERDAS Imagine and ArcGIS, the image processing and GIS softwares respectively, were used to conduct the digital analysis. The flowchart shows the methodology used for digital analysis (Fig.2).

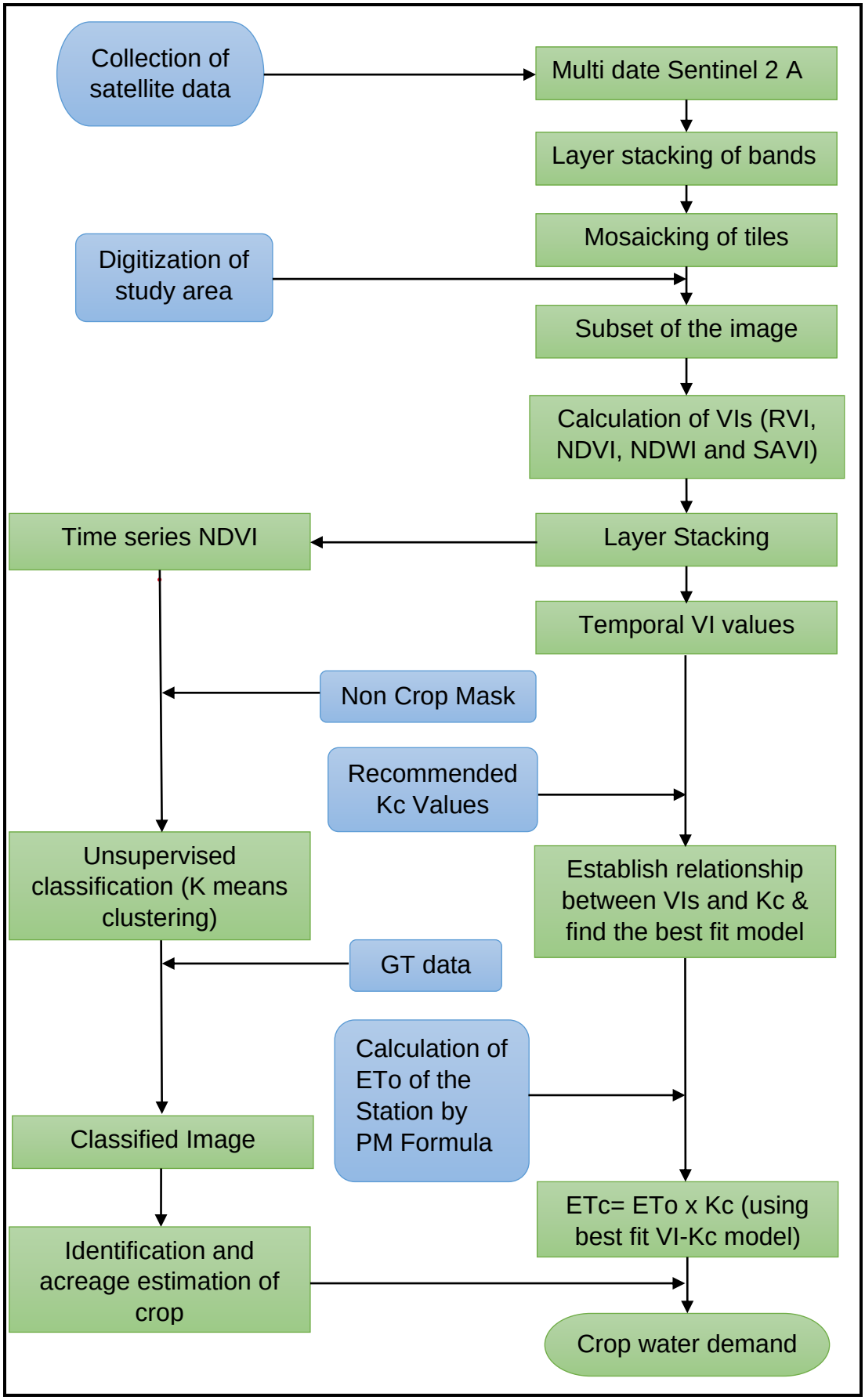

Fig.2 Flowchart for the digital analysis

3.6 Ground Truth Data Collection

Ground truth data collection was synchronized with satellite data acquisition. During the field visit, specific data was gathered, such as the GPS coordinates of the crop area using an android smartphone with the geotagging facility, the sowing date, the crop growth stage, height of the crop, other intercrops, the crop infestation, the soil type, the moisture condition and the crop calendar. The detailed procedure for data collection from ground truth sites is given in this section.

3.6.1 Planning GT

The criteria for the selection of locations of points/stations/areas for the ground truth survey were:

1. Easy accessibility from roads.
2. Dominant cultivation areas of the study crop.
3. The satellite images with identified crop areas of the previous year.

GT plan was prepared using the following information:

1. Location of the crop in previous years
2. Road network map of the study area
3. Google map app/Google Earth website
4. Toposheet

On the base map, locations with a chance of finding standing chickpea crops were noted. Printouts of potential visitation zones were brought to the field to reduce field navigation. Due to the possibility of differing sowing and harvesting dates in various regions, GT was scheduled thrice during the study period – once in the fourth week of December 2021, followed in the second week of January and then finally in the first week of March 2022.

3.6.2 Equipments used for ground truth survey

1. Ground Truth proforma sheets (Fig. 3)
2. Android smartphone with GPS (Fig. 4)

GROUND TRUTH PROFORMA SHEET

			Date:	Site ID
Sl. No.	Name of observed variable/ item		Details/ Value of item	
1	Location	Village		
		Taluka		
		District		
2	GPS readings (in the middle of the field)	Latitude		
		Longitude		
		Elevation		
3	Crop type/ LULC			
4	Growth stage			
5	Field size in meters (approximate), L×W			
6	Date of sowing/ harvest (approx./ expected)			
7	Plant height			
8	Visual soil exposure, Soil moisture condition			
9	Farmer details			

Take photos of:

1. Full view of main crop (from the side)
2. Selected plant to identify growth stage
3. Field showing the surrounding situation
4. Other side of the road

Freehand field sketch (Mark north arrow, site, roads and surrounding details)

Fig. 3 Ground Truth Proforma Sheet

Fig. 4 Android Smartphone with GPS

3.6.3 The Ground Truth work

In the study region, the ground truth work for the chickpea crop was completed between 25 - 27 December 2021, 9 – 11 January and 4 - 6 March 2022. Data from 39 sites were gathered using the following method:

1. The representative sites for the crop under study were found while navigating the fields in the study region. The GPS readings were taken from the center of the field to prevent issues of mixed pixels.
2. Critical observation of the crop stage, the spread of the crop and nearby crops as well as distinguishing characteristics of the area were made.
3. Depending on the availability of the farmer in the field, information on the date of sowing, the variety of crops, the likely date of harvest, the weather etc. were acquired by interviewing the farmer. This information was then entered into the proforma of the GT Sheet.
4. Geo-tagged android smartphones were used to snap pictures at each location, showing:
   a. Overall view of the crop
   b. Growth stage of the crop

c. Root development of the crop

d. Soil moisture condition

e. Adjacent field boundary/opposite side of the crop location

f. Distance/direction boards on the nearby road.

g. Other co-existing crops

Additionally, the digital snapshot automatically included the latitude and longitude of the station.

5. A rough sketch was made on the GT proforma sheet to depict the location, direction and features of the surrounding area. On the sketch made on the GT sheet, the position of the point of observation was indicated.
6. Each GT site was properly indexed and serial numbers of the photos taken at each place were also recorded. The observed sites were assigned sequential ID numbers 1, 2, 3,…… and 39.

   In addition, approximate (rough) polygons were constructed indicating the locations of the crops of interest and the nearby crops.
7. On the GT sheet itself, any particular findings or details on the crops being studied in that particular region were noted. e.g. poor crop conditions in specific patches, late sowing, weed infestation etc.

Table 2 provides information about the GT stations and the main crops grown there.

Table 2. Geographical Locations and crops of the GT sites

Sr. No	Location	Latitude (N)	Longitude (E)	Major Crops
1	Pachmuri	20º 45' 58.4"	77º 00' 12.4"	Chickpea, Red gram
2	Ugwa fata	20º 48' 01.9"	77º 00' 08.2"	Chickpea, Red gram, Flax seed
3	Gandhigram	20º 50' 52.5"	76º 59' 45.6"	Chickpea, Cotton, Red gram
4	Kinkhed	20º 52' 16.9"	77º 01' 22.2"	Chickpea, Cotton, Red gram
5	Aapatapa	20º 50' 29.4"	77º 10' 04.1"	Chickpea, Red gram
6	Valya	20º 41' 19.4"	76º 55' 44.5"	Chickpea, Red gram
7	Kanheri Gawli	20º 40' 21.1"	76º 52' 11.1"	Chickpea, Red gram, Sugarcane
8	Talegaon Bk.	20º 30' 22.1"	21º 6' 53.1936"	Chickpea, Red gram
9	Gramin Patur	20º 28' 38.7"	76º 56' 47.0"	Chickpea, Red gram
10	PDKV campus	20º 41' 58.2"	77º 02' 28.9"	Chickpea, Mustard, Cotton
11	PDKV campus	20º 42' 55.5"	77º 03' 12.6"	Chickpea
12	Dhaga	21º 05' 51.5652"	77º 05' 28.6764"	Chickpea

13	PDKV campus	20º 42' 42.7"	77º 04' 05.7"	Chickpea, Mustard
14	Khaparwadi Bk.	21º 2' 7.0692"	77º 03' 34.2252"	Chickpea
15	PDKV campus	20º 42' 02.3"	77º 03' 53.4"	Chickpea, Cotton, Red gram, Sorghum, Citrus
16	PDKV campus	20º 42' 15.1"	77º 03' 22.4"	Chickpea, Soyabean
17	PDKV campus	20º 42' 07.8"	77º 01' 49.6"	Chickpea, Linseed
18	Kolambi	20º 41' 51.0"	77º 15' 57.3"	Chickpea
19	Borgaon	20º 39' 10.8"	77º 15' 45.4"	Chickpea
20	Digras Bk.	20º 31' 14.5"	76º 51' 9.0"	Chickpea, Citrus, Wheat
21	Vyalla	20º 40' 34.6"	76º 53' 28.1"	Chickpea
22	Ridhora	20º 41' 26.2"	76º 56' 35.9"	Chickpea
23	Wadegaon Hingana	20º 33' 05.8"	76º 51' 09.9"	Chickpea, Red gram, Citrus
24	Hingana	20º 32' 17.3"	76º 51' 34.4"	Chickpea, Red gram, Citrus
25	Degaon	20º 35' 31.8"	76º 50' 38.3"	Chickpea, Maize, Citrus
26	Rel	20º 56' 23.7192"	77º 02' 41.4024"	Chickpea, Red gram
27	Sukali	20º 34' 37.7"	77º 01' 04.6"	Chickpea, Onion
28	Karanja	20º 51' 41.9976"	76º 49' 20.2548"	Chickpea, Red gram
29	Redhawa	20º 33' 42.8"	77º 06' 20.4"	Chickpea, Cotton
30	Atkali	20º 33' 54.0"	77º 04' 45.5"	Chickpea
31	Borgaon	20º 37' 49.9"	77º 15' 55.1"	Chickpea, Wheat
32	Pinjar	20º 33' 9.8"	77º 15' 37.9"	Chickpea, Wheat, Sorghum
33	Donad	20º 33' 42.2"	77º 12' 1.7"	Chickpea
34	Patur Nandapur	20º 35' 54.1"	77º 16' 43.4"	Chickpea
35	Barsitakli	20º 34' 26.4"	77º 3' 10.6"	Chickpea, Red gram, Cotton
36	Sakhari	20º 47' 13.4808"	77º 23' 49.1532"	Chickpea, Wheat, Banana
37	Chikhalgaon	20º 31' 42.4"	76º 58' 1.0"	Chickpea, Red gram
38	Chikhalgaon	20º 33' 58.8"	76º 58' 34.8"	Chickpea, Groundnut, Citrus
39	Khapurkhed	20º 59' 19.7952"	76º 52' 47.1468"	Chickpea, Red gram

3.6.4 GT Data Processing

The following digital processing was done to the GT data that was gathered during fieldwork:

1. Filled up GT survey sheets with sketches, were scanned and put in a specific folder, in.jpeg format. Plate 3 displays an example of a GT proforma sheet with recorded data and a field sketch.
2. The left/right side of the GT point is indicated on the images acquired during the GT survey by the numbers 1L1, 1L2, 1R1, 1R2 etc. To indicate

the left/right side of the GT point, the photos collected during the GT survey were indexed using the GT location points 1L1, 1L2, 1R1, 1R2 etc. Plates 4a, 4b, 4c, 4d and 5 show a few GT images taken during field observations of chickpea and other crops.

3. Creation of the GT point shape file (Point Vector Layer): The GT point shape/vector file was created with the relevant annotations and attribute information corresponding to each location was added (Fig.5). Along with the respective GT sites, the accompanying photos were linked. All the information related to a GT site can be extracted just by a click on that particular GT site location on the point vector layer as Arcmap can support the identification of all the information.

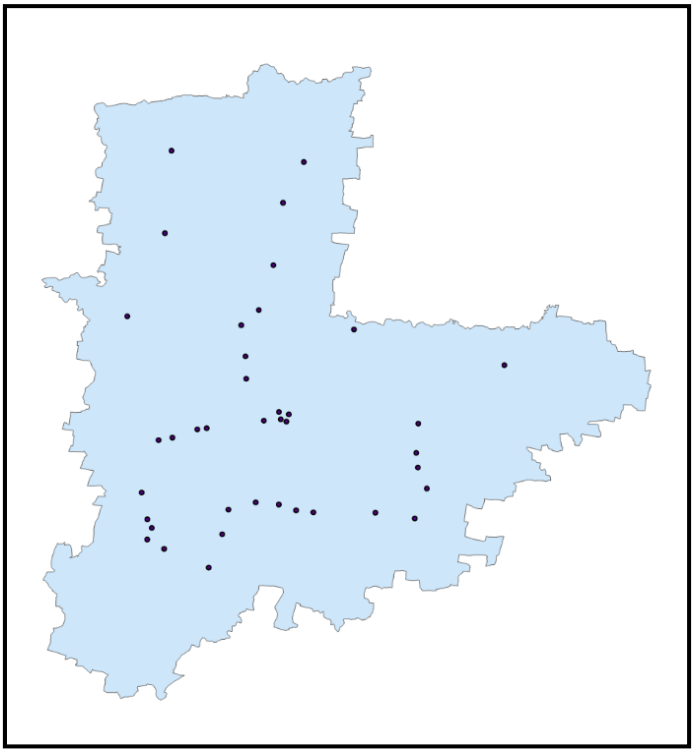

Fig. 5 Point vector map of the study area

GROUND TRUTH PROFORMA SHEET

			Date: 25/12/21 Site ID 3
Sl.No.	Name of observed variable/ item		Details/ Value of item
1	Location	Village	Gandhigram (Sangavi kh)
		Taluka	Akola
		District	Akola
2	GPS readings (in the middle of field)	Latitude	20° 50' 52.5" N
		Longitude	76° 59' 45.6" E
		Elevation	285 m
3	Crop type/ LULC		Chickpea, Cotton, Redgram
4	Growth stage		50% flowering (for chickpea) i.e., at 7th week
5	Field size in meters (approximate), L×W		120 x 180
6	Date of sowing/ harvest (approx./ expected)		5 Oct 2021
7	Plant height		≈32 cm
8	Visual soil exposure, Soil moisture condition		Dry
9	Farmer details		Hari

Take photos of:

1. Full view of main crop (from side)
2. Selected plant to identify growth stage
3. Field showing surrounding situation
4. Other side of road

Free hand field sketch(Mark north arrow,site,roads and surrounding details)

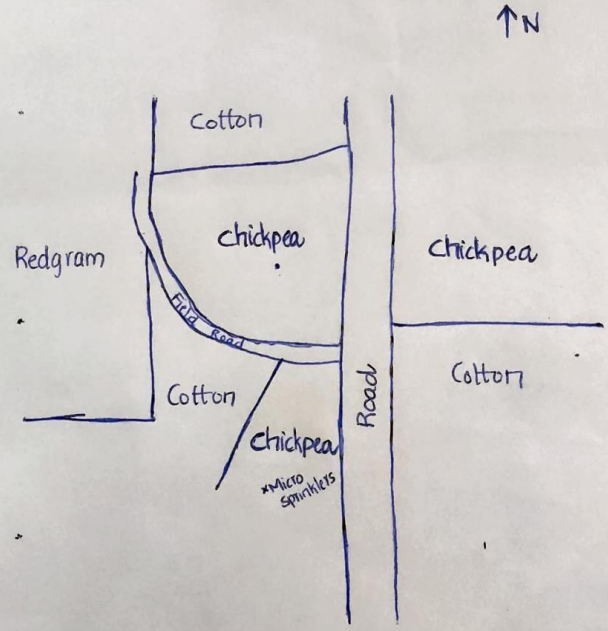

Plate 3. GT proforma sheet with recorded data and field sketch

Plate 4a. Observations of chickpea crop during GT

Plate 4b. Observations of chickpea crop during GT

Plate 4c. Observations of chickpea crop during GT

Plate 4d. Observations of chickpea crop during GT

Plate 5. Observations of other crops during GT

3.7 Determination of age of Chickpea crop

Fields of chickpea were visited for collecting ground truth data. The criteria for choosing the field were completely arbitrary, however, having a farmer in the field was an advantage. By speaking with the farmers, information about the sowing date, the variety and the anticipated harvesting data was gathered. Visual observations were used to determine the age of the crop in the absence of a farmer in the field or the absence of information on the age of the crop. In this instance, stages of chickpea development, depicted in Fig. 6**,** were used to indirectly determine the crop age. The criterion for determining crop age is given in Table 3. This criterion was somewhat modified to fit local situations with the help of experts (Table 4).

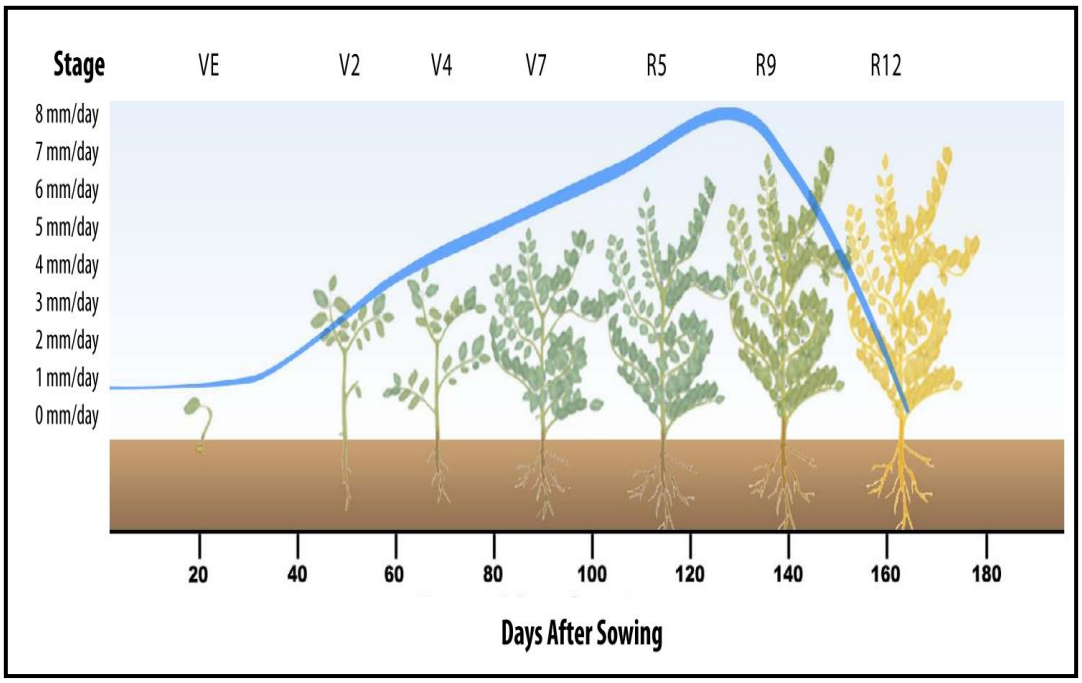

*Source: www.insidecotton.com

Fig.6 Stages of chickpea development

Table 3. Growth stages of chickpea

Sr. No	Stage	Stage length (days)	Description
1	VG	7 to 15	Germination
2	VE	40 to 80	Emergence - The seedling emerges
3	V1		First node - First multifoliate leaf at first node fully unfolded
4	V2		Second node - First multifoliate leaf at second node fully unfolded
5	V3		Third node - First multifoliate leaf at third node fully unfolded
6	V(n)		Nth-node - First multifoliate leaf at nth node fully unfolded
7	R1	20 to 30	Initiation of flowering – One flower bud at any node on the main stem
8	R2		Calyx opening – Bud grows but is still sterile, sepals begin to form
9	R3		Anthesis – Pollination occurs before the bud opens
10	R4		Wings extend – Flower petals extend to form a flower
11	R5		Flower collapses
12	R6	10 to 15	Pod initiation – One pod found in any nod on the main stem
13	R7		Full pod – One fully expanded pod present
14	R8	10 to 15	Beginning seed – One fully expanded pod in which seed cotyledon growth is visible
15	R9		Full seed – One pod on the main stem filled with seeds when fresh
16	R10	20 to 30	Beginning maturity – one pod on the main stem turns to a light golden-yellow color
17	R11		50% of pods are golden yellow
18	R12		90% of pods are golden yellow

*Source: www.grdc.com.au

Table 4. Modification of detection criterion of chickpea crop stage as per local conditions

Sr. No	Stage	Identifying characteristics	Days past sowing (as per reference)	Modified days	Approx. weeks
1	Germination and Emergence	The plumule emerges and the first two leaves are scales. The first true leaf has two or three pairs of leaflets plus a terminal leaflet.	0 – 30	6 - 10	1
2	Early vegetative	Thick strong and woody primary branches grow from buds at the lowest nodes of the plumular shoot as well as the lateral branches of the seedling	31 – 75	11 - 15	2
3	Late vegetative	Secondary branches are formed		16 – 35	3 – 5
4	Initiation of flowering	Flowering commences on the main stem and lower branches.	76 – 105	36 – 40	6
5	50% flowering	At least one open flower developed in 50% of total plants		41 – 50	7
6	Pod initiation	The setting of pods commences on the main stem	106 – 120	51 – 60	8 – 9
7	Early pod development	The rapid growth of pod wall	121 – 135	61 -75	10 – 11
8	Pod development	The seed grows and fills the pod	136 – 148	76 – 90	12 – 13
9	Physiological maturity	90% of the stems and pods become light golden yellow	149 - 165	91 - 120	14 and above

*Information based on personal communication with regional experts

3.8 Reference Image Date

3.8.1 Determination of Reference Image (RI) Date

Eleven satellite images were available for the rabi crop season as shown in Table 1. For results with better accuracy, the ground truth data collection was conducted thrice - during 25 - 27 December 2021, thereafter, during 9 – 11 January and finally, during 4 - 6 March 2022. Twice in the first half and then once in the second half of the ideal crop period. The exact date of the field visit and the date of the satellite overpass were matched for the satellite images of 27 December 2021 and hence chosen as the standard image or reference image (RI). This makes it easier to correlate the exact crop stage with the crop spectral data that was derived from the image.

3.8.2 Criteria for week-wise distribution of data

Once the age of the crop on the reference image date (27 December 2021) has been established, the trial-and-error method was devised as the criteria to determine the age of the crop on other image dates and it is provided in Table 5. The value of the vegetation indices of the chickpea crop was distributed accordingly.

Table 5. Criteria for week-wise distribution of data

Sr. No	Date of image	The time interval between successive images		Cumulative interval from RI date	Interval (Approx. weeks)	Age determined (weeks)
		Days	Weeks			
1	07-11-2021	20	2.9	7.1	3	RI-7
2	27-11-2021	15	2.1	4.2	2	RI-4
3	12-12-2021	15	2.1	2.1	2	RI-2
4	27-12-2021	RI date. Age on this date was determined as per GT data				
5	06-01-2022	10	1.4	1.4	1	RI+1
6	26-01-2022	20	2.9	4.3	3	RI+4
7	10-02-2022	15	2.1	6.4	2	RI+6
8	25-02-2022	15	2.1	8.5	2	RI+8
9	12-03-2022	15	2.1	10.6	2	RI+10
10	27-03-2022	15	2.1	12.7	2	RI+12
11	06-04-2022	10	1.4	14.1	1	RI+13

3.9 Multispectral Vegetation Indices (VIs)

Based on the reflectance of solar radiation hitting the surface, remote sensing satellites create images. The reflectance of solar radiation varies with the characteristics of the surface as well as with the incident spectral bands. Hence, characteristics of the surface can be better determined by combining reflectance data from two or more spectral bands, called index. Spectral vegetation indices or simply, vegetation indices are measurements of greenness of a surface that are made by combining mostly red (RED) and near-infrared (NIR) bands. Green vegetation strongly absorbs the red region of visible light while strongly reflecting invisible NIR wavelengths. Healthy vegetation appears green in color to human eyes as the reflectance is highest for the green region of visible light. Hence, different researchers proposed several vegetation indices as differences, ratios, ratios of differences and linear combinations of spectral data, mainly in R and NIR regions. The leaf area index and vegetation cover are closely related to all of the vegetation indices.

To determine normal growing conditions in a region for a specific time of year, VI values can be averaged across time. The health of the vegetation there about the norm can then be determined by further study. VIs can indicate where vegetation is thriving and where it is struggling over time, as well as changes in vegetation brought on by human activity. In this study, an effort has been made to include significant vegetation indices like Ratio Vegetation Index (RVI), Normalized Difference Vegetation Index (NDVI), Normalized Difference Water Index (NDWI) and Soil Adjusted Vegetation Index (SAVI) to explore their relationship with crop coefficients, and ultimately, determine the irrigation water requirement.

3.9.1 Ratio Vegetation Index (RVI)

The ratio vegetation index (RVI) is the first proposed but is still one of the most commonly used indices. It was given by the formula (Jordan, 1969):

$$RVI = NIR / RED \qquad \text{---------- 2}$$

Where. NIR and RED are the reflectances in near-infrared and red bands respectively.

RVI is close to 1 when NIR and RED bands have similar reflectances. RVI increases with the amount of green vegetation in a pixel. The RVI values are not constrained and can rise well above 1. Typically, RVI values over 30 are considered to be quite high. Bare soil RVI values are often close to 1. During the period of peak growth, RVI is quite sensitive to changes in vegetation. When there is little foliage cover, it is not very sensitive.

3.9.2 Normalized Difference Vegetation Index (NDVI)

Rouse et al. were the first to develop NDVI (1974) which is the most well-known and widely adopted index. It is the ratio between the difference of reflectances in near-infrared (NIR) and red (RED) bands and the sum of reflectances in near-infrared (NIR) and red (RED) bands. It is calculated for each pixel in the image, as:

$$NDVI = \frac{(NIR-RED)}{(NIR+RED)} \qquad \text{---------- 3}$$

The range of the NDVI is +1.0 to -1.0. Rocks and bare soils have positive but lower NDVI values near 0. Owing to their high NIR and low RED reflectances, vegetation yields positive NDVI values. With the increase in green vegetation in a pixel, the NDVI value can rise to 1. On the contrary, negative NDVI values were given by water, clouds and snow due to their higher reflectance in the red band rather than in the NIR bands. NDVI value corresponding to deep water is negative and approaches -1. Barren areas of rock, sand and snow are represented by values near zero, from -0.1 to 0.1. Shrubs and grasslands are represented by low positive values, approximately 0.2 to 0.4 whereas, a high NDVI value (approaching 1) indicates temperate and tropical rainforests. Typically, NDVI ranges from -0.1 to 0.6, from a not-very-green area to a very-green area.

3.9.3 Normalized Difference Water Index (NDWI)

NDWI introduced by Gao (1996), measures moisture content in soil and plants and is calculated analogous to NDVI, as:

$$NDWI = \frac{(NIR-SWIR)}{(NIR+SWIR)} \qquad \text{---------- 4}$$

Where,

NIR = Near infra-red range with wavelengths in the range of 841– 876 nm

SWIR = Part of the spectrum with wavelengths in the range of 1628–1652nm

While calculating NDWI, a short-wave near-infrared (SWIR) wavelength is employed, which is a water absorption band, instead of using the red range in NDVI calculation. It covers a wide range of wavelengths from 1500 to 1750 nm. Since SWIR is not affected by pigments, NDWI is a more reliable correlate for grain yield than NDVI since visible light is susceptible to pigments.

During drought conditions when the vegetation largely depends on water stress, NDWI is considered to be better than NDVI, as the vegetative characteristics majorly depend on water stress.

NDWI is dimensionless and based on the hardwood content and the kind of vegetation and cover, it ranges from -1 to +1. High vegetation water content and vegetation fraction cover are correlated with high NDWI readings. Low vegetation water content and low vegetation fraction cover are correlated with low NDWI readings. When there is water stress, NDWI will drop. Hence, adequate water is represented by high NDWI values whereas water stress is indicated by lower NDWI values.

3.9.4 Soil Adjusted Vegetation Index (SAVI)

Huete(1988) proposed the Soil Adjusted Vegetation Index (SAVI) as:

$$SAVI = \frac{(NIR-RED)}{(NIR+RED+L)}(1+L) \quad \text{---------- 5}$$

Where,

NIR = Near Infra-red band reflectance

RED = Red band reflectance

L = Soil normalization factor. Usually, taken as 0.5.

The soil normalization factor, L was introduced to minimize the effect of soil brightness and to produce vegetation isolines independent of the soil background. Depending on the vegetation density, the L factor varies from 0 to infinity. When, L= 0, SAVI is equal to NDVI. Huete (1988) proposed there might be two or three optimal adjustment factor (L) depending on the canopy density (L = 0.25 for higher vegetation density; L = 0.5 for intermediate vegetation; L = 1 for low vegetation).

SAVI is a better index than NDVI for intermediate canopies as it minimizes spatial and temporal soil differences due to wetting (Qi et al., 1993). Hence, SAVI is most suitable for partial canopies.

3.10 Processing of Satellite Data for extracting Vegetation Indices

Multispectral vegetation indices (VIs) namely Ratio Vegetation Index (RVI), Normalized Difference Vegetation Index (NDVI), Normalized Difference Water Index (NDWI) and Soil Adjusted Vegetation Index (SAVI) were extracted from multidate subset images of all the 11 dates of satellite pass given in Table 1. Using the Model Builder Tool in ERDAS Imagine software, separate images for every vegetation index were generated corresponding to each day of the satellite overpass. Using the Raster menu in the ERDAS Imagine software, stacking of these images of each vegetation indices was done.

3.11 Generating Spectral Vegetation Indices Profile for Chickpea Crop

The crop vector layer representing the fields visited during the ground truth survey was processed in the ERDAS Imagine environment along with the layer stack images for the various vegetation indices viz. RVI, NDVI, NDWI and SAVI. The temporal values of the vegetation indices for each GT site corresponding to the respective image dates were compiled.

Each crop site was categorized based on the age of the crop in weeks on the reference image date and then, the corresponding temporal values of each VI were distributed accordingly. For each week, corresponding VI values were averaged out. The weeks past sowing along the abscissa and corresponding average VI values on the ordinate were plotted to derive the overall trend of multi-temporal VI for the chickpea crop. The spectral VI

profiles of chickpea crops are shown by the trend of VIs with increasing crop age.

3.12 Identification and Acreage Estimation of Chickpea Crop

The classification of multi-date remote sensing data was done using a hybrid technique based on K-means clustering and visual classification. The pixels are grouped into several clusters based on the similarity in their spectral properties using the K-means clustering method of unsupervised classification and then followed by a supervised classification in which spectrally similar classes are discriminated using visual vector analysis. The process is outlined in a flowchart, as seen in Fig. 7 and the details are as given below:

3.12.1 Preparation of Reference Temporal Spectral Profiles (RTSP)

Gathering pure chickpea locations was the emphasis of the ground truth survey. However, in addition to this crop, signatures for other co-existing crops like wheat, onion etc. were also gathered. On the images, the spatial coordinates of GT sites were transferred. Crop polygons (training sites) were marked on the image with an acquisition date close to the date of the field observation in accordance with the information gathered during field trips. NDVI image for each satellite image acquisition date was created and a corresponding layer stack was formed. For the training crop polygons (training windows), multidate average NDVI values were derived. The general signature of the crop is obtained by the NDVI values on the different acquisition dates plotted against the ideal crop period i.e. November to March. Signatures of the crop were developed accordingly. The reference temporal spectral profile (RTSP) of chickpea are provided by these signatures and thus aids in crop identification.

3.12.2 Data load reduction of multi-date RS dataset

The non crop mask (NCM) was created from the information that was already available about built-up areas, slopes, forests, wastelands etc. All pixels that belonged to non-agricultural areas were masked off in order to limit the number of data pixels that needed to be subjected to K- means clustering. NCM image assigned the value 1 for pixels belonging to agricultural areas whereas 0 for non-agricultural areas, forests and perennials.

3.12.3 K- means clustering

NDVI stack dataset after non crop masking was used for unsupervised classification. K-means clustering method of unsupervised classification was performed using ERDAS Imagine software. A total of 50 classes were chosen at a convergence threshold of 0.999 and with 30 iterations. A classified raster image consisting of 50 classes was generated by the end of K-means clustering. A signature file with the signatures of all 50 classes was also obtained. The Temporal Spectral Profile (TSPs) for each class is generated from the signature file. The available RTSP of the chickpea crop and the extensive local knowledge of the analyst were then used to visually compare each of these TSPs from the 50 classes.

TSPs of some clusters weren't assigned to the RTSP of chickpea. These clusters were classified as "Mix crop." A few cluster classes in the classified image remained "unclassified" due to a lack of RTSPs. The final output of classification was stored separately.

3.12.4 Supervised classification

The GT point layer was overlaid on the cluster file and multi-date subsets. The visual interpretation was performed for unclassified pixels and/or pixels that could not be assigned to any crop class with confidence using available RTSPs. Visual analysis was used to assess and label crop polygons.

3.12.5 Integration of classified images/vector and acreage estimation

The final classified image was generated by integrating the results of both the supervised and unsupervised classification and crop recoding. The area corresponding to each class can be added to the attribute table by the Table menu option in the ERDAS Imagine Software. The area coverage of the chickpea crop is obtained from the attribute table of recoded image. The estimated total acreage of the rabi chickpea crop of the study area was thus determined.

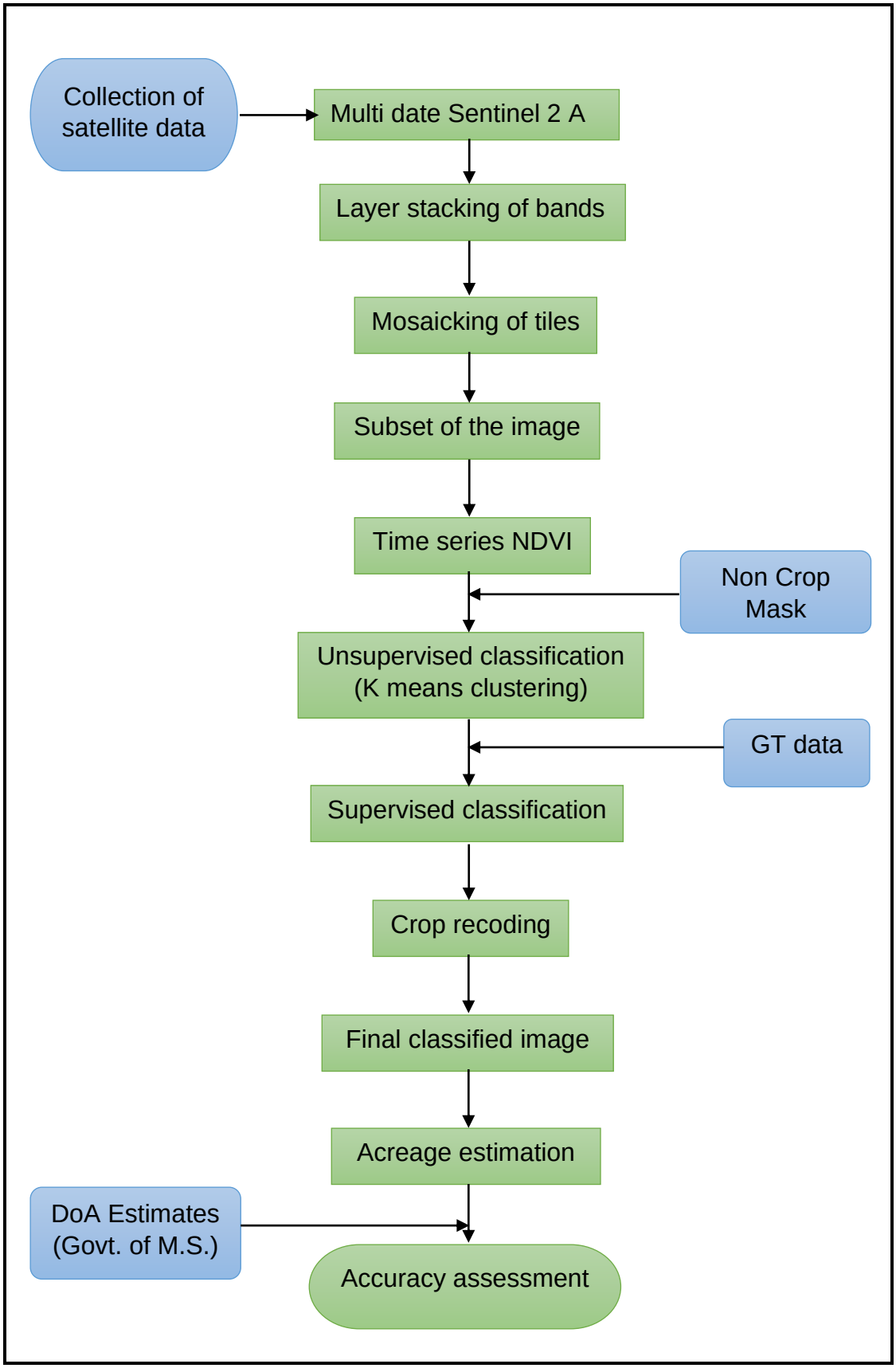

Fig. 7 Flowchart for acreage estimation

3.13 Establishing relation between vegetation indices (VIs) and crop coefficients (Kc)

The different vegetation indices (VIs) viz. RVI, NDVI, NDWI and SAVI were taken into consideration for establishing their link with the crop coefficients of chickpea. GT vector file was laid over each VI layer stack in the viewer of ERDAS Imagine software. Temporal VI values of each site were obtained one by one and these values were exported to a Microsoft Excel Sheet. According to the age of the crop on the reference image date, these values of each VI were then allocated in the corresponding week number. The average values for each week of each VI for the chickpea crop were then calculated.

To establish the relationship of crop coefficients with estimated VIs and thus to model the VI-Kc correlations, crop coefficients suggested by MPKV Rahuri for chickpea (Table 6) were employed. The recommendation of crop coefficients (Kc) was made based on the three different approaches to determining reference evapotranspiration. However, due to the worldwide acceptance of the approach, crop coefficient values derived from the FAO Penman-Monteith method were adopted for further investigation.

The scattered diagram was obtained by plotting the average weekly values of the vegetative indices for chickpea, including RVI, NDVI, NDWI and SAVI, against the corresponding recommended weekly crop coefficients (Kc). The trend lines and corresponding R^2 values were obtained. Different orders of both linear and polynomial equations were tested. However, the relevance of the linear equations was greater. Each relation was subjected to simple linear regression analysis. The correlations between suggested crop coefficients (Kc) and vegetative indices (VIs) were then examined and the best-fit models were found and assessed.

VIs and Kc relationship is derived using simple linear regression analysis that can be utilized to analyze a satellite image. A degree of fit is determined by the coefficient of determination (R^2), which is obtained from simple regression analysis (R^2=0 being no fit and R^2=1 being ideal fit). Another indicator of how well the two independent data sets match is the root-mean-square error (RMSE). This analysis also shows bias and variance from

the 1:1 line. The models were assessed using the R^2 and root-mean-square error (RMSE), as well as frequently used parameters like percent deviation (PD) and the Willmott index of agreement (D).

Table 6. Recommended chickpea crop coefficients

Week after sowing	Kc for chickpea based on the method of calculating reference ET		
	Penman-Monteith	Pan Evaporation	Hargreaves-Samani
1	0.85	0.77	0.83
2	0.84	0.75	0.79
3	0.88	0.79	0.80
4	0.95	0.86	0.83
5	1.04	0.95	0.89
6	1.12	1.04	0.95
7	1.18	1.11	1.01
8	1.21	1.15	1.05
9	1.20	1.15	1.06
10	1.15	1.10	1.04
11	1.05	1.01	0.97
12	0.91	0.88	0.86
13	0.75	0.72	0.72
14	0.57	0.53	0.55
15	0.38	0.35	0.37
16	0.23	0.19	0.21
17	0.12	0.09	0.11

*Source: MPKV, Rahui (2012)

3.14 Estimation of Reference Evapotranspiration (ET_o)

For determining reference evapotranspiration, the FAO Penman-Monteith method using weather information like radiation, air temperature, air humidity and wind speed is advised as the only accepted method. It was derived for a hypothetical, 0.12 m uniform height, actively growing and adequately watered crop with a surface resistance of 70 dsm-1 and an albedo of 0.23 (FAO 56 PM; Allen *et al*.1998).

FAO Penman-Monteith equation is given as:

$$ETo = \frac{0.408\Delta(R_n - G) + \gamma \frac{900}{T+273} u_2 (e_s - e_a)}{\Delta + \gamma(1 + 0.34\, u_2)} \quad \text{---------- 6}$$

Where,

ETo	=	Reference Evapotranspiration (mm day^{-1})
Δ	=	Slope of saturation vapour curve (kPa $^0C^{-1}$)
R_n	=	Net radiation at the crop surface (MJ m^{-2} day^{-1})
G	=	Soil heat flux density (MJ m^{-2} day^{-1})
γ	=	Psychometric constant (kPa $^0C^{-1}$)
T	=	Mean air temperature (^0C)
u_2	=	Wind speed at 2.0 m height (ms^{-1})
e_s	=	Saturation vapour pressure (kPa)
e_a	=	Actual vapour pressure (kPa)
$(e_s - e_a)$	=	Saturation vapour pressure deficit (kPa)

The calculation of the reference evapotranspiration (ETo) was done using this equation. According to the procedures outlined in FAO-56, all the associated terms in the equation were assessed based on their empirical relationship with the climatological data of the station.

Microsoft Excel was used to perform precise ETo calculations by entering the factors such as the maximum temperature, minimum temperature, relative humidity and wind speed. The study used weekly values of the ETo.

3.15 Utilization of the developed relationship for real-time irrigation water management

The best VI versus Kc correlation was discovered using the aforementioned methods. By using the best-performing VI-Kc relation for chickpea, the weekly crop coefficients for the crop were calculated from the estimated VI data. The weekly reference evapotranspiration (ETo) of the selected station in the research area was calculated for each week of the rabi season 2021–22, which corresponds to the chickpea crop period. In the district under study, the weekly crop evapotranspiration (ETc) of chickpea was

calculated by multiplying the weekly ETo by Kc. The total evapotranspiration of the crop is calculated as the sum of ETc for all weeks of the growing season. The area under crop assessed by remote sensing is multiplied by the associated crop evapotranspiration values to determine the water demand/water extraction amount. The water requirements for all the weeks of the growth season were added up to determine the overall water need for chickpea in the study area.

CHAPTER IV

RESULTS AND DISCUSSION

The present investigation has been undertaken to comprehend the behavior of multispectral vegetation indices derived from remote sensing satellite images throughout the growth period of the chickpea crop. GIS and remote sensing techniques were employed for crop identification and acreage estimation. The relationship between vegetation indices (VIs) and crop coefficients (Kc) of chickpea was investigated. After the models describing the relationship between vegetation indices and crop coefficients were established, the best-performing model was selected. This best fit model was used to predict the weekly and total water requirement of the chickpea crop and ultimately its weekly and total water demand for the study area. This chapter goes into more detail about the relevant results.

4.1 Generation of layer stack images of vegetation indices

The Sentinel 2A satellite data of the research area for 11 dates during the crop growing season of the chickpea were obtained. Composite images with all the required bands were prepared for each tile after resampling the 11^{th} band. Composites of the same date were merged to form the mosaic. The methodology described in 3.2 was used to obtain a subset of the study area from each mosaic. These images were processed using the ERDAS Imagine software by running models for the four vegetation indices under study, namely Ratio Vegetation Index (RVI), Normalized Difference Vegetation Index (NDVI), Normalized Difference Water Index (NDWI), and Soil Adjusted Vegetation Index (SAVI), for each of the eleven dates of the satellite overpass. A total of 44 images were generated for all four vegetation indices. A layer stack of each vegetation index was obtained by stacking all the corresponding images in chronological order. The four stack layer images of the vegetation indices namely, RVI stack, NDVI stack, NDWI stack, and SAVI stack were obtained and are displayed in Plate 6.

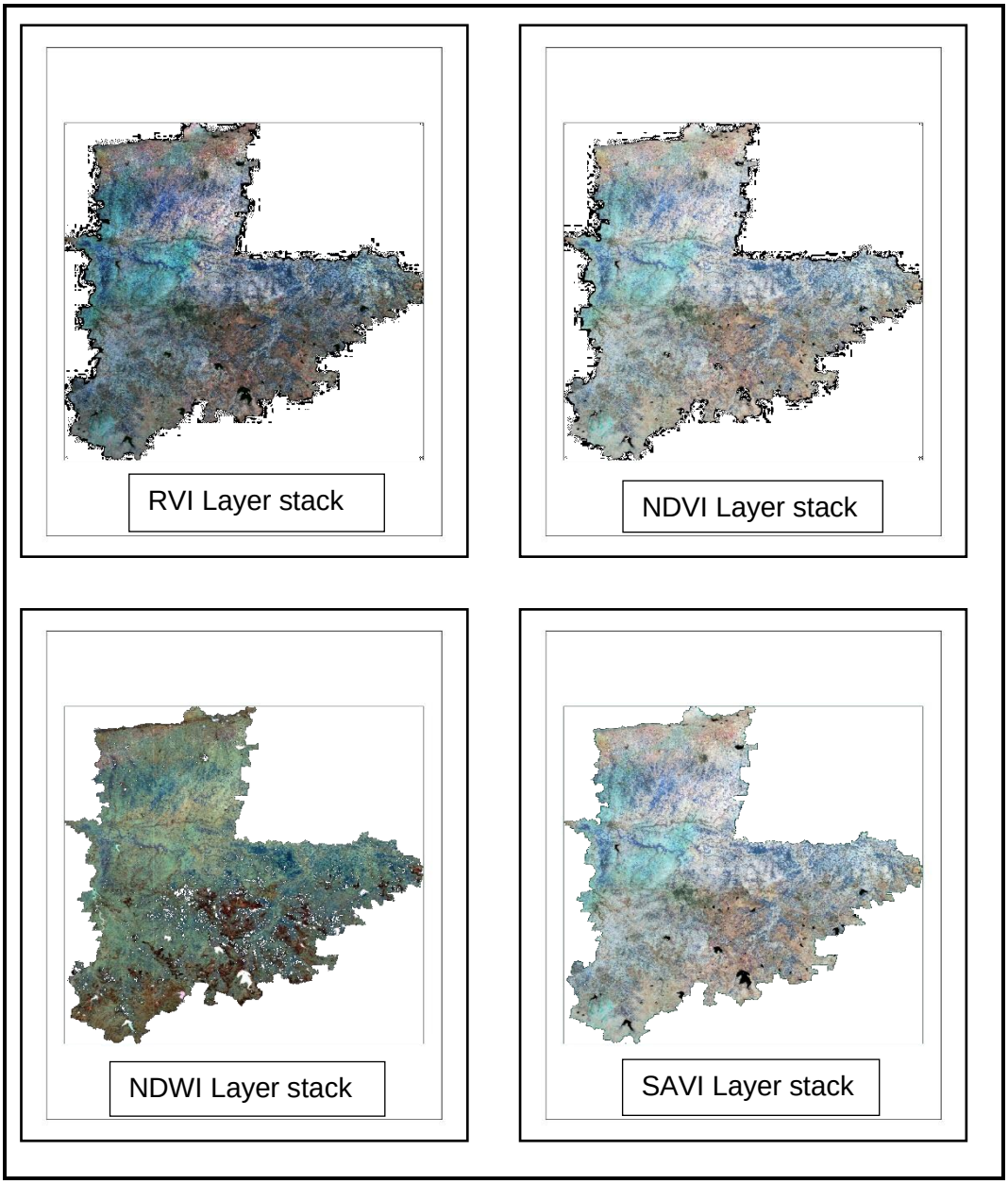

Plate 6. Layer stack images of vegetation indices

4.2 Extraction of Vegetation Indices for pure crop pixels

Digitization of fields visited during the ground truth survey was done. The value of the site-specific vegetation indices was obtained by superimposing the GT vector layer on the VI stack layers. The temporal values of all four vegetation indices for pure crop sites were obtained during the period of satellite data acquisition. These site-specific multi-date values of the vegetation indices were used for further study.

4.3 Spectral profile of Chickpea crop

The age of the chickpea crop was determined using the information gathered from the farmers during the ground truth survey like sowing date, variety, and expected harvesting date. The criterion used to approximate the age of the chickpea crop is elaborated in section 3.7 and the exact age of the chickpea crop was ascertained using modified criteria as per discussion with the regional experts to fit the local conditions is comprehended in Table 7. The site-specific VI values on each day of the satellite overpass were distributed corresponding to the determined age of the crop in weeks by referring to age as on ground truth date and reference image date. The weekly values of each vegetation index viz. RVI, NDVI, NDWI, and SAVI of all the GT sites are displayed in Tables 8, 9, 10 and 11 respectively. The values of different sites for each week were averaged to obtain a mean VI value corresponding to each week and are shown in Table 12. As the condition of the chickpea crop varied at each site, the weekly mean VI value served as the representation of the mean of all those crop conditions corresponding to the same week irrespective of changes in vegetation and soil.

Table 7. Age of chickpea crop on reference image date for all the GT sites

GT site ID	Major stage	Stage No.	Observed characteristics	Age (in weeks) on the date of	
				GT	RI
1	Initiation of flowering	4	Flowering commences on the main stem and lower branches.	6	6
2	50% flowering	5	At least one open flower developed in 50% of total plants	7	7
3	50% flowering	5	At least one open flower developed in 50% of total plants	7	7
4	Pod initiation	6	The setting of pods commences on the main stem	8	8
5	Late vegetative	3	Secondary branches are formed	4	4
6	Pod initiation	6	The setting of pods commences on the main stem	8	8
7	Late vegetative	3	Secondary branches are formed	4	4
8	Initiation of flowering	4	Flowering commences on the main stem and lower branches.	6	6
9	Initiation of flowering	4	Flowering commences on the main stem and lower branches.	6	6
10	Pod initiation	6	The setting of pods commences on the main stem	8	6

11	Early vegetative	2	Thick strong and woody primary branches grow from buds at the lowest nodes of the plumular shoot as well as the lateral branches of the seedling	2	0
12	Late vegetative	3	Secondary branches are formed	4	2
13	Late vegetative	3	Secondary branches are formed	5	3
14	Late vegetative	3	Secondary branches are formed	4	2
15	Initiation of flowering	4	Flowering commences on the main stem and lower branches.	6	4
16	Late vegetative	3	Secondary branches are formed	4	2
17	Late vegetative	3	Secondary branches are formed	4	2
18	Physiological maturity	9	90% of the stems and pods become light golden yellow	15	6
19	Physiological maturity	9	90% of the stems and pods become light golden yellow	15	6
20	Physiological maturity	9	90% of the stems and pods become light golden yellow	14	5
21	Physiological maturity	9	90% of the stems and pods become light golden yellow	15	6
22	Physiological maturity	9	90% of the stems and pods become light golden yellow	14	5
23	Late vegetative	3	Secondary branches are formed	5	5
24	Initiation of flowering	4	Flowering commences on the main stem and lower branches.	6	6
25	Physiological maturity	9	90% of the stems and pods become light golden yellow	14	5
26	Late vegetative	3	Secondary branches are formed	4	4
27	Late vegetative	3	Secondary branches are formed	5	5
28	Initiation of flowering	4	Flowering commences on the main stem and lower branches.	6	6
29	Physiological maturity	9	90% of the stems and pods become light golden yellow	14	5
30	Late vegetative	3	Secondary branches are formed	4	4
31	Physiological maturity	9	90% of the stems and pods become light golden yellow	14	5
32	Physiological maturity	9	90% of the stems and pods become light golden yellow	15	6
33	Physiological maturity	9	90% of the stems and pods become light golden yellow	15	6
34	Physiological maturity	9	90% of the stems and pods become light golden yellow	14	5
35	Late vegetative	3	Secondary branches are formed	3	3
36	Physiological maturity	9	90% of the stems and pods become light golden yellow	14	5
37	Late vegetative	3	Secondary branches are formed	5	5
38	Physiological maturity	9	90% of the stems and pods become light golden yellow	15	6
39	Physiological maturity	9	90% of the stems and pods become light golden yellow	14	5

Table 8. Weekly RVI values of chickpea

Weeks past sowing	GROUND TRUTH POINTS																			
	1	2	3	4	5	6	7	8	9	10	11	12	13	14	15	16	17	18	19	20
1				1.588		1.423			3.207		1.408		2.11				1.454		1.452	
2	1.367				1.552		1.37	3.789		1.395		1.964		1.578	1.679			1.356		4.338
3		1.773	1.784			1.533			2.671		1.81		2.037			1.631	1.871		1.666	
4	1.659			2.097	2.317		1.717	2.647		1.813		2.029		1.401	1.574			1.753		3.101
5		1.928	2.19		2.483	1.516			2.55		2.79	1.442	1.732	1.186			2.7		2.007	
6	2.366			2.649		1.407	2.559	2.407	2.255	2.86	2.877		1.594		1.624	2.455	2.366	1.896	1.836	2.94
7	2.244	2.71	3.481				2.495	1.808		2.566					1.257			1.781		1.973
8		2.441	3.074	3.446	2.771							1.441		1.383		2.424				
9				2.384		1.646			1.843		2.712		1.401				2.138		2.018	
10	2.254				2.381		2.592	1.576		2.346		1.299		1.32	1.512			2.144		1.709
11		1.72	2.58			1.368			1.743		2.282		1.192			1.996	1.392		1.858	
12	1.788			1.651	1.443		2.058	1.451		1.596		1.347		1.289	1.385			1.656		1.5
13		1.308	1.907			1.251			2.031		1.863		1.314				1.079		1.886	
14	1.278			1.241	1.159		1.349	1.378		1.19		1.218		1.138	1.265	1.466		1.232		1.433
15		1.223	1.282			1.302			1.847		1.18		1.383				1.125		1.294	
16	1.255			1.2	1.198		1.266	1.392		1.212		1.298		1.215	1.302	1.505		1.222		1.336
17		1.165	1.056		1.015	1.182			1.796		1.055	1.145	1.307	1.062			1.047		1.149	
18	1.115			1.106		1.172	1.142	1.322	1.869	1.156	1.155		1.347		1.199	1.306	1.12	1.108	1.193	1.235

Table 8. contd.

Weeks past sowing	GROUND TRUTH POINTS																			Mean RVI
	21	22	23	24	25	26	27	28	29	30	31	32	33	34	35	36	37	38	39	
1	1.613	1.428		2.326	2.004			1.992	1.772				1.387				1.474		1.226	1.742
2			1.35			2.494	1.402			1.638	1.358	1.544		1.349	1.396	1.629		1.593		1.807
3	1.732	2.138		2.372	1.715			1.839	1.619			1.589	1.618	1.488		1.665	1.658	1.904		1.815
4		1.831	1.481			1.841	1.649			1.558	1.828				1.742		1.656		1.294	1.849
5	1.735		1.861	2.939	1.39			1.967	1.374				2.194		1.832					1.990
6	1.944			2.557	1.62	2.049	2.52	1.85	1.4	1.564	2.486	1.75	2.01	1.52		1.933		1.483	1.214	2.066
7		2.085				1.47	2.181			1.158	2.242						1.641			2.072
8			2.132									1.914		1.927	1.997	2.199		1.977	1.484	2.187
9	2.092	2.189		2.484	1.457			1.941	1.522				2.234				1.711			1.985
10			1.812			1.511	2.561			1.383	2.924	1.598		1.883	2.015	1.665		1.941	1.353	1.894
11	2.082	2.204		2.06	1.263			1.668	1.45				1.693				1.542			1.770
12			1.642			1.406	2.209			1.289	2.69	1.306		1.507	2.232	1.248		1.602	1.187	1.613
13	2.123	1.318		2.25	1.375			1.506	1.477				1.085				1.114		1.009	1.523
14			1.411			1.311	2.153			1.216	1.665	1.165		1.306	1.552	1.149		1.441		1.351
15	1.516	1.208		2.114	1.345			1.347	1.362			1.144	1.123	1.161		1.146	1.187	1.265		1.328
16		1.23	1.356			1.368	1.27			1.252	1.235				1.445		1.263			1.291
17	1.161		1.172	1.874	1.278			1.178	1.24				1.016		1.209					1.216
18	1.169			1.8	1.281	1.297	1.169	1.249	1.204	1.185	1.096		1.07							1.243

Table 9. Weekly NDVI values of chickpea

Weeks past sowing	GROUND TRUTH POINTS																			
	1	2	3	4	5	6	7	8	9	10	11	12	13	14	15	16	17	18	19	20
1				0.238		0.188			0.522		0.183		0.361				0.197		0.197	
2	0.181				0.24		0.182	0.597		0.19		0.346		0.248	0.276			0.177		0.639
3		0.259	0.262			0.187			0.444		0.269		0.325			0.421	0.285		0.229	
4	0.236			0.345	0.389		0.252	0.445		0.278		0.331		0.152	0.21			0.262		0.507
5		0.309	0.362		0.412	0.203			0.422		0.457	0.181	0.262	0.091			0.444		0.326	
6	0.406			0.452		0.169	0.438	0.413	0.386	0.482	0.484		0.229		0.238	0.38	0.406	0.309	0.295	0.492
7	0.384	0.457	0.545				0.426	0.295		0.437					0.136			0.289		0.332
8		0.431	0.531	0.576	0.488							0.156		0.132		0.406				
9				0.409		0.244			0.296		0.461		0.167				0.363		0.337	
10	0.39				0.415		0.452	0.213		0.408		0.109		0.118	0.191			0.367		0.255
11		0.268	0.431			0.168			0.273		0.384		0.108			0.16	0.176		0.3	
12	0.285			0.245	0.176		0.352	0.179		0.228		0.14		0.117	0.155			0.247		0.196
13		0.14	0.307			0.12			0.333		0.297		0.142				0.052		0.302	
14	0.122			0.107	0.074		0.149	0.159		0.087		0.098		0.065	0.117	0.177		0.104		0.178
15		0.1	0.123			0.131			0.298		0.083		0.161				0.059		0.128	
16	0.109			0.085	0.084		0.113	0.163		0.09		0.126		0.091	0.128	0.159		0.094		0.141
17		0.081	0.036		0.017	0.088			0.277		0.035	0.073	0.134	0.038			0.031		0.075	
18	0.054			0.05		0.079	0.066	0.138	0.303	0.072	0.072		0.148		0.09	0.104	0.056	0.051	0.088	0.105

Table 9. contd.

Weeks past sowing	GROUND TRUTH POINTS																			Mean NDVI
	21	22	23	24	25	26	27	28	29	30	31	32	33	34	35	36	37	38	39	
1	0.245	0.189		0.401	0.339			0.336	0.286				0.176				0.204		0.119	0.261
2			0.175			0.445	0.193			0.265	0.178	0.237		0.174	0.19	0.262		0.252		0.272
3	0.248	0.347		0.394	0.243			0.277	0.215			0.205	0.214	0.172		0.228	0.226	0.293		0.273
4		0.283	0.18			0.286	0.233			0.205	0.282				0.259		0.235		0.112	0.274
5	0.263		0.293	0.476	0.164			0.317	0.159				0.363		0.287					0.305
6	0.321			0.438	0.237	0.344	0.432	0.298	0.167	0.22	0.426	0.273	0.336	0.206		0.318		0.194	0.097	0.330
7		0.355				0.206	0.373			0.1	0.384						0.254			0.332
8			0.366									0.311		0.315	0.333	0.381		0.328	0.173	0.352
9	0.353	0.373		0.426	0.186			0.32	0.207				0.382				0.262			0.319
10			0.285			0.191	0.447			0.144	0.503	0.221		0.304	0.337	0.242		0.319	0.132	0.287
11	0.347	0.37		0.343	0.133			0.255	0.194				0.261				0.221			0.259
12			0.242			0.162	0.385			0.117	0.47	0.123		0.198	0.39	0.099		0.23	0.072	0.218
13	0.352	0.143		0.375	0.163			0.204	0.195				0.054				0.067		0.021	0.193
14			0.17			0.135	0.366			0.097	0.249	0.076		0.133	0.216	0.069		0.181		0.142
15	0.205	0.094		0.358	0.147			0.148	0.153			0.067	0.058	0.075		0.068	0.085	0.117		0.133
16		0.098	0.149			0.154	0.115			0.107	0.1				0.182		0.112			0.120
17	0.079		0.084	0.296	0.124			0.086	0.11				0.017		0.099					0.094
18	0.078			0.286	0.123	0.129	0.078	0.111	0.093	0.085	0.046		0.034							0.102

Table 10. Weekly NDWI values of chickpea

Weeks past sowing	GROUND TRUTH POINTS																			
	1	2	3	4	5	6	7	8	9	10	11	12	13	14	15	16	17	18	19	20
1				0.128		0.035			0.254		0.113		0.116				0.051		0.055	
2	0.057				0.154		0.057	0.338		0.04		0.122		0.046	0.064			0.02		0.312
3		0.134	0.12			0.065			0.235		0.174		0.116			0.06	0.12		0.114	
4	0.126			0.146	0.224		0.127	0.226		0.141		0.125		-0.048	0.033			0.105		0.251
5		0.149	0.201		0.257	0.056			0.203		0.281	0.045	0.082	-0.073			0.232		0.188	
6	0.189			0.234		0.025	0.239	0.065	0.217	0.226	0.277		0.077		0.073	0.16	0.206	0.125	0.173	0.207
7	0.229	0.207	0.268				0.215	0.117		0.235					0.006			0.146		0.115
8		0.195	0.292	0.299	0.287							0.007		-0.03		0.208				
9				0.241		0.089			0.153		0.275		0.015				0.192		0.177	
10	0.249				0.282		0.291	0.047		0.256		0.01		-0.012	0.063			0.224		0.077
11		0.092	0.228			0.025			0.127		0.213		-0.031			0.11	0.059		0.16	
12	0.163			0.133	0.105		0.198	-0.026		0.131				-0.034	0.029			0.135		0.01
13		0.025	0.172			0.012			0.171		0.192		0.001				-0.058		0.163	
14	0.042			0.021	-0.042		0.073	-0.057		-0.004		-0.013		-0.073	0.009	0.048		0.014		-0.026
15		-0.014	0.03			-0.02			0.157		-0.025		0.01				-0.061		0.034	
16	0.032			0.006	0.019		-0.012	-0.026		0.004		0.015		-0.026	0.009	0.078		0.004		-0.037
17		-0.066	-0.005		-0.082	-0.057			0.121		-0.016	-0.06	-0.041	-0.11			-0.105		-0.054	
18	-0.021			-0.025		-0.035	-0.038	-0.066	0.153	-0.033	0.034		0.003		-0.018	-0.001	-0.061	-0.041	-0.047	-0.082

Table 10. contd.

Weeks past sowing	GROUND TRUTH POINTS																		Mean NDWI
	21	22	23	24	25	26	27	28	29	30	31	32	33	34	35	36	37	38	39	
1	0.048	0.079		0.212	0.077			0.133	0.071				0.073				0.032		-0.058	0.089
2			0.085			0.148	-0.02			0.061	0.123	0.148		0.029	0.01	0.06		0.062		0.096
3	0.086	0.174		0.234	0.03			0.107	0.043			0.142	0.079	0.02		0.041	-0.013	0.099		0.104
4		0.155	0.078			0.043	0.081			0.064	0.18				0.063		0.066		-0.015	0.109
5	0.051		0.244	0.293	-0.067			0.089	-0.027				0.2		0.128					0.133
6	0.128			0.273	0.07	0.095	0.249	0.079	0.052	0.043	0.198	0.151	0.189	0.061		0.158		0.036	0.004	0.142
7		0.189				-0.007	0.148			-0.035	0.196						0.116			0.143
8			0.233									0.176		0.15	0.151	0.206		0.135	-0.007	0.165
9	0.178	0.209		0.259	0.029			0.121	0.057				0.204				0.121			0.154
10			0.222			0.046	0.275			0.024	0.316	0.14		0.139	0.194	0.163		0.16	-0.004	0.151
11	0.17	0.188		0.204	-0.014			0.075	0.053				0.116				0.05			0.108
12			0.161			0.026	0.222			-0.001	0.288	0.038		0.038	0.198	-0.028		0.056	-0.051	0.081
13	0.201	0.036		0.22	0.006			0.039	0.056				-0.029				-0.079		-0.09	0.062
14			0.078			-0.032	0.199			-0.022	0.134	0.003		-0.019	0.034	-0.05		0.013		0.015
15	0.091	-0.014		0.208	0.008			-0.022	0.02			-0.002	-0.034	-0.052		-0.058	-0.06	-0.035		0.008
16		0.002	0.011			0.012	-0.001			0.02	0.017				0.035		-0.022			0.007
17	-0.047		-0.053	0.148	-0.016			-0.072	-0.034				-0.047		-0.077					-0.035
18	-0.038			0.154	-0.008	-0.03	-0.07	-0.042	-0.022	-0.012	-0.016		-0.003							-0.015

Table 11. Weekly SAVI values of chickpea

Weeks past sowing	GROUND TRUTH POINTS																			
	1	2	3	4	5	6	7	8	9	10	11	12	13	14	15	16	17	18	19	20
1				0.235		0.284			0.785		0.277		0.543				0.299		0.298	
2	0.268				0.357		0.27	0.893		0.283		0.516		0.251	0.411			0.263		0.956
3		0.386	0.391			0.278			0.663		0.401		0.485			0.629	0.425		0.34	
4	0.356			0.521	0.587		0.381	0.671		0.42		0.499		0.155	0.318			0.397		0.764
5		0.463	0.543		0.618	0.305			0.634		0.685	0.271	0.394	0.078			0.667		0.489	
6	0.609			0.678		0.254	0.657	0.619	0.578	0.723	0.726		0.344		0.357	0.571	0.609	0.464	0.442	0.738
7	0.574	0.682	0.814				0.636	0.44		0.652					0.202			0.431		0.495
8		0.648	0.799	0.867	0.734							0.237		0.158		0.611				
9				0.613		0.366			0.445		0.692		0.251				0.544		0.506	
10	0.587				0.624		0.68	0.322		0.614		0.166		0.134	0.288			0.552		0.385
11		0.4	0.645			0.251			0.408		0.574		0.16			0.238	0.263		0.449	
12	0.428			0.369	0.265		0.529	0.269		0.343		0.211		0.131	0.233			0.371		0.295
13		0.209	0.459			0.179			0.499		0.444		0.212				0.077		0.452	
14	0.183			0.161	0.11		0.223	0.238		0.13		0.147		0.065	0.175	0.265		0.156		0.267
15		0.15	0.185			0.197			0.446		0.124		0.241				0.088		0.192	
16	0.163			0.127	0.126		0.169	0.244		0.135		0.19		0.104	0.192	0.238	0.039	0.142		0.212
17		0.122	0.053		0.025	0.132			0.416		0.053	0.109	0.201	0.025			0.047		0.112	
18	0.082			0.075		0.119	0.099	0.208	0.454	0.108	0.108		0.222		0.135	0.156	0.085	0.077	0.132	0.158

Table 11. contd.

Weeks past sowing	GROUND TRUTH POINTS																		Mean SAVI
	21	22	23	24	25	26	27	28	29	30	31	32	33	34	35	36	37	38	39	
1	0.369	0.287		0.603	0.511			0.507	0.431				0.267				0.308		0.181	0.386
2			0.26			0.666	0.286			0.395	0.264	0.354		0.259	0.283	0.391		0.376		0.401
3	0.369	0.518		0.588	0.361			0.412	0.319			0.304	0.318	0.255		0.339	0.336	0.437		0.407
4		0.427	0.273			0.431	0.352			0.31	0.426				0.392		0.355		0.171	0.410
5	0.395		0.441	0.714	0.246			0.476	0.238				0.544		0.43					0.454
6	0.481			0.656	0.355	0.516	0.648	0.447	0.25	0.33	0.639	0.409	0.503	0.309		0.477		0.292	0.145	0.494
7		0.529				0.306	0.556			0.147	0.573						0.378			0.494
8			0.551									0.469		0.474	0.502	0.574		0.494	0.262	0.527
9	0.53	0.559		0.639	0.279			0.48	0.311				0.572				0.393			0.479
10			0.429			0.288	0.672			0.217	0.755	0.332		0.457	0.507	0.364		0.48	0.199	0.431
11	0.519	0.553		0.513	0.198			0.38	0.29				0.39				0.329			0.386
12			0.364			0.245	0.578			0.176	0.707	0.186		0.299	0.585	0.15		0.346	0.109	0.327
13	0.526	0.214		0.562	0.243			0.304	0.291				0.081				0.099		0.031	0.287
14			0.256			0.202	0.548			0.146	0.374	0.114		0.199	0.324	0.104		0.271		0.212
15	0.308	0.141		0.537	0.221			0.222	0.23			0.101	0.087	0.112		0.102	0.128	0.176		0.199
16		0.147	0.224			0.23	0.172			0.161	0.15				0.273		0.168			0.178
17	0.119		0.126	0.444	0.186			0.13	0.165				0.026		0.148					0.139
18	0.117			0.429	0.184	0.194	0.117	0.166	0.139	0.127	0.069		0.051							0.152

Table 12. Weekly mean VI values of chickpea crop

Weeks past sowing	Mean value of vegetation indices			
	RVI	NDVI	NDWI	SAVI
1	1.742	0.261	0.089	0.386
2	1.807	0.272	0.096	0.401
3	1.815	0.273	0.104	0.407
4	1.849	0.274	0.109	0.410
5	1.990	0.305	0.133	0.454
6	2.066	0.330	0.142	0.494
7	2.072	0.332	0.143	0.494
8	2.187	0.352	0.165	0.527
9	1.985	0.319	0.154	0.479
10	1.894	0.287	0.151	0.431
11	1.770	0.259	0.108	0.386
12	1.613	0.218	0.081	0.327
13	1.523	0.193	0.062	0.287
14	1.351	0.142	0.015	0.212
15	1.328	0.133	0.008	0.199
16	1.291	0.120	0.007	0.178
17	1.216	0.094	-0.035	0.139
18	1.243	0.102	-0.015	0.152

4.3.1 RVI profile of Chickpea

The mean RVI values for chickpea crop corresponding to various growth stages (weeks past sowing) were acquired through the aforementioned procedures. The RVI trend along the life cycle of the chickpea crop is depicted by the plot of RVI versus weeks past sowing. Smoothed data is represented by the dotted line that is drawn through the scattered points and is shown in Fig. 8. This trend satisfies the polynomial equation of fourth order:

$$y = 0.0002x^4 - 0.0055x^3 + 0.0466x^2 - 0.0736x + 1.7727 \qquad R^2 = 0.9733 \text{ --- } 7$$

Where,

y = RVI

x = Weeks past sowing

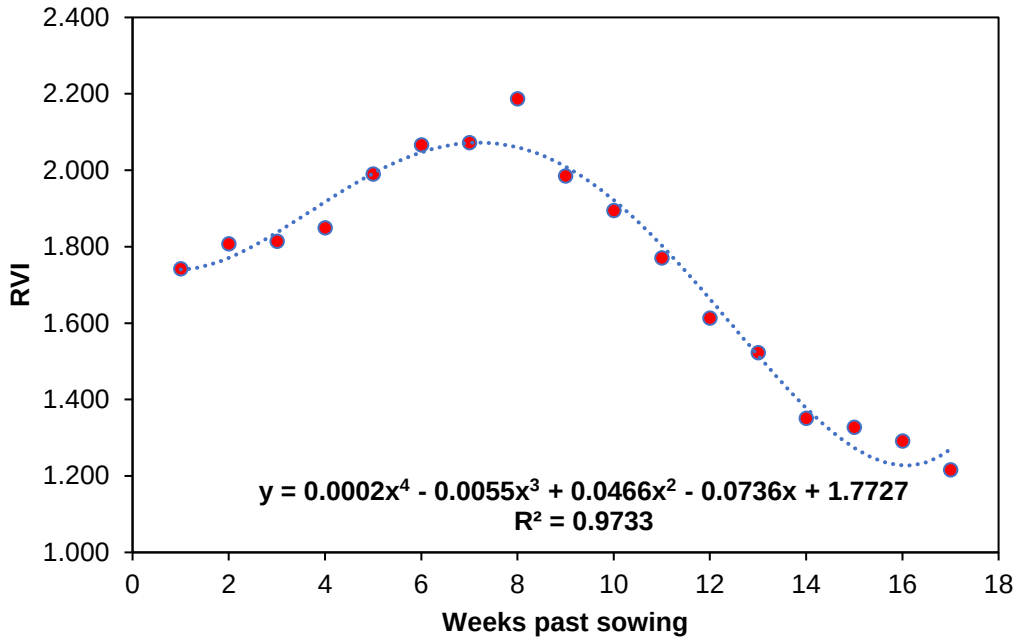

Fig. 8 RVI profile of chickpea

It is observed that the RVI value first increases, reaches a maximum value, and, then decreases. The initial crop stages corresponding to germination and emergence exhibit a low RVI value of 1.742 and then increase up to the 8th week corresponding to the pod initiation stage. The value of RVI was found to be higher between the 5th to 9th weeks past sowing corresponding to the maximum vegetative (grand growth) and pod initiation stages. During the mid-season stage, the values were nearly similar and then, go on decreasing till the physiological maturity stage at the 14th week. Since 90% of the stems and pods turn light golden yellow by then, indicating senescence and thus giving a dried appearance, the rate of decrease in RVI is low, thereafter.

A general resemblance in the pattern was observed when temporal patterns of RVI and Kc were plotted together as shown in Fig. 9. The peak values of both RVI and Kc were observed at the midseason stage while throughout the crop growth period, both RVI and Kc trends exhibit similarity. However, the RVI value decreases at a slower rate than Kc in the late season stage after the peak.

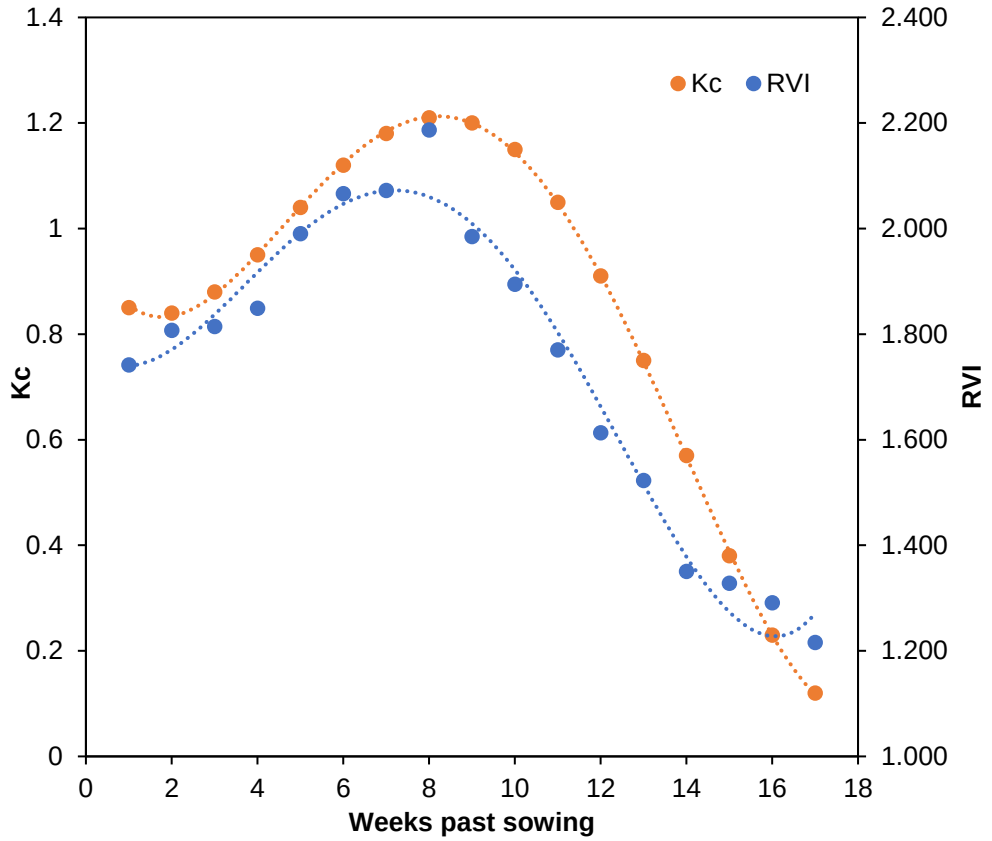

Fig. 9 Comparison of RVI and Kc patterns of chickpea

4.3.2 NDVI Profile of chickpea

The trend of NDVI along the crop growth cycle of chickpea is obtained by plotting NDVI values against weeks past sowing. The NDVI trend is shown in Fig. 10 and obeys the fourth order polynomial equation:

$$y = 4E\text{-}05x^4 - 0.0015x^3 + 0.0139x^2 - 0.0323x + 0.2827 \qquad R^2 = 0.9819 \text{ --- } 8$$

Where,

y = NDVI

x = Weeks past sowing

The initial stage of the crop was found to be characterized by lower NDVI values starting from 0.261 and then progressing to touch the peak value of 0.352 by the 8th week. The NDVI values in this midseason stage from the 5th to the 9th week are observed to be higher which indicates higher rates of photosynthesis and after which it undergoes a gradual fall till physiological maturity. The trendline exhibits a uniform rate of change of both increase up to the peak and decrease from the peak.

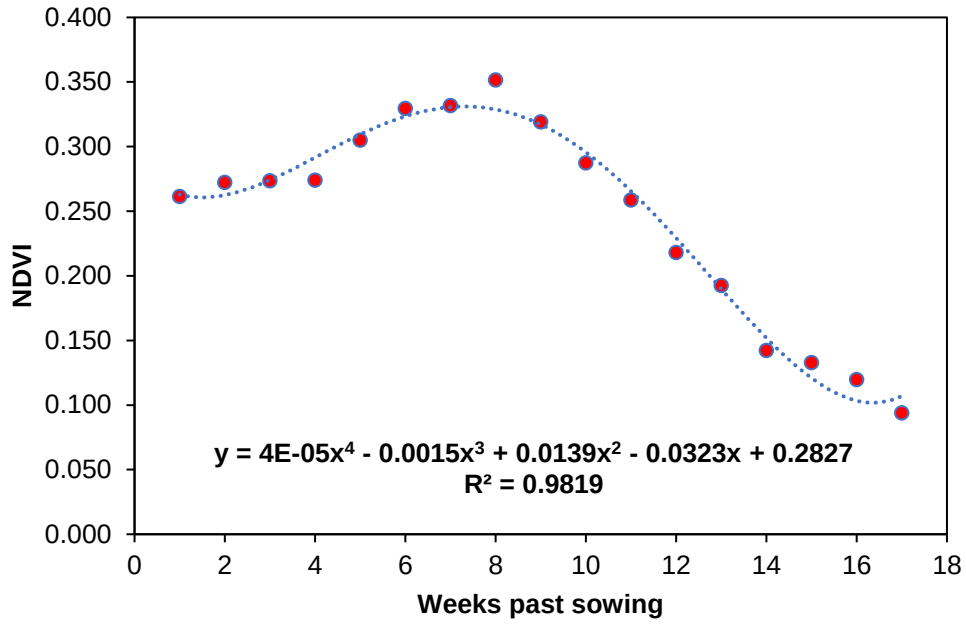

Fig. 10 NDVI profile of chickpea

On plotting Kc and NDVI together against weeks past sowing, the temporal variation of both NDVI and crop coefficients were observed to be almost similar as shown in Fig. 11. However, the rate of change of NDVI was found to be comparatively lower than that of Kc.

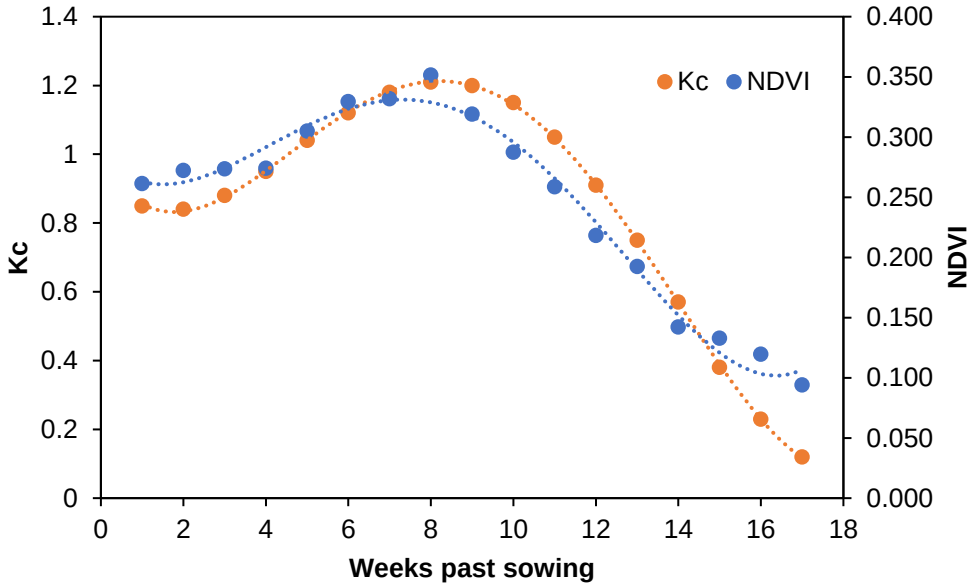

Fig. 11 Comparison of Kc and NDVI patterns of chickpea

4.3.3 NDWI profile of chickpea

The temporal trend of NDWI is given by the plot between NDWI and weeks past sowing as shown in Fig. 12. The NDWI was found to be increasing from 0.089 to 0.165 up to the 8th week. The values were found to be higher in general from the 5th to the 10th week after which the value decreases at a faster rate up to the senescence. The trendline obeys the polynomial equation of the fourth order:

$y = 3E\text{-}05x^4 – 0.0011x^3 + 0.0104x^2 – 0.0229x + 0.1036$ $R^2 = 0.977$------ 9

Where,

y = NDWI

x = Weeks past sowing

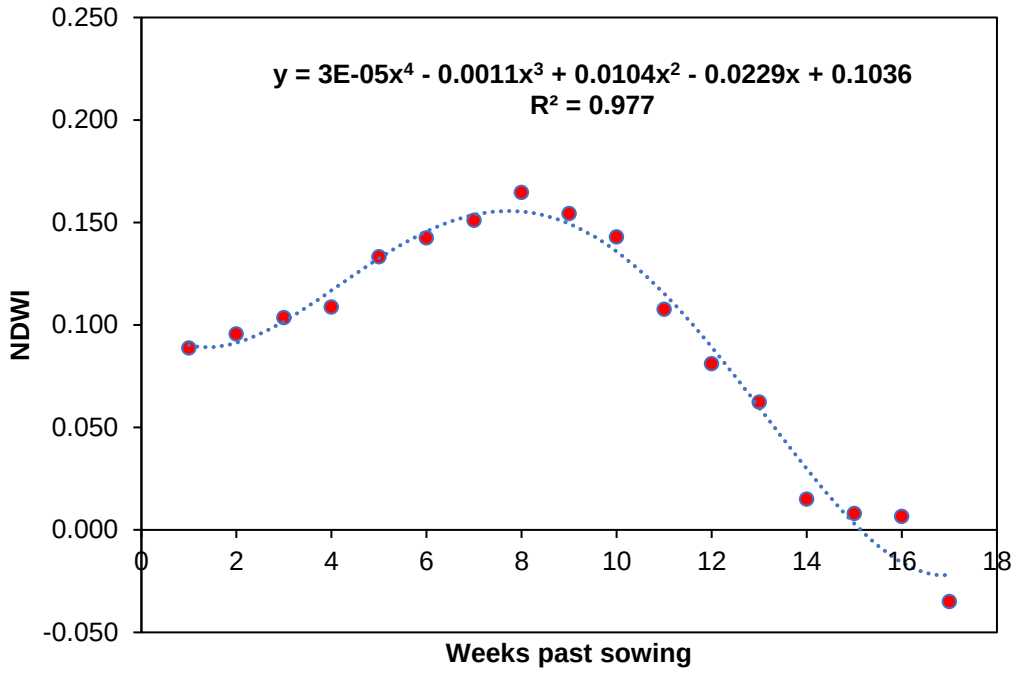

Fig. 12 NDWI profile of chickpea

The temporal trend of NDWI and crop coefficients is found to be highly similar to each other as shown in Fig. 13. This indicates greater chances for modeling crop coefficients in terms of NDWI.

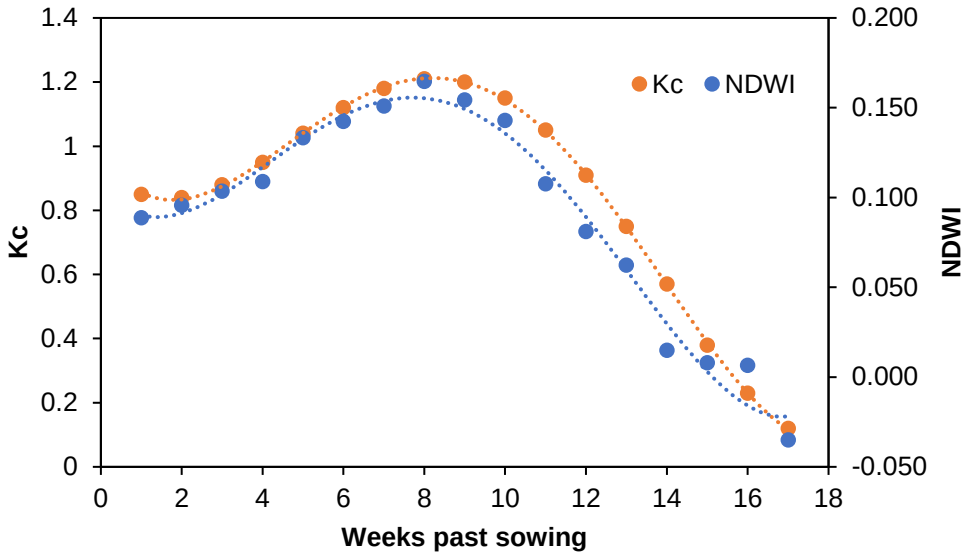

Fig. 13 Comparison of Kc and NDWI patterns of chickpea

4.3.4 SAVI profile of chickpea

The temporal development of SAVI along the life cycle of chickpea is obtained by plotting SAVI values against weeks past sowing as shown in Fig. 14. The SAVI values were observed to be increasing at the beginning from 0.386 to 0.527 up to the 8th week, after which the trend shows a gradual decrease till the senescence. Comparatively, higher values were observed from the 5th to the 9th week. The trendline is characterized by a uniform rate of change throughout the lifecycle and obeys the fourth order polynomial equation:

$$y = 7E\text{-}05x^4 - 0.0023x^3 + 0.0207x^2 - 0.046x + 0.4148 \qquad R^2 = 0.9819 \text{ ---10}$$

Where,

y = SAVI

x = Weeks past sowing

On comparison of SAVI and Kc (Fig. 15), both the trends were found to be almost similar. SAVI values were found to be higher in the initial stages than the Kc. However, both curves touch the peak by the 8th week after which, SAVI values were found to be undergoing a gradual decrease and also, lower than the Kc till the 14th week of physiological maturity. In general, the rate of change of SAVI was found to be comparatively lower than that of Kc throughout the crop cycle.

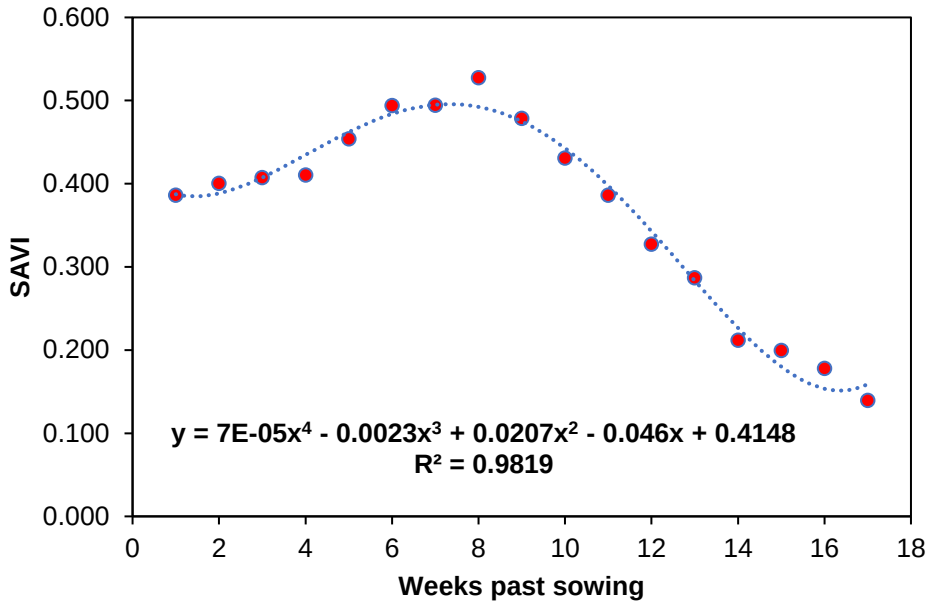

Fig. 14 SAVI profile of chickpea

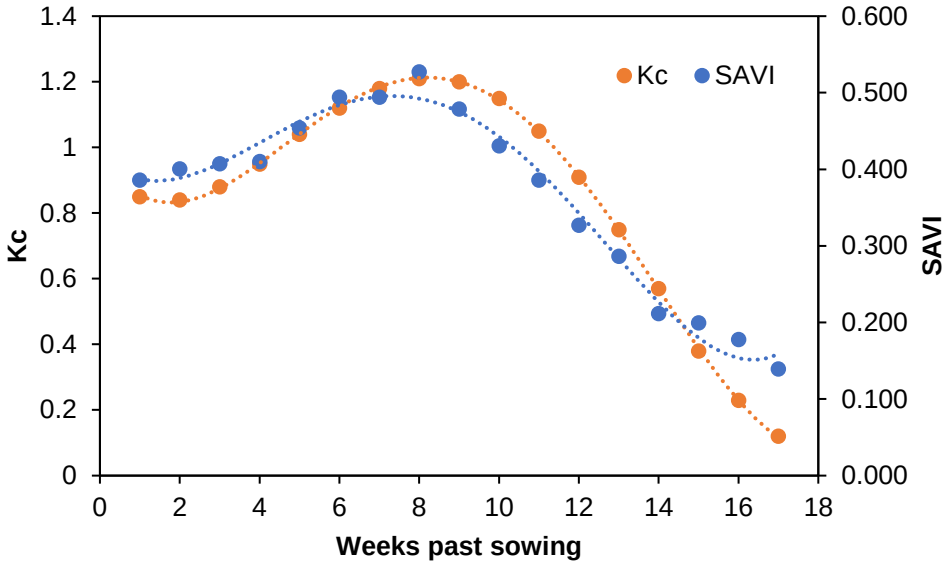

Fig. 15 Comparison of Kc and SAVI patterns of chickpea

4.3.5 Overall trend of VIs for chickpea

Weekly mean VI values of chickpea crop are tabulated in Table 12. All the VI profiles illustrated from 4.3.1 to 4.3.4 depict similar behavior of first starting from a lower value during the initial stages of germination and emergence and then going on increasing up to the 8th week through the vegetative growth and initial reproductive stages indicating increasing

photosynthetic activity. Peak values of each VI were obtained on the 8th week corresponding to pod initiation and thereafter, VI value undergoes a gradual decrease throughout the late season stage till the senescence indicating yellowing of leaves and stem owing to the reduction in photosynthetic activity. As the plants get dried more and more towards the later stages, the value even falls below the initial value and the VI values were observed to be nearly stable during maturity. Furthermore, all the VIs yielded higher values during the 5th to 10th week corresponding to late vegetative and early pod development stages respectively indicating the midseason stage of maximum growth, in general. During the midseason stage, all the VIs yielded nearly constant values during the 6th and 7th week corresponding to the initiation of flowering and 50% flowering respectively.

4.4 Identification and acreage estimation of chickpea crop

A hybrid classification method based on K-means clustering and visual analysis is adopted for the identification and acreage estimation of chickpea crop using multidate time series remote sensing data of Sentinel 2A satellite.

Time series NDVI layer stack was prepared using the NDVI images derived from subsets. The geographical locations of GT sites were transferred onto the image by incorporating the shape file. For each day of the satellite overpass, the average NDVI values of the fields of chickpea, wheat, and onion which are grown in the similar period were obtained. Graphs representing NDVI values for various dates of satellite image acquisition were plotted for chickpea, onion, and wheat. These graphs display the Reference Temporal Spectral Profiles (RTSPs) of the corresponding class. RTSPs representing different sowing dates of the chickpea crop were prepared in addition to the general RTSP.

Non crop mask was layered on the NDVI stack to reduce data load, and the resulting multilayer dataset representing the cropped area was then used for further processing. K-means clustering method of unsupervised classification was carried out on this resultant multilayer dataset and a classified image with 50 classes of clusters was generated. Signatures of all these classes were obtained from the attribute table and then, exported to Microsoft excel. Temporal spectral profiles (TSPs) for each class were

prepared based on their signatures. The cluster classes were assigned to a certain crop or other with which it matches the most after visual comparison with known RTSPs with the help of an expert. TSPs of 13 classes were found to match with RTSPs of chickpea crop. The output of unsupervised classification is depicted as Fig. 16 and was further used for supervised classification by visual analysis and signature editor tool. Crop recoding was performed on the output of supervised classification to create a real thematic map by combining similar clusters. The spatial distribution of chickpea and other crops is represented by choosing different colors for different classes. The final classified image is shown in Fig. 17.

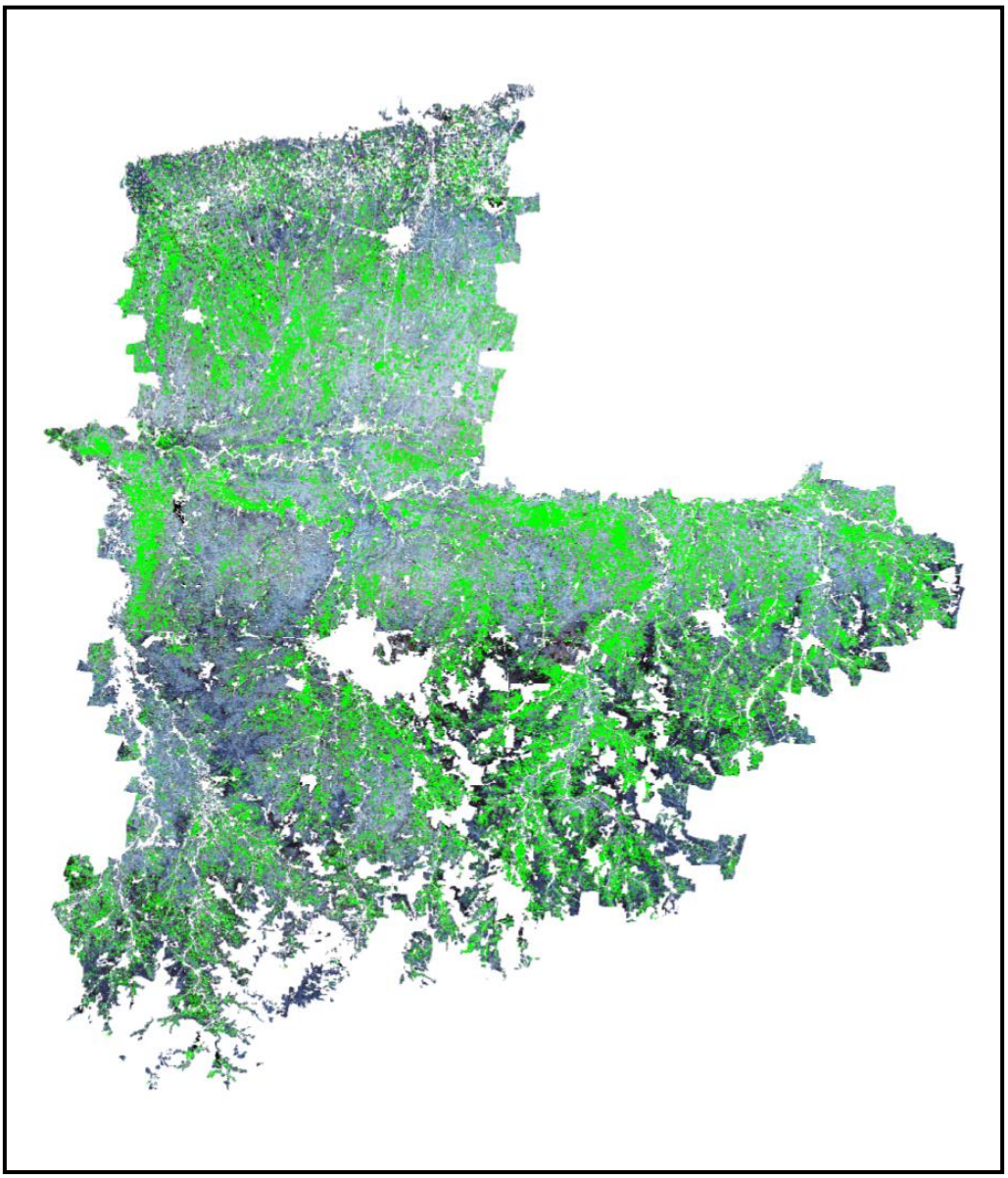

Fig. 16 Classified image obtained after unsupervised classification

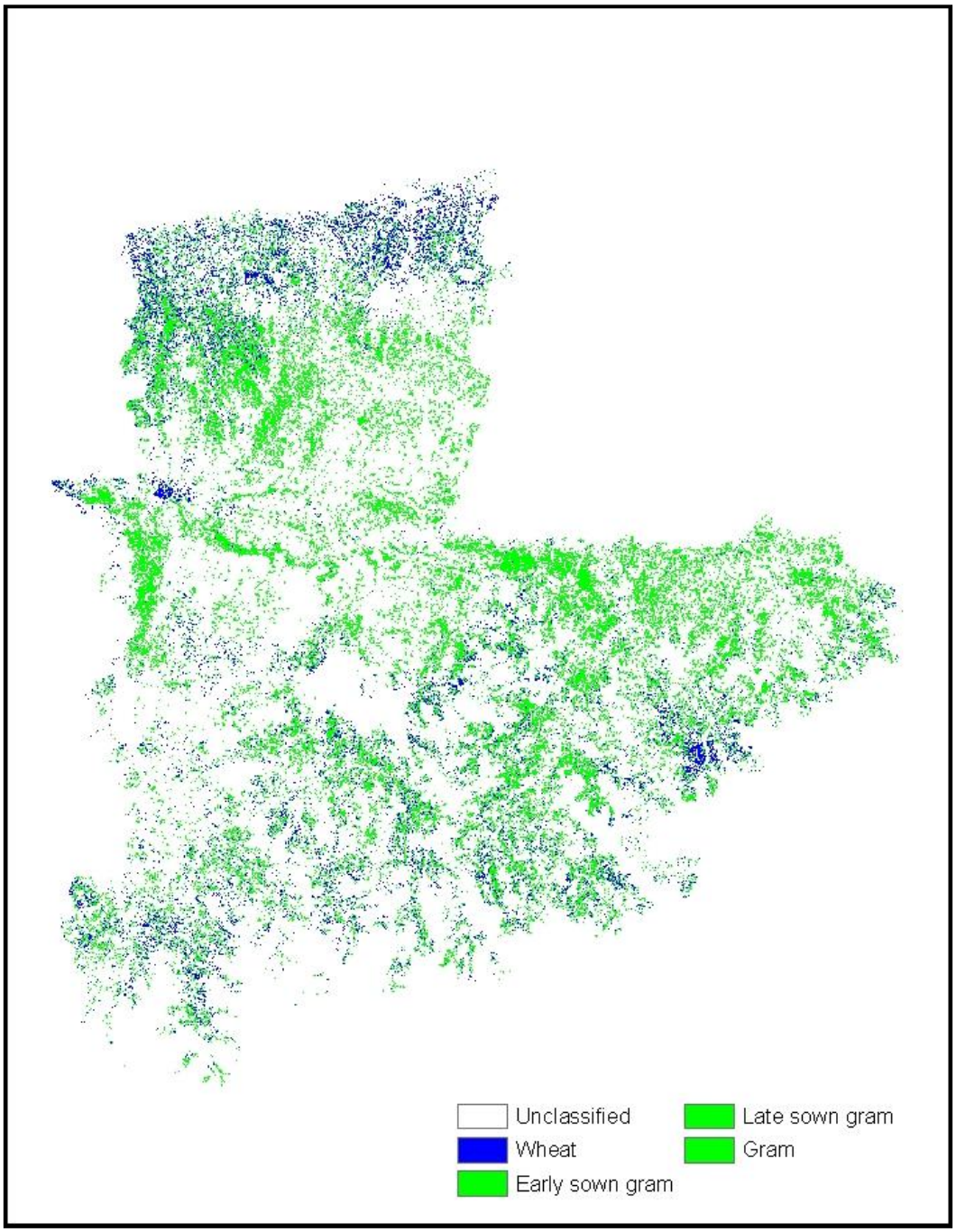

Fig. 17 Final Classified image

Using the Table menu option in ERDAS Imagine Software, the area coverage of each class was displayed in the attribute table of the recoded image. The estimated acreage of chickpea crop in the Akola district is obtained from the attribute table as 95576 hectares. It is noted that numerous linear features, such as highways and canals, were accurately categorized as non-crop classes in the current analysis.

In the study area, the chickpea crop area was estimated by remote sensing to be 95576 ha, 3.12 percent more than the actual acreage of 92681 ha recorded by the Department of Agriculture, Government of Maharashtra. Overestimation is assumed to be the result of mixed crop pixels due to the smaller fields or the presence of similar spectral profiles of co-existing crops. Though chickpea is predominantly a rainfed crop, in irrigated chickpea fields, soil moisture may have affected the reflectance.

The results obtained are in agreement with similar studies conducted by Coppa (2006) for barley, canola, chickpeas, lentils and wheat, Dheeravath *et al.* (2010), Mukherji *et al.* (2010) for wheat and Pimpale *et al.* (2015) for wheat.

4.5 Relationship between crop coefficients and VIs for chickpea

The average weekly values of the vegetation indices viz. RVI, NDVI, NDWI, and SAVI (Table 12) of chickpea were plotted against the weekly crop coefficients (Kc) based on the PM method as advised by MPKV Rahuri (described in 3.13). The relationship between the vegetation indices and crop coefficients was investigated using simple linear regression analysis and a strong linear relation was identified. The correlation between the recommended weekly crop coefficients for the chickpea crop and the vegetation indices namely, RVI, NDVI, NDWI, and SAVI are depicted in Figures 18a–18d. Linear prediction models were generated from the regression analysis and are given as:

$Kc = 1.0608\ RVI - 0.992$ $R^2 = 0.884$ ---------- 11

$Kc = 3.9966\ NDVI - 0.13$ $R^2 = 0.9097$ ---------- 12

$Kc = 5.5309\ NDWI + 0.3508$ $R^2 = 0.955$ ---------- 13

$Kc = 2.6733\ SAVI - 0.1281$ $R^2 = 0.9135$ ---------- 14

The generated models were statistically analyzed using the most used statistical measures, namely the coefficient of determination (R^2), mean standard error (MSE), root mean square error (RMSE), percent deviation (PD), and the Willmott index of agreement (D). The outcomes of statistical analysis are comprehended in Table 13.

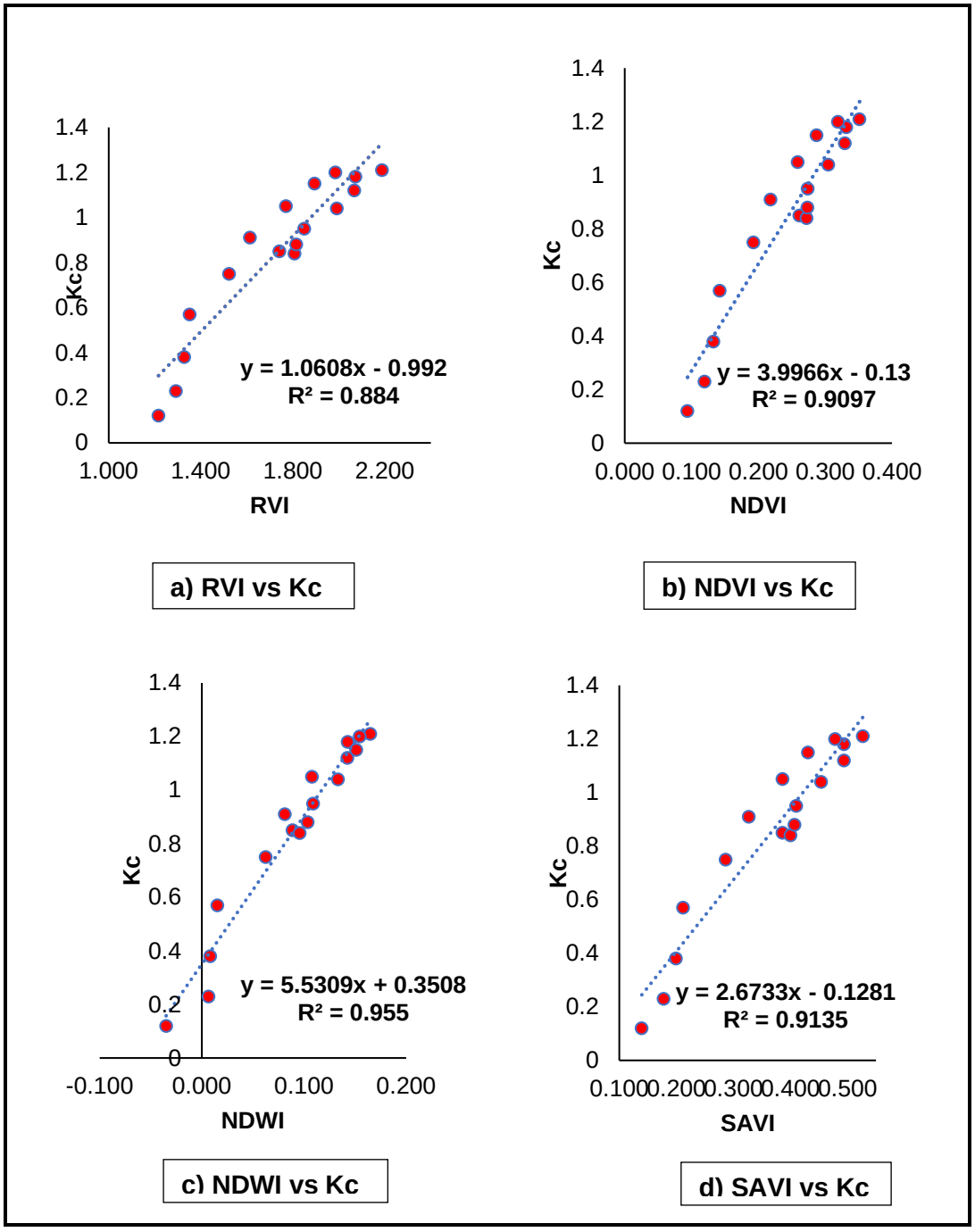

Fig. 18 (a, b, c and d) Relationships of crop coefficients with vegetation indices

All the regression models were found to be statistically significant with a very low p-value. Vegetation indices are correlated to canopy structure, canopy photosynthesis and LAI, in general. Each vegetation indices have been found to have a strong correlation with recommended crop coefficients of chickpea with high R^2 values. However, the NDWI-Kc model exhibited the best performance amongst all models with the highest R^2 and D values of 0.9550 and 0.9884 respectively along with the lowest values for SE, RMSE

and PD of 0.0743, 0.0698 and 4.1016 respectively. It may be because the chickpea is mostly a rainfed crop and NDWI is a better indicator of vegetative characteristics in water stress conditions.

Both the SAVI-Kc model and NDVI-Kc model showed similar trends with R^2 values of 0.9135 and 0.9097 respectively. Hence, both the models confirm reasonable results with SE, RMSE, PD and D values of 0.1030, 0.0968, 7.3089 and 0.9770 respectively for the SAVI-Kc model and 0.1053, 0.0989, 7.3852 and 0.9759 for NDVI-Kc model. SAVI is a better indicator of vegetation growth for partial canopies as it eliminates soil noise effects. However, the similarity of SAVI with NDVI might be due to the higher vegetation density.

On the other hand, the RVI-Kc model showcased comparatively poor performance with an R^2 value of 0.8840 suggesting it is less accurate in forming linear relationships. This might be because RVI is just a simple ratio and doesn't entirely account for the greenness of vegetation.

The findings were in agreement with similar studies by El-Shirbeny *et al.* (2014) using NDVI for wheat, Pimpale *et al.* (2014) using NDVI in chickpea, Parmar and Gontia (2016) using NDVI and SAVI for groundnut and Pimpale *et al.* (2019) using RVI, SAVI, NDVI, TNDVI and MSAVI2 for sorghum. Most of the studies were observed to be utilizing NDVI to derive crop coefficients from remotely sensed data.

Table 13. Statistical analysis of VI-Kc prediction models

Regression model	RVI - Kc	NDVI - Kc	NDWI - Kc	SAVI - Kc
Intercept	-0.9920	-0.1300	0.3508	-0.1281
Coefficient	1.0608	3.9966	5.5309	2.6733
SE	0.1193	0.1053	0.0743	0.1030
R^2	0.8840	0.9097	0.9550	0.9135
P- value	2.06E-08	3.1E-09	1.63E-11	2.24E-09
RMSE	0.1121	0.0989	0.0698	0.0968
PD	10.1738	7.3852	4.1016	7.3089
D	0.9684	0.9759	0.9884	0.9770

4.6 Utilization of the developed relationship for real time irrigation water management

As discussed in 4.5, it was found that the vegetation index NDWI and recommended crop coefficients (Kc) of chickpea had a strong correlation. Hence, weekly crop coefficients were derived based on the obtained linear regression equation. The FAO Penman-Monteith method was used to estimate the reference evapotranspiration (ETo) for the Akola district during the study period based on the daily meteorological data (Annexure I) and the detailed calculations are given in Annexure II. The reference evapotranspiration (ETo) was multiplied by the NDWI-Kc model derived crop coefficient (Kc) to estimate the crop evapotranspiration (ETc) of chickpea for the study area. Table 14 displays the estimated weekly values of the reference evapotranspiration ETo and crop evapotranspiration ETc.

The total crop evapotranspiration (ETc) throughout the life cycle of the rabi chickpea crop in the Akola district during 2021-22 was calculated as 248.23 mm. The weekly water demand of the chickpea crop was estimated by multiplying the corresponding weekly crop evapotranspiration with the estimated crop acreage as described in 4.4 and the calculations are given in Annexure III. Table 15 comprehends the crop water demand of the rabi chickpea crop in Akola. The total water demand of chickpea was obtained as 213.4138 Mm^3. Weekly water demand shows the highest values during midseason stages indicating the need for irrigation, especially during midseason stages when the growth is maximum.

These results are in agreement with similar studies by Hafeez *et al*. (2002) for paddy, Pimpale *et al.* (2015) for wheat and González *et al.* (2018) for silage corn.

Table 14. Reference evapotranspiration (ETo, mm) and crop evapotranspiration (ETc, mm) of rabi chickpea in Akola district 2021-22

MET. Week	Weeks past sowing	NDWI	Kc derived	ETo (mm)	ETc (mm)
47	1	0.0888	0.84	18.68	15.73
48	2	0.0957	0.88	16.46	14.49
49	3	0.1036	0.92	12.73	11.75
50	4	0.1088	0.95	15.81	15.06
51	5	0.1333	1.09	13.35	14.53
52	6	0.1424	1.14	15.56	17.72
1	7	0.1426	1.14	13.96	15.91
2	8	0.1647	1.26	13.56	17.11
3	9	0.1544	1.20	15.80	19.03
4	10	0.1510	1.19	18.20	21.59
5	11	0.1076	0.95	18.78	17.76
6	12	0.0811	0.80	20.54	16.41
7	13	0.0623	0.70	22.14	15.40
8	14	0.0150	0.43	24.93	10.81
9	15	0.0081	0.40	27.06	10.70
10	16	0.0066	0.39	25.24	9.77
11	17	-0.0350	0.16	28.43	4.47
TOTAL					**248.23**

Table 15. Crop water demand (Mm^3) of rabi chickpea in Akola district (2021-22)

MET. Week	Weeks past sowing	ETc (mm)	Crop Acreage (ha)	*Water demand	
				m^3	**Mm^3
47	1	15.73	95576	15031513.76	15.03
48	2	14.49	95576	13847217.39	13.85
49	3	11.75	95576	11234030.54	11.23
50	4	15.06	95576	14390202.16	14.39
51	5	14.53	95576	13883616.78	13.88
52	6	17.72	95576	16933585.11	16.93
1	7	15.91	95576	15209930.64	15.21
2	8	17.11	95576	16349113.88	16.35
3	9	19.03	95576	18188150.51	18.19
4	10	21.59	95576	20634401.21	20.63
5	11	17.76	95576	16973140.75	16.97
6	12	16.41	95576	15686947.02	15.69
7	13	15.40	95576	14716444.17	14.72
8	14	10.81	95576	10335462.75	10.34
9	15	10.70	95576	-	-
10	16	9.77	95576	-	-
11	17	4.47	95576	-	-
Total		**248.23**		**213413756.66**	**213.4138**

*Since water is needed only up to physiological maturity, water demand calculations are done only up to 14th week

**Mm^3 = Million cubic meters

CHAPTER V

SUMMARY AND CONCLUSIONS

Water resource management is crucial for increasing water use efficiency in the current scenario of water challenges due to increasing population, water resource depletion, and abrupt climate changes. The agricultural sector being the major shareholder of water consumption across the globe, precise irrigation water management is the need of the hour. To meet this need, current irrigation scheduling techniques must be improved to take into account the actual irrigation water requirement of crops. The FAO-56 provides revised guidelines for calculating the water needs of crops that are applicable globally. Crop coefficients and reference evapotranspiration are used to calculate the crop water requirement of plants. However, the method uses time-based tabular crop coefficients that lack spatial variability. Multispectral vegetation indices (VIs) based on remote sensing share the same pattern as crop coefficients (Kc), and can thus be used as a substitute for crop coefficients to produce spatial values that can help with precision irrigation water management. Hence, the current investigation entitled "Estimation of Evapotranspiration of Chickpea using Vegetation Indices Based Crop Coefficients" was conducted to investigate the spectral behavior of the chickpea crop, estimate acreage, establish a relationship between VIs and crop coefficients and utilize the best derived VI-Kc relationship for water demand calculations.

The study was carried out in the predominantly chickpea-growing district of Akola in Maharashtra. Though the moisture sensitive chickpea crop is predominantly grown in rabi season, precise application of irrigation especially at critical growth stages like grand growth, flowering and pod formation stages considerably increases yield and quality of produce. The suitability of the four most often used vegetative indices (VIs), namely RVI, NDVI, NDWI, and SAVI, was examined to create a relationship with the crop coefficients of the chickpea crop. Multidate Sentinel 2A images were digitally processed to generate the VIs under study, and the values obtained were organized in accordance with the crop age in weeks. The identification and

acreage estimation was performed using the hybrid classification method while the FAO Penman-Monteith method was employed to estimate the reference evapotranspiration (ETo). The correlation between VIs and PM-based Kc values was established using simple regression analysis and the best VI-Kc relationship was identified. The Kc derived from the best-performing regression model was used to estimate the real-time crop water requirement using the relation ETc= ETo x Kc. The water demand of the chickpea crop in the study area was determined based on the actual crop water requirement.

The following paragraphs provide an overview of the main findings and conclusions of the research.

The study of the spectral behavior of chickpea indicated that all the VI profiles namely, RVI, NDVI, NDWI, and SAVI, have similar behavior of beginning with a lower value during the early stage of germination and emergence and gradually increasing up until the eighth week through the vegetative growth and early reproductive stages, signifying increasing photosynthetic activity. After attaining peak values in the 8^{th} week corresponding to pod initiation, VIs showed a decline throughout the late season stage till the senescence. Towards the later stages, the value even falls below the initial value. The comparison of VIs with Kc throughout the course of the growth period of chickpea revealed that the development trends of all VIs are almost identical to those of crop coefficients. Both VIs and Kc adhere to the growth curve pattern.

The general observation signifies all VIs peak when the crop reaches its maximum effective green cover, which also happens to be when the Kc is at its highest point. Thereafter, the VIs begins to decline as the crop ages and eventually reach very low values.

Identification and acreage estimation of chickpea crop based on the hybrid classification approach estimated the acreage in the near range of actual acreage recorded by the Department of Agriculture, Government of Maharashtra. An overestimation of 3.12% was observed. However, these remote sensing estimations were acquired far earlier than the Department of Agriculture's published figures.

Among the four vegetative indices studied—RVI, NDVI, NDWI, and SAVI—NDWI produced the highest correlation with crop coefficients of chickpea crop, with very significant R^2 and D values of 0.9550 and 0.9884, respectively, and the lowest SE, RMSE, and PD values of 0.0743, 0.0698, and 4.1016, respectively. Hence, to forecast the spatial crop coefficient of chickpea, the developed NDWI-Kc model (Kc = 5.5309 NDWI + 0.3508) can be utilized.

The weekly crop coefficients of chickpea were derived from the best-performing regression model, the NDWIxKc model. FAO-PM method was employed to estimate the reference evapotranspiration based on the meteorological data of the study area. The actual crop evapotranspiration of the chickpea crop in the study area is calculated as the product of reference evapotranspiration and Kc derived from the regression model. The total crop evapotranspiration of chickpea throughout the growth period was found to be 248.23 mm in the Akola district while the total water demand for chickpea crop in the entire study area is 213.4138 Mm^3. Crop water requirement and irrigation water requirement are synonymous in the study area, due to the lack of rains during the rabi season.

Conclusions

The conclusions drawn from the results of the current investigation are given below:

1. All of the vegetation indices (VIs) followed a similar trend to crop coefficients. Conversely, temporal fluctuations in VIs can be used to track phenological information. The defined VI patterns can be used to determine the likely date of planting. Since the patterns of VIs and Kc are similar, Kc can be estimated using vegetative indices for chickpea crop. This finding validates the central hypothesis of the study.
2. Identification and acreage estimation of chickpea crop revealed that, with a percent deviation of 3.12, the estimated acreages were found to be fairly near to the actual measurements. Hence, remote sensing and GIS techniques can be used to produce accurate and timely estimations of crop acreages.

3. In terms of the linear association of vegetation index with recommended crop coefficients of chickpea, NDWI exhibited the highest superiority. Hence, the established VI-Kc correlation can replace traditional tabular Kc in the FAO-56 procedures.
4. A remote sensing and GIS integrated approach can be used to deliver an adequate amount of irrigation water at various locations in accordance with the actual crop water demand, resulting in effective irrigation water management. This strategy can also be applied in cases of scarcity of water to provide the optimum irrigation water as lifesaving irrigation to avoid crop failure.
5. An expert system for precise irrigation scheduling can be formed using automatic weather stations and real-time, high-resolution data from remote sensors.

CHAPTER VI

LITERATURE CITED

Akkara MS, Pimpale AR, Wadatkar SB and Rajankar PB (2022). Role of Multispectral Vegetation Indices in Precision Agriculture – A Review. Int. J. Ag. Env. Biotech., 15(Special Issue): 277-285.

Allen RG, Jensen ME, Wright JL and Burman RD (1989). Operational estimates of evapotranspiration. J. Agron., 81 :650-662.

Allen RG, Smith M, Pereira LS and Perrier A (1994). An update for the calculation of reference evapotranspiration.

Allen RG, Pereira LS, Raes D and Smith M (1998). Crop Evapotranspiration-Guidelines for Computing Crop Water Requirements. FAO Irrigation and Drainage Paper 56, Rome, Italy, pp 300.

Allen RG (1999). Concept paper – Accuracy of predictions of project-wide evapotranspiration using crop coefficients and reference evapotranspiration in a large irrigation project. In Proc. United States Committee on Irrigation and Drainage Conference on 'Benchmarking Irrigation System Performance Using Water Measurement and Water Balances', San Luis Obispo, CA, during 10-13 March 1999.

Allen RG, Smith M, Pereira LS, Raes D and Wright JL (2000). Revised FAO Procedures for Calculating Evapotranspiration: Irrigation and Drainage Paper No. 56 for testing in Idaho. In Proc. Watershed Management and Operations Management. Fort Collins, CO, during 20-24 June 2000.

Allen RG, Walter IA, Elliott R, Howell TA, Itenfisu D and Jensen ME (2005). The ASCE standardized reference evapotranspiration equation.

Anonymous (2012). Krishi Darshani-2012. Mahatma Phule Krishi Vidyapeeth, Rahuri, Maharashtra, pp. 8 -9.

Anonymous (2013). Krishi Darshani-2013. Mahatma Phule Krishi Vidyapeeth, Rahuri, Maharashtra, pp. 9.

Anonymous (2017). Agriculture Contingency Plan for District: AKOLA. accessed 2 September 2021 <www.agricoop.nic.in/sites/default/files/MH11-%20Akola>

Arshad A, Bakhsh A, Azzam A, Ali S and Awais M (2018). Computing Spatio - Temporal Water Demand of Wheat Crop Using GIS and Remote Sensing - A Case Study of Faisalabad Irrigation District, Pakistan. J. Agri. Res., 3(6): 178.

Ayyangar R, Rao PPN and Rao KR (1980). Crop covers and crop phenological information from red and infrared spectral responses. J. Indian Society of Remote Sensing, 8: 23-29.

Barnes EM, Sudduth KA, Hummel JW, Lesch SM and Corwin DL (2003). Remote and ground-based sensor techniques to map soil properties. Photogramm. Eng. Remote Sensing, 69: 619-630.

Bausch WC (1993). Soil background effects on reflectance-based crop coefficients for corn. Remote Sens. Environ., 46: 1-10.

Bausch WC and Neale CMU (1987). Crop coefficients derived from reflected canopy radiation: A concept Trans. ASAE., 30(3): 703-709.

Bhatt CK and Nain AS (2018). Rice Acreage Estimation Using Sentinel-1A Dual Polarised SAR Data in Udham Singh Nagar (Uttarakhand). International Journal of Current Microbiology and Applied Sciences, 7(4): 2319-7706.

Blaney HF and Criddle WD (1950). Determining water requirements of irrigated areas from climatological and irrigation data. USDA (SCS)TP., 96: 48

Brown PW, Mancino CF, Young MH, Thompson TL, Wierenga PJ and Kopec OM (2001). Penman Monteith crop coefficients for use with desert turf systems. Crop Science, 41: 1197-1206.

Campos TM, Garcia HFJ, Camps VG, Grau MG, Nutini F, Busetto L and Boschetti M (2017). Exploitation of SAR and Optical Sentinel Data to Detect Rice Crop and Estimate Seasonal Dynamics of Leaf Area Index. Remote sensing, 9: 248

Chai K (2018). Detecting Rice Cropping Patterns with Sentinel-1 Multitemporal Imagery. Enschede, Netherland.

Chen CF, Son NT, Chen CR, Chang LY and Chiang SH (2016). Rice crop mapping using Sentinel-1A phenological metrics. The International Archives of the Photogrammetry, Remote Sensing and Spatial Information Sciences, 41(B8): 12-19.

Coppa IPM (2006). The use of remote sensing data for broad acre grain crop monitoring in South-East Australia. Ph.D. Thesis. RMIT Melbourne.

CottonInfo (2012). WATERpak - a guide for irrigation management in cotton and grain farming systems. accessed 20 December 2021 <http://www.cottoninfo.com.au/publications/waterpak>

Crop statistics (2022). Districtwise Area, Production and Productivity. accessed 23 June 2022 <http://www.maharashtra.gov.in>

Csillik O and Belgiu M (2017). Cropland mapping from Sentinel-2 time series data using object-based image analysis. The 20th AGILE International Conference on Geographic Information Science: Societal Geo-innovation Celebrating 20 years of GIS research, 9-12.

Dadhwal VK and Parihar JS (1985). Estimation of 1983-84 wheat acreage of Karnal district (Haryana) using Landsat MSS digital data. Technical

Note, IRS-UP/SAC/CPFfTN/09/85. Space Applications Centre. Ahmedabad, India.

Deoli V and Kumar D (2019). Remote Sensing and GIS approach for Spatiotemporal Mapping of Ramganga Reservoir. Int. J. Curr. Microbiol. App. Sci., 8(5): 775-783.

Desta F, Bissa M and Korbu L (2015). Crop water requirement determination of chickpea in the central vertisol areas of Ethiopia using FAO CROPWAT model. African Journal of Agricultural Research, 10(7): 685-689.

Dheeravath V, Thenkabail PS, Chandrakantha G, Noojipady P, Reddy GPO, Biradar CM, Gumma MK and Velpuri M (2010). Irrigated areas of India derived using MODIS 500 m time series for the years 2001-2003. ISPRS Journal of Photogrammetry and Remote sensing, 65: 42-59.

Dingre SK, Gorantiwar SD and Kadam S (2021). Correlating the field water balance derived crop coefficient (Kc) and canopy reflectance-based NDVI for irrigated sugarcane. Springer, DOI:10.1007/s11119-020-09774-8.

Doorenbos J and Pruitt WO (1977). Crop water requirements. FAO Irrigation Drainage Paper No. 24, FAO, Rome.

El-Shirbeny MA, Abd-Elraouf MA, Badr MA and Bauomy EM (2014). Assessment of wheat crop coefficient using remote sensing techniques. World Research Journal of Agricultural Sciences, ISSN: 2326-7266, 1(2): 12-16.

FAO (2005). Report. Agriculture, food and water – A contribution to the world water Development.

Farg E, Arafat SM, Abd EI-Wahed MS and EL-Gindy AM (2012). Estimation of evapotranspiration ETc and crop coefficient Kc of wheat in south Nile delta of Egypt using integrated FA0-56 approach and remote sensing data. The Egyptian Journal of Remote Sensing and Space Science, 15(1): 83-89.

French AN, Hunsaker DJ, Sanchez CA, Saber M, Gonzalez JR and Anderson R (2020). Satellite-based NDVI crop coefficients and evapotranspiration with eddy covariance validation for multiple durum wheat fields in the US Southwest. Agricultural Water Management, 239: 106-266.

Gamal R, El-Shirbeny M, Abou-Hadid A, Swelam A, El-Gindy AG, Arafa Y and Nangia V (2022). Identification and Quantification of Actual Evapotranspiration Using Integrated Satellite Data for Sustainable Water Management in Dry Areas. Agronomy, 12(9): 21-43.

Gao BC (1996). NDWI- A normalized difference water index for remote sensing of vegetation liquid water from space. Remote Sensing of Environment, 58(3): 257-266.

Gears C and Erasmus D (2001). Review of mapping, Geographic Information Systems: Key concerns in the South African sugar industry Proceedings South African Sugar Technologist's Association, 75: 34-37.

Gomez MG (2017). Joint use of Sentinel-1 and Sentinel-2 for land cover classification: A machine learning approach. Sweden.

Gontia NK and Tiwari KN (2010). Estimation of crop coefficient and Evapotranspiration of wheat (Triticum aestivum) in an irrigation command using remote sensing and GIS. J. Water Resources Management, 24: 399-414.

Gonzalez AR, Sanchez DGR and Duarte JIS (2020). Development of crop coefficient for forage safflower based on vegetation indices. Technologia y ciencias del agua, ISSN 2007-2422, 11(6): 29-60.

Grains Research and Development Corporation (2022). GrowNotes™-GRDC. accessed 20 December 2021 <http://www.grdc.com.au/resources-and-publications/grownotes>

Guruge PAP (1996). The use of remote sensing data for identifying development of sugarcane in Buttala area. Proc. of XVII Asian Conference on Remote Sensing.

Hafeez MM, CheminY, Bouman BAM and Van De Giesen N (2002). Estimation of spatially distributed evapotranspiation through remote sensing: A case study for irrigated rice in the Philippines. Proceedings of the International workshop on water-wise rice production, 8-11 April, Pjilippines: International Rice Research Institute, pp. 347-356.

Hassan DF, Abdalkadhum AJ, Mohammed RJ and Shaban A (2022). Integration remote sensing and meteorological data to monitoring plant phenology and estimation crop coefficient and evapotranspiration. Journal of Ecological Engineering, 23(4).

Howell TA, Evett SR, Tolk JA and Schneider AD (2004). Evapotranspiration of Full, Deficit-Irrigated and Dryland Cotton on the Northern Texas High Plains. J. lrrig. and Drain. Eng., 130(4): 277-285.

Howell TA, Evett SR, Tolk JA, Copeland KS, Dusek DA and Colaizzi PD (2006). Crop coefficients developed at Bushland, Texas for corn, wheat, sorghum, soybean, cotton, and alfalfa. In Proc. World Water and Environmental Resources Congress. Examining the Confluence of Environmental and Water Concerns, May 21-25, Omaha, Nebraska.

Hudait M and Patel PP (2022). Crop-type mapping and acreage estimation in smallholding plots using Sentinel-2 images and machine learning algorithms: Some comparisons. The Egyptian Journal of Remote Sensing and Space Science, 25(1): 147-156.

Huete AR (1988). A soil adjusted vegetation index (SAVI). J. Remote Sens. Environ., 25: 295-309.

Hunsaker DJ (1999). Basal crop coefficients and water use for early maturity cotton. Trans. ASAE., 42(4): 927-936.

Hunsaker DJ, Pinter PJ, Barnes EM and Kimball BA (2003). Estimating cotton evapotranspiration crop coefficients with a multispectral vegetation index. J. lrrig Sci., 22: 95-104.

Jackson RD, ldso SB, Reginato RJ and Pinter PJ (1980). Remotely sensed crop temperatures and reflectances as inputs to irrigation scheduling. In: Irrigation and drainage special conference proceedings, 23-25 July, Boise, Idaho. ASCE, New York, pp 390-397.

Jackson RD and Huete AR (1991). Interpreting vegetation indices. Preventive veterinary medicine, 11(3-4): 185-200.

Jagtap SS and Jones JW (1989). Stability of crop coefficients under different climatic and irrigation management practices. J. lrrig. Sci., 10: 231-244.

Jordan CF (1969). Derivation of leaf area index from quality of light on the forest floor. Ecology, 50: 663-666.

Kadam S.A., S.D. Gorantiwar, S.D. Dahiwalkar, S.R. Satpute and P.G. Popale (2017). Relationship between spectral reflectance, NDVI and water stress conditions of soybean (Glycine max. L). J. Agric Res. Technol., 42(3): 149-153.

Kamble B, Kilic A and Hubbard (2013). Estimating Crop Coefficients Using Remote Sensing Based Vegetation Index. Remote Sens., 5: 1588-1602.

Kimothi MM, Kalubarm MH, Dutta S, Thapa R and Sood RK (1997). Remote sensing of horticultural plantations in Kumarsain tehsil in Shimla district, Himachal Pradesh. J. Indian Society of Remote Sensing, 25: 19-26.

Lasko K, Vadrevu P, Tran VT and Justice C (2018). Mapping Double and sinlge Crop Paddy Rice with Sentnel-1A at varying Spatial Scales and Polarizations in Hanoi, Vietnam. IEEE Journal of Selected Topics in Applied Earth Observation and Remote Sensing, 11(2): 498-512.

Mamta K, Patel NR and Khayruloevich PY (2013). Estimation of crop water requirement in rice-wheat system from multi-temporal AWIFS satellite data. International journal of geomatics and geosciences, 4(1): 61-74.

Marek GW, Auvermann BW, Marek TH and Hefiin K (2006). Evaluating the use of reference evapotranspiration data as an estimator of feed yard evaporation. ASAE Paper No. 064025. In Proc. 2006 International ASABE Annual Conference, Portland, Oregon: ASABE.

Mariana M, Ronald C, Sergio J and Waldo B (2021). Maize crop coefficient estimation based on spectral vegetation indices and vegetation cover fraction derived from UAV-based multispectral images. Journal of Agronomy, 11: 668-686.

Mehta R, Pandey V, Lunagaria MM and Anilkumar (2016). Reference and crop evapotranspiration estimation for mustard and chickpea at different locations of Gujarat. International Journal of Advanced Research and Review, 1(6): 48-56.

Mohammed EA, Ali AM, Badr MA, Bauomy EM (2014). Assessment of wheat crop coefficient using remote sensing techniques. World Research Journal of Agricultural Sciences, 1(2): 12-16.

Mohite JD, Sawant SA, Kumar A, Prajapati M, Pusapati SV, Singh D and Pappula S (2018). Operational near real time rice area mapping using multi-temporal sentinel-1 sar observations. The International Archives of the Photogrammetry, Remote Sensing and Spatial Information Sciences, 42(4): 1-5.

Monteith JL (1965). Evaporation and environment. In G.E. Fogg (ed.) The state and movement of water in living organisms. In Proc. Symp. Soc. Exp. Biol., 19: 205–234.

Moran MS, Clarke TR, Inoue Y and Vidal A (1994). Estimating crop water deficit using the relation between the surface-air temperature and spectral vegetation index. Remote Sens. Environ., 49: 246-263.

Moran MS, Mass SJ and Pinter PJ (1995). Combining remote sensing and modeling for estimating surface evaporation and biomass production. Remote Sensing Review, 12: 335-353.

Mukherjee J, Gebru G, Sood A, Mahey RK, Bal SK, Singh H and Sidhu PK (2010). Wheat yield and acreage prediction using LISS-III and AWiFS sensors data of Indian remote sensing satellite of Rupnager district of Punjab, India. Italian Journal of Remote Sensing, 42(3): 115-127.

Munshi MK (1982). A Study of the Determination ol Wheat Crop Statistics in India through the Utilisation of Landsat Data. Ph.D. Thesis. lIT Delhi.

Narciso G and Schmidt E (1999). Identification and classification of sugarcane based on satellite remote sensing. Agricultural Research Council, Institute for Soil, Climate and Water. Private Bag X79, Pretoria, 0001.

Neale CMU, Bausch WC and Heerman DF (1989). Development of Reflectance based crop coefficients for corn. Trans. ASAE., 28: 773-780.

Nemani RR and Running SW (1989). Testing a theoretical climate-soil-leaf area hydrologic equilibrium of forests using satellite data and ecosystem simulation. Agricultural and Forest Meteorology, 44(3-4): 245-260.

Ozcan O, Musaoglu N and Ustundag B (2014). Crop water requirement estimation of wheat cultivated fields by remote sensing and GIS. J. Food, Agri. and Environ., 12(1): 289-293.

Pakhale G, Gupta P and Nale J (2010). Crop and irrigation water requirement estimation by remote sensing and GIS: A case study of Karnal district. Haryana, India. Int. J. Engineering and Technology, 2(4): 207-211.

Palacios EV, Palacios LS and Mejia ES (2012). Models of Crop Growth and Remote Sensing for Estimating Crop Yield in Irrigated Agriculture. < http: II cigr. ageng 2012.org/documentos/orales/O-SW.pdf dated 20.04.2013>: 1-6.

Pandey V, Patel VJ, Vadodaria RP, Patel HR and Shekh AM (2008). Irrigation water requirement and production potentials of major crops over Narmada canal command area in Gujarat. Journal of Agrometeorology, 10: 314-320.

Panigrahy S and Chakraborty M (1996). A case study for Burdhaman district of West Bengal. Indo-U.S Workshop on Remote Sensing and its applications, Mumbai, India.

Parmar HV and Gontia NK (2016). Remote Sensing based vegetation indices an crop coefficient relationship for estimation of crop evapotranspiration in Ozat-II canal command. Journal of Agrometerology, 18(1): 137-139.

Penman HL (1948). Natural evaporation from open water, bare soil, and grass. Proc. Roy. Soc. London, 193: 120-146.

Pimpale AR, Rajankar PB, Wadatkar SB and Ramteke IK (2014). Determination of spatial crop coefficient of chickpea using remote sensing and GIS. American International Journal of Research in Formal, Applied and Natural Sciences, 14(349): 59-64.

Pimpale AR, Rajankar PB, Wadatkar SB and Ramteke IK (2015). Application of remote sensing and GIS for acreage estimation of wheat. International Journal of Engineering, Business and Enterprise Applications, 12(2): 167-171.

Pimpale AR, Rajankar PB, Wadatkar SB, Wanjari SS and Ramteke IK (2015). Estimation of water requirement of wheat using multi-spectral vegetation indices. Journal of Agrometeorology, 17(2): 208-212.

Pimpale AR, Wadatkar SB, Pimpale RA, Rajankar PB and Ramteke IK (2019). Comparative performance of different multispectral vegetation indices for determination of crop coefficients of rabi sorghum. International Journal of Agricultural Sciences, 2(6): 8164-8167.

Qi J, Huete AR, Moran MS, Chehbouni A and Jackson RD (1993). Interpretation of vegetation indices derived from multi-temporal SPOT images, Remote Sens. Environ., 44: 89-101.

Rawat KS and Mishra AK (2020). Retrieval of Kc from SEBAL and comparison among NDVI and LAI based Kc. International journal of advanced research in engineering and technology, 11(9): 1108-1111.

Ray SS and Oadhwal VK (2001). Estimation of crop evapotranspiration of irrigation command area using remote sensing and GIS. Agric. Water Manage., 49: 239-249.

Reyes-González A, Kjaersgaard J, Trooien T, Hay C and Ahiablame L (2018). Estimation of crop evapotranspiration using satellite remote sensing-based vegetation index. Advances in Meteorology, 2018.

Robertson A, Gitelson A, Peng Y, Walter-Shea E, Leavitt B and Arkebauer T (2013). Continuous monitoring of crop reflectance, vegetation fraction, and identification of developmental stages using a four band radiometer. Agronomy Journal, 105(6): 1769-1779.

Rouse JW, Haas RH, Schell JA and Deering OW (1973). Monitoring vegetation systems in the Great Plains with ERTS. Third ERTS Symposium, NASA, SP-351(I): 309-317.

Salah ER, Abdelghani C and Benoit D (2010). Combining Satellite Remote Sensing Data with the FAO-56 Dual approach for water use mapping in irrigated wheat fields of a semi-arid region Remote Sens., 2010(2): 375-387. ISSN 2072-4292 doi:10.3390/rs2010375.

Sandholt I, Rasmussen K and Andersen J (2002). A simple interpretation of the surface temperature/vegetation index space for assessment of surface moisture status. Remote Sens. Environ., 79(2-3): 213-224.

Santos C, Lorite IJ, Tasumi M, Allen RG and Fereres E (2007). Integrating satellite- based evapotranspiration with simulation models for irrigation management at the scheme level. J. Irri. Sci., 3: 277–288.

Shao G, Han W, Zhang H, Liu S (2021). Mapping maize crop coefficient Kc using random forest algorithm based on leaf area index and UAV-based multispectral vegetation indices. Agricultural Water Management, 252:106-906.

Sharma R (1995). Coconut inventory using remote sensing data. SAC Courier. 20. Space Applications Centre, Ahmedabad, India.

Silva KF, de Moraes DH, Mesquita M, de Oliveira HF, Nascimento WM, Battisti R and Flores RA (2021). Water requirement and crop coefficient of three chickpea cultivars for the edaphoclimatic conditions of the Brazilian savannah biome. Irrigation Science, 39(5): 607-616.

Singh SK, Dutta S and Dharaiya N (2016). Remote Sensing Indices for Crop Water Management. International Journal of Engineering Sciences & Research Technology, ISSN: 2277-9655.

Spiliotopoulos M, Loukas A (2019). Hybrid Methodology for the Estimation of Crop Coefficients Based on Satellite Imagery and Ground Based Measurements. Water, 11: 13-64.

Subbarao NV, Mani JK, Shrivastava A, Srinivas K and Varghese AO (2021). Acreage estimation of kharif rice crop using Sentinel-1 temporal SAR data. Spatial Information Research, 29(4): 495-505.

Suleiman AA, Tojo SCM and Hoogenboom G (2007). Evaluation of FA0-56 crop coefficient procedures for deficit irrigation management of cotton in a humid-climate. Agric. Water Manage., 91(1-3): 33-42.

Sutariya S, Ankur H and Tiwari M (2021). Estimation of Actual Evapotranspiration in Panam Canal Command Using Remote Sensing and Geographical Information System (GIS). International Journal of Environment and Geoinformatics, 8(2): 193-199.

Tasumi M, Allen RG, Trezza R, Morse A and Kramber W (2006). Application of MODIS and Landsat based evapotranspiration for western states water management. Doctoral dissertation, Colorado State University, Libraries.

Thornthwaite CW (1948). An approach toward a rational classification of climate. The Geographical Review, 38(1): 55-94.

Torbick N, Chowdhury D, Salas W and Qi J (2017). Monitoring Rice Agriculture across Myanmar Using Time Series Sentinel-1 Assisted by Landsat-8 and PALSAR-2. Remote sensing, 9: 119.

United States Geological Survey (2022). EarthExplorer. accessed 15 April 2022 <http://www.earthexplorer.usgs.gov>

Vaidyanathan A (2011). Report of the Expert Committee on Agricultural Statistics. Directorate of Economics and Statistics, Department of Agriculture and Cooperation, New Delhi.

Wiegand CL and Richardson AJ (1990). Use of spectral vegetation indices to infer leaf area, evapotranspiration and yield. I. Rationale. Agronomy Journal, 82(3): 623-9.

Wright JL (1982). New evapotranspiration crop coefficients. J. lrrig. Drain. Div. ASCE, 108: 57-74.

Zhang Yu, Han W, Niu X and Li G (2019). Maize Crop Coefficient Estimated from UAV Measured Multispectral Vegetation Indices. Sensors, 19: 235-250. doi:10.3390/s19235250.

Zolfagharnejad H, Kamkar B and Abdi O (2017). Vegetation index-deduced crop coefficient of wheat (triticum aestivum) using remote sensing: case study on four basins of Golestan Province, Iran. International journal of agricultural and biosystems engineering, 11(7): 498-501.

ANNEXURE I

Daily Meteorological Data of Akola (2021-22)

MET Week	Date	Temperature (ºC)		Relative Humidity (%)		Wind Speed (km/hr)	BSH (hrs)	Rainfall (mm)
		Max.	Min.	I	II			
47	19-11-2021	33	20.6	84	41	2.7	6.8	0.0
	20-11-2021	32.4	21.2	72	60	4	4.3	0.0
	21-11-2021	30	21.2	86	56	3.9	2.4	1.4
	22-11-2021	31.8	21.8	90	54	2.8	6.3	0.0
	23-11-2021	32.2	20.6	90	53	0.2	4.6	0.0
	24-11-2021	32.4	19.6	86	47	0.4	7.3	0.0
	25-11-2021	32.6	17.5	91	47	0.6	6.3	0.0
48	26-11-2021	32.2	15.4	86	36	0.2	7.7	0.0
	27-11-2021	31.2	14.2	73	18	0.7	8.3	0.0
	28-11-2021	31.4	12.2	60	23	1.4	8.7	0.0
	29-11-2021	30.2	13	66	26	1.5	8.3	0.0
	30-11-2021	30.4	15.4	77	27	1.7	6.7	0.0
	01-12-2021	28.4	16	66	32	1.6	3.5	0.0
	02-12-2021	29.6	15	84	44	1.4	4.1	0.0
49	03-12-2021	26.6	17.8	85	42	0.8	0	0.0
	04-12-2021	26.6	13.2	88	44	2.3	0.4	0.0
	05-12-2021	26	14.8	82	40	0.3	5.8	0.0
	06-12-2021	30.2	14.5	92	44	0.5	7.3	0.0
	07-12-2021	29	14.4	89	50	0.2	1.6	0.0
	08-12-2021	28.8	17.5	83	50	0.7	4.6	0.0
	09-12-2021	28.6	18.5	73	38	0.9	2.6	0.0
50	10-12-2021	30.2	16	84	39	1.7	6	0.0
	11-12-2021	29.8	13.5	87	36	0.8	7	0.0
	12-12-2021	29.5	14.2	80	39	0.8	6.4	0.0
	13-12-2021	28.6	12.2	80	33	1.3	6.9	0.0
	14-12-2021	28.8	12.4	77	33	1.3	7.4	0.0
	15-12-2021	28.2	13	72	34	2.3	5.6	0.0
	16-12-2021	28.5	12.5	71	35	1.8	4.5	0.0
51	17-12-2021	28	12.5	70	33	1.5	4.5	0.0
	18-12-2021	28.8	11.5	88	37	0.2	6.7	0.0
	19-12-2021	27.8	10.2	84	36	0.3	6.6	0.0
	20-12-2021	27.6	5.8	92	23	0.5	6.4	0.0
	21-12-2021	25.6	7	81	32	1.1	7.9	0.0
	22-12-2021	26	6.9	83	20	0.2	8.3	0.0
	23-12-2021	29.3	8	85	23	0.3	8.5	0.0
52	24-12-2021	30	10.5	80	40	0.1	8.3	0.0
	25-12-2021	27.4	14.2	78	38	0.5	7.6	0.0
	26-12-2021	28.4	11.4	91	32	0.6	8.3	0.0
	27-12-2021	29.2	11.6	91	31	0.2	7.3	0.0
	28-12-2021	29.2	13.4	80	64	0.5	7.6	0.0
	29-12-2021	28.6	13.2	98	67	1.4	1.3	42.6

	30-12-2021	22.4	12.5	86	62	2.6	3.3	0.0
	31-12-2021	22	13.1	89	68	3.5	0.2	0.0
1	01-01-2022	23.4	13.2	93	65	1.3	1.2	0.0
	02-01-2022	23	13.6	96	55	0.3	4.6	0.0
	03-01-2022	26.6	13.5	93	44	0.9	6.5	0.0
	04-01-2022	27.2	12.8	95	41	0.7	7	0.0
	05-01-2022	28.4	13.3	87	35	0.2	7	0.0
	06-01-2022	29.2	12.8	87	42	0.7	7.3	0.0
	07-01-2022	29.4	13.5	93	47	0.9	5.9	0.0
2	08-01-2022	28.4	14.2	88	46	1.6	6.9	0.0
	09-01-2022	29.4	17	94	65	1.9	5.3	0.0
	10-01-2022	24.6	12.5	83	57	1.4	1.3	0.0
	11-01-2022	24.8	15.2	84	68	0.5	5.6	0.0
	12-01-2022	23.2	14.2	87	65	0.2	0	0.0
	13-01-2022	23.8	12.4	89	50	0.5	2.8	0.0
	14-01-2022	25.5	16.4	83	82	3.1	5.5	0.0
3	15-01-2022	19.4	11.5	98	59	0.7	0	1.0
	16-01-2022	24.8	12.5	96	52	1.2	6.1	0.0
	17-01-2022	25.8	12.2	93	51	2.4	7	0.0
	18-01-2022	28	12	91	53	0.7	7.7	0.0
	19-01-2022	27.4	10.5	88	40	0.9	7.7	0.0
	20-01-2022	28.8	9.4	88	36	0.6	8.4	0.0
	21-01-2022	28.8	11.5	73	33	2	8.9	0.0
4	22-01-2022	28.6	11	76	38	1.9	8.8	0.0
	23-01-2022	28.8	14.4	74	34	5.4	8.1	0.0
	24-01-2022	25.2	10.3	75	34	5.7	7	0.0
	25-01-2022	22.8	7	78	31	1.6	6.2	0.0
	26-01-2022	23.6	6.6	79	37	0.6	7.5	0.0
	27-01-2022	24	5	79	32	0.3	8.7	0.0
	28-01-2022	24.4	4.2	67	32	0.4	9	0.0
5	29-01-2022	24.6	4.5	72	32	1	7.4	0.0
	30-01-2022	26	6.2	80	39	0.3	8.9	0.0
	31-01-2022	24.8	7	64	20	0.4	9.3	0.0
	01-02-2022	30.8	10	69	19	1.3	9.2	0.0
	02-02-2022	31	9	77	23	0.5	9.1	0.0
	03-02-2022	31.2	11	74	19	0.4	9	0.0
	04-02-2022	31.4	13.9	79	24	5.5	9	0.0
6	05-02-2022	26	6	71	19	1.9	8.5	0.0
	06-02-2022	28.2	7.8	73	30	0.7	8.7	0.0
	07-02-2022	29.8	9.6	70	28	1.3	8.7	0.0
	08-02-2022	30.8	11.5	60	29	0.8	8.7	0.0
	09-02-2022	32.8	11	65	33	1.7	7.5	0.0
	10-02-2022	30	11.2	69	21	3	7.9	0.0
	11-02-2022	31	8.5	70	30	2.1	8.5	0.0
7	12-02-2022	28	9.2	59	26	1.4	9.3	0.0
	13-02-2022	29.2	8	79	32	1.7	9	0.0
	14-02-2022	29	11.6	87	25	0.9	8.7	0.0
	15-02-2022	31	15.2	73	27	1.5	8	0.0

	16-02-2022	30.2	13	72	24	1.4	7.9	0.0
	17-02-2022	32	17.4	53	38	1.5	8.6	0.0
	18-02-2022	29.6	15.6	84	39	5.6	5.9	0.0
	19-02-2022	31.2	17.6	76	35	2.6	5.9	0.0
	20-02-2022	33	17.5	75	33	1.1	5.9	0.0
	21-02-2022	32.6	11	76	25	3.2	9.2	0.0
8	22-02-2022	32.8	10.4	68	14	1.3	9.1	0.0
	23-02-2022	35	14	69	19	1.5	9.3	0.0
	24-02-2022	36.4	17.5	67	21	2.2	8.8	0.0
	25-02-2022	35.4	13.5	72	17	2.5	8.7	0.0
	26-02-2022	33.6	16.3	54	17	2.1	8.9	0.0
	27-02-2022	35.8	16.4	68	22	4.3	8	0.0
	28-02-2022	35	15.5	72	24	2.3	8.2	0.0
9	01-03-2022	35.2	17	78	22	1.5	7.8	0.0
	02-03-2022	35.2	16.2	63	20	2	7.3	0.0
	03-03-2022	35.8	18.6	57	21	2.6	7.6	0.0
	04-03-2022	35	16.2	65	27	2.4	4.8	0.0
	05-03-2022	35.6	16.7	69	23	1.1	8.2	0.0
	06-03-2022	35.2	17.5	80	26	1.4	7.6	0.0
	07-03-2022	35	18	83	30	2.3	7.9	0.0
10	08-03-2022	35.2	20.6	77	25	2.8	7.2	0.0
	09-03-2022	33.4	17	67	41	2.5	5.6	0.0
	10-03-2022	29.2	14.3	64	25	3.1	1	0.0
	11-03-2022	35	16.5	75	28	0.6	7.3	0.0
	12-03-2022	35.6	17.2	57	18	1.3	8.1	0.0
	13-03-2022	36.2	14.5	53	24	1.4	8.8	0.0
	14-03-2022	34	14.2	48	13	1.1	9	0.0
11	15-03-2022	37.5	14.5	68	25	0.9	8	0.0
	16-03-2022	36.6	16	64	22	0.9	9.1	0.0
	17-03-2022	40.8	19	62	16	2.5	9.1	0.0
	18-03-2022	41.6	18.5	63	15	2.7	9.3	0.0

ANNEXURE II

ETo calculations of Akola district (2021-22)

Date	Week	Altitude	J day	T	P	Ɣ	Δ	U2	eTmax	eTmin	es	ea	es-ea	dr	δ	Deg	Min	φ	Tanφ	Tan δ	ωs	Ra	N	Rs	Rso	Rns	Rnl	Rn	G	ETo (mm)	
1	2	3	4	5	6	7	8	9	10	11	12	13	14	15	16	17	18	19	20	21	22	23	24	25	26	27	28	29	30	31	32
19-11-2021	47	285	323	26.8	97.976	0.065	0.207	0.691	5.030	2.427	3.728	2.050	1.678	1.025	-0.350	20	42	0.361	0.378	-0.365	1.433	26.860	10.950	15.055	20.298	11.593	3.617	7.976	0	3.132	
20-11-2021	47	285	324	26.8	97.976	0.065	0.207	1.023	4.863	2.518	3.691	2.365	1.325	1.025	-0.353	20	42	0.361	0.378	-0.369	1.431	26.760	10.938	11.950	20.222	9.201	2.221	6.981	0	2.899	18.680
21-11-2021	47	285	325	25.6	97.976	0.065	0.195	0.998	4.243	2.518	3.380	2.271	1.110	1.025	-0.357	20	42	0.361	0.378	-0.373	1.430	26.662	10.926	9.594	20.149	7.387	1.478	5.909	0	2.436	
22-11-2021	47	285	326	26.8	97.976	0.065	0.207	0.716	4.701	2.612	3.657	2.445	1.212	1.026	-0.360	20	42	0.361	0.378	-0.377	1.428	26.567	10.915	14.309	20.077	11.018	2.947	8.070	0	2.956	
23-11-2021	47	285	327	26.4	97.976	0.065	0.203	0.051	4.809	2.427	3.618	2.366	1.251	1.026	-0.363	20	42	0.361	0.378	-0.380	1.427	26.475	10.904	12.203	20.007	9.396	2.335	7.061	0	2.218	
24-11-2021	47	285	328	26	97.976	0.065	0.199	0.102	4.863	2.281	3.572	2.124	1.448	1.026	-0.367	20	42	0.361	0.378	-0.384	1.425	26.386	10.894	15.437	19.940	11.887	3.722	8.164	0	2.596	
25-11-2021	47	285	329	25.05	97.976	0.065	0.189	0.153	4.918	2.000	3.459	2.066	1.393	1.027	-0.370	20	42	0.361	0.378	-0.388	1.424	26.300	10.883	14.187	19.875	10.924	3.315	7.609	0	2.442	
26-11-2021	48	285	330	23.8	97.976	0.065	0.177	0.051	4.809	1.750	3.279	1.618	1.661	1.027	-0.373	20	42	0.361	0.378	-0.391	1.423	26.216	10.873	15.837	19.812	12.194	4.523	7.671	0	2.347	
27-11-2021	48	285	331	22.7	97.976	0.065	0.167	0.179	4.544	1.619	3.082	1.000	2.082	1.027	-0.376	20	42	0.361	0.378	-0.394	1.421	26.136	10.864	16.518	19.751	12.719	5.882	6.837	0	2.286	16.463
28-11-2021	48	285	332	21.8	97.976	0.065	0.159	0.358	4.596	1.421	3.009	0.955	2.054	1.028	-0.378	20	42	0.361	0.378	-0.397	1.420	26.059	10.855	16.958	19.692	13.057	6.166	6.891	0	2.557	
29-11-2021	48	285	333	21.6	97.976	0.065	0.158	0.384	4.292	1.498	2.895	1.052	1.843	1.028	-0.381	20	42	0.361	0.378	-0.400	1.419	25.984	10.846	16.439	19.636	12.658	5.700	6.958	0	2.543	
30-11-2021	48	285	334	22.9	97.976	0.065	0.169	0.435	4.341	1.750	3.046	1.260	1.786	1.028	-0.383	20	42	0.361	0.378	-0.403	1.418	25.913	10.837	14.489	19.583	11.156	4.487	6.670	0	2.518	
01-12-2021	48	285	335	22.2	97.976	0.065	0.163	0.409	3.869	1.818	2.844	1.219	1.625	1.029	-0.386	20	42	0.361	0.378	-0.406	1.417	25.845	10.829	10.638	19.531	8.191	2.673	5.518	0	2.104	
02-12-2021	48	285	336	22.3	97.976	0.065	0.164	0.358	4.147	1.705	2.926	1.629	1.297	1.029	-0.388	20	42	0.361	0.378	-0.409	1.416	25.781	10.821	11.329	19.482	8.723	2.632	6.091	0	2.108	
03-12-2021	49	285	337	22.2	97.976	0.065	0.163	0.205	3.483	2.038	2.760	1.598	1.163	1.029	-0.390	20	42	0.361	0.378	-0.411	1.415	25.719	10.814	6.430	19.436	4.951	0.589	4.362	0	1.45	
04-12-2021	49	285	338	19.9	97.976	0.065	0.144	0.588	3.483	1.517	2.500	1.434	1.066	1.029	-0.392	20	42	0.361	0.378	-0.414	1.414	25.661	10.807	6.890	19.392	5.305	0.811	4.495	0	1.754	12.727
05-12-2021	49	285	339	20.4	97.976	0.065	0.148	0.077	3.361	1.684	2.522	1.363	1.160	1.030	-0.394	20	42	0.361	0.378	-0.416	1.413	25.606	10.800	13.277	19.351	10.223	3.713	6.510	0	1.912	
06-12-2021	49	285	340	22.35	97.976	0.065	0.164	0.128	4.292	1.651	2.972	1.704	1.268	1.030	-0.396	20	42	0.361	0.378	-0.418	1.412	25.555	10.794	15.030	19.312	11.573	4.137	7.436	0	2.284	
07-12-2021	49	285	341	21.7	97.976	0.065	0.159	0.051	4.006	1.641	2.823	1.731	1.092	1.030	-0.398	20	42	0.361	0.378	-0.420	1.411	25.507	10.788	8.268	19.276	6.367	1.327	5.039	0	1.499	
08-12-2021	49	285	342	23.15	97.976	0.065	0.171	0.179	3.960	2.000	2.980	1.820	1.160	1.030	-0.399	20	42	0.361	0.378	-0.422	1.411	25.462	10.783	11.797	19.242	9.084	2.734	6.349	0	2.017	
09-12-2021	49	285	343	23.55	97.976	0.065	0.175	0.230	3.914	2.130	3.022	1.521	1.501	1.031	-0.401	20	42	0.361	0.378	-0.424	1.410	25.421	10.778	9.422	19.211	7.255	1.988	5.267	0	1.812	
10-12-2021	50	285	344	23.1	97.976	0.065	0.171	0.435	4.292	1.818	3.055	1.601	1.455	1.031	-0.402	20	42	0.361	0.378	-0.425	1.409	25.384	10.773	13.415	19.182	10.329	3.667	6.662	0	2.400	
11-12-2021	50	285	345	21.65	97.976	0.065	0.158	0.205	4.195	1.547	2.871	1.428	1.443	1.031	-0.403	20	42	0.361	0.378	-0.427	1.409	25.350	10.769	14.576	19.157	11.224	4.351	6.873	0	2.204	
12-12-2021	50	285	346	21.85	97.976	0.065	0.160	0.205	4.123	1.619	2.871	1.452	1.419	1.031	-0.404	20	42	0.361	0.378	-0.428	1.408	25.319	10.765	13.856	19.134	10.669	4.009	6.660	0	2.144	
13-12-2021	50	285	347	20.4	97.976	0.065	0.148	0.333	3.914	1.421	2.668	1.214	1.453	1.031	-0.405	20	42	0.361	0.378	-0.429	1.408	25.292	10.762	14.431	19.113	11.112	4.548	6.564	0	2.235	15.805
14-12-2021	50	285	348	20.6	97.976	0.065	0.150	0.333	3.960	1.440	2.700	1.208	1.492	1.032	-0.406	20	42	0.361	0.378	-0.430	1.408	25.269	10.759	15.007	19.095	11.556	4.855	6.701	0	2.287	
15-12-2021	50	285	349	20.6	97.976	0.065	0.150	0.588	3.824	1.498	2.661	1.189	1.472	1.032	-0.407	20	42	0.361	0.378	-0.431	1.407	25.249	10.756	12.885	19.080	9.921	3.857	6.065	0	2.384	
16-12-2021	50	285	350	20.5	97.976	0.065	0.149	0.460	3.891	1.449	2.670	1.196	1.475	1.032	-0.408	20	42	0.361	0.378	-0.432	1.407	25.232	10.754	11.587	19.068	8.922	3.220	5.702	0	2.150	
17-12-2021	51	285	351	20.25	97.976	0.065	0.147	0.384	3.780	1.449	2.615	1.131	1.484	1.032	-0.408	20	42	0.361	0.378	-0.432	1.407	25.220	10.752	11.582	19.059	8.919	3.281	5.638	0	2.048	
18-12-2021	51	285	352	20.15	97.976	0.065	0.146	0.051	3.960	1.357	2.658	1.330	1.329	1.032	-0.409	20	42	0.361	0.378	-0.433	1.407	25.211	10.751	14.159	19.052	10.902	4.255	6.647	0	1.929	13.353
19-12-2021	51	285	353	19	97.976	0.065	0.137	0.077	3.736	1.245	2.490	1.195	1.295	1.032	-0.409	20	42	0.361	0.378	-0.433	1.406	25.205	10.750	14.039	19.048	10.810	4.331	6.479	0	1.875	
20-12-2021	51	285	354	16.7	97.976	0.065	0.121	0.128	3.693	0.922	2.308	0.849	1.459	1.032	-0.409	20	42	0.361	0.378	-0.433	1.406	25.204	10.749	13.804	19.046	10.629	4.628	6.001	0	1.766	
21-12-2021	51	285	355	16.3	97.976	0.065	0.118	0.281	3.283	1.002	2.142	0.931	1.211	1.032	-0.409	20	42	0.361	0.378	-0.433	1.406	25.205	10.749	15.563	19.048	11.984	5.344	6.639	0	2.053	
22-12-2021	51	285	356	16.45	97.976	0.065	0.119	0.051	3.361	0.995	2.178	0.749	1.429	1.033	-0.409	20	42	0.361	0.378	-0.433	1.406	25.211	10.750	16.036	19.052	12.347	5.973	6.374	0	1.751	
23-12-2021	51	285	357	18.65	97.976	0.065	0.134	0.077	4.076	1.073	2.574	0.925	1.650	1.033	-0.409	20	42	0.361	0.378	-0.433	1.407	25.220	10.750	16.275	19.059	12.532	5.909	6.623	0	1.931	
24-12-2021	52	285	358	20.25	97.976	0.065	0.147	0.026	4.243	1.270	2.756	1.356	1.400	1.033	-0.408	20	42	0.361	0.378	-0.433	1.407	25.233	10.752	16.048	19.068	12.357	5.088	7.269	0	2.082	15.561
25-12-2021	52	285	359	20.8	97.976	0.065	0.151	0.128	3.650	1.619	2.635	1.325	1.310	1.033	-0.408	20	42	0.361	0.378	-0.432	1.407	25.249	10.753	15.235	19.081	11.731	4.780	6.950	0	2.108	
26-12-2021	52	285	360	19.9	97.976	0.065	0.144	0.153	3.869	1.348	2.608	1.232	1.376	1.033	-0.407	20	42	0.361	0.378	-0.431	1.407	25.269	10.755	16.068	19.096	12.372	5.273	7.099	0	2.161	
27-12-2021	52	285	361	20.4	97.976	0.065	0.148	0.051	4.052	1.366	2.709	1.250	1.459	1.033	-0.407	20	42	0.361	0.378	-0.431	1.407	25.293	10.758	14.905	19.114	11.477	4.721	6.756	0	1.973	

28-12-2021	52	285	362	21.3	97.976	0.065	0.155	0.128	4.052	1.537	2.795	1.912	0.883	1.033	-0.406	20	42	0.361	0.378	-0.430	1.408	25.320	10.761	15.272	19.134	11.759	3.944	7.816	0	2.318	
29-12-2021	52	285	363	20.9	97.976	0.065	0.152	0.358	3.914	1.517	2.716	2.055	0.661	1.033	-0.405	20	42	0.361	0.378	-0.428	1.408	25.351	10.764	7.869	19.157	6.059	1.049	5.010	0	1.590	
30-12-2021	52	285	364	17.45	97.976	0.065	0.126	0.665	2.709	1.449	2.079	1.463	0.616	1.033	-0.404	20	42	0.361	0.378	-0.427	1.409	25.385	10.767	10.236	19.183	7.882	2.214	5.668	0	1.817	
31-12-2021	52	285	365	17.55	97.976	0.065	0.127	0.895	2.644	1.508	2.076	1.570	0.506	1.033	-0.403	20	42	0.361	0.378	-0.426	1.409	25.423	10.772	6.592	19.212	5.076	0.653	4.422	0	1.512	
01-01-2022	1	285	1	18.3	97.976	0.065	0.132	0.333	2.878	1.517	2.198	1.641	0.557	1.033	-0.401	20	42	0.361	0.378	-0.424	1.410	25.472	10.777	7.786	19.249	5.995	1.117	4.879	0	1.467	
02-01-2022	1	285	2	18.3	97.976	0.065	0.132	0.077	2.809	1.558	2.184	1.520	0.663	1.033	-0.400	20	42	0.361	0.378	-0.422	1.411	25.518	10.782	11.823	19.284	9.104	2.833	6.270	0	1.749	13.963
03-01-2022	1	285	3	20.05	97.976	0.065	0.145	0.230	3.483	1.547	2.515	1.486	1.029	1.033	-0.398	20	42	0.361	0.378	-0.420	1.411	25.567	10.787	14.095	19.321	10.853	3.908	6.945	0	2.129	
04-01-2022	1	285	4	20	97.976	0.065	0.145	0.179	3.607	1.478	2.543	1.442	1.101	1.033	-0.396	20	42	0.361	0.378	-0.418	1.412	25.619	10.793	14.713	19.361	11.329	4.223	7.106	0	2.147	
05-01-2022	1	285	5	20.85	97.976	0.065	0.152	0.051	3.869	1.527	2.698	1.341	1.357	1.033	-0.395	20	42	0.361	0.378	-0.416	1.413	25.675	10.799	14.740	19.403	11.350	4.419	6.931	0	2.031	
06-01-2022	1	285	6	21	97.976	0.065	0.153	0.179	4.052	1.478	2.765	1.494	1.271	1.033	-0.393	20	42	0.361	0.378	-0.414	1.414	25.735	10.806	15.126	19.448	11.647	4.360	7.287	0	2.252	
07-01-2022	1	285	7	21.45	97.976	0.065	0.156	0.230	4.099	1.547	2.823	1.683	1.140	1.033	-0.391	20	42	0.361	0.378	-0.412	1.415	25.797	10.813	13.487	19.495	10.385	3.431	6.954	0	2.189	
08-01-2022	2	285	8	21.3	97.976	0.065	0.155	0.409	3.869	1.619	2.744	1.602	1.142	1.033	-0.388	20	42	0.361	0.378	-0.409	1.416	25.863	10.820	14.712	19.545	11.328	4.011	7.317	0	2.426	
09-01-2022	2	285	9	23.2	97.976	0.065	0.172	0.486	4.099	1.938	3.018	2.243	0.775	1.033	-0.386	20	42	0.361	0.378	-0.407	1.417	25.932	10.828	12.830	19.597	9.879	2.638	7.241	0	2.350	
10-01-2022	2	285	10	18.55	97.976	0.065	0.134	0.358	3.093	1.449	2.271	1.483	0.788	1.033	-0.384	20	42	0.361	0.378	-0.404	1.418	26.005	10.836	8.061	19.652	6.207	1.229	4.978	0	1.588	
11-01-2022	2	285	11	20	97.976	0.065	0.145	0.128	3.130	1.727	2.429	1.790	0.639	1.032	-0.381	20	42	0.361	0.378	-0.401	1.419	26.081	10.844	13.254	19.709	10.206	3.090	7.116	0	2.052	13.559
12-01-2022	2	285	12	18.7	97.976	0.065	0.135	0.051	2.844	1.619	2.232	1.629	0.603	1.032	-0.379	20	42	0.361	0.378	-0.398	1.420	26.159	10.853	6.540	19.769	5.036	0.555	4.480	0	1.256	
13-01-2022	2	285	13	18.1	97.976	0.065	0.130	0.128	2.948	1.440	2.194	1.378	0.816	1.032	-0.376	20	42	0.361	0.378	-0.395	1.421	26.241	10.862	9.942	19.831	7.656	2.031	5.625	0	1.615	
14-01-2022	2	285	14	20.95	97.976	0.065	0.152	0.793	3.263	1.865	2.564	2.112	0.452	1.032	-0.373	20	42	0.361	0.378	-0.392	1.422	26.326	10.872	13.241	19.895	10.195	2.751	7.444	0	2.273	
15-01-2022	3	285	15	15.45	97.976	0.065	0.113	0.179	2.253	1.357	1.805	1.330	0.475	1.032	-0.370	20	42	0.361	0.378	-0.388	1.424	26.414	10.882	6.604	19.961	5.085	0.588	4.497	0	1.232	
16-01-2022	3	285	16	18.65	97.976	0.065	0.134	0.307	3.130	1.449	2.290	1.510	0.780	1.032	-0.367	20	42	0.361	0.378	-0.385	1.425	26.505	10.892	14.049	20.030	10.817	3.574	7.243	0	2.158	15.799
17-01-2022	3	285	17	19	97.976	0.065	0.137	0.614	3.322	1.421	2.372	1.508	0.864	1.032	-0.364	20	42	0.361	0.378	-0.381	1.426	26.599	10.902	15.189	20.101	11.696	4.037	7.659	0	2.478	
18-01-2022	3	285	18	20	97.976	0.065	0.145	0.179	3.780	1.403	2.591	1.640	0.951	1.031	-0.361	20	42	0.361	0.378	-0.377	1.428	26.696	10.913	16.092	20.174	12.391	4.249	8.142	0	2.408	
19-01-2022	3	285	19	18.95	97.976	0.065	0.137	0.230	3.650	1.270	2.460	1.289	1.171	1.031	-0.357	20	42	0.361	0.378	-0.373	1.429	26.796	10.924	16.142	20.250	12.430	4.718	7.712	0	2.340	
20-01-2022	3	285	20	19.1	97.976	0.065	0.138	0.153	3.960	1.179	2.570	1.232	1.338	1.031	-0.354	20	42	0.361	0.378	-0.369	1.431	26.898	10.936	17.055	20.327	13.132	5.203	7.929	0	2.360	
21-01-2022	3	285	21	20.15	97.976	0.065	0.146	0.512	3.960	1.357	2.658	1.149	1.510	1.031	-0.350	20	42	0.361	0.378	-0.365	1.432	27.003	10.948	17.727	20.406	13.650	5.701	7.949	0	2.822	
22-01-2022	4	285	22	19.8	97.976	0.065	0.143	0.486	3.914	1.313	2.613	1.242	1.371	1.031	-0.347	20	42	0.361	0.378	-0.361	1.434	27.111	10.960	17.662	20.488	13.600	5.435	8.164	0	2.786	
23-01-2022	4	285	23	21.6	97.976	0.065	0.158	1.381	3.960	1.641	2.800	1.280	1.520	1.030	-0.343	20	42	0.361	0.378	-0.357	1.436	27.221	10.972	16.853	20.571	12.977	5.099	7.877	0	3.649	
24-01-2022	4	285	24	17.75	97.976	0.065	0.128	1.458	3.206	1.253	2.229	1.015	1.214	1.030	-0.339	20	42	0.361	0.378	-0.353	1.437	27.334	10.985	15.542	20.656	11.968	4.670	7.298	0	3.275	
25-01-2022	4	285	25	14.9	97.976	0.065	0.109	0.409	2.776	1.002	1.889	0.821	1.068	1.030	-0.335	20	42	0.361	0.378	-0.348	1.439	27.449	10.998	14.599	20.743	11.241	4.338	6.904	0	2.162	18.204
26-01-2022	4	285	26	15.1	97.976	0.065	0.110	0.153	2.913	0.975	1.944	0.924	1.020	1.030	-0.331	20	42	0.361	0.378	-0.344	1.441	27.567	11.012	16.280	20.832	12.535	4.928	7.607	0	2.093	
27-01-2022	4	285	27	14.5	97.976	0.065	0.107	0.077	2.984	0.872	1.928	0.822	1.106	1.030	-0.327	20	42	0.361	0.378	-0.339	1.442	27.687	11.025	17.846	20.923	13.741	5.770	7.971	0	2.099	
28-01-2022	4	285	28	14.3	97.976	0.065	0.106	0.102	3.056	0.825	1.941	0.765	1.175	1.029	-0.322	20	42	0.361	0.378	-0.334	1.444	27.809	11.039	18.288	21.015	14.082	6.051	8.031	0	2.141	
29-01-2022	5	285	29	14.55	97.976	0.065	0.107	0.256	3.093	0.842	1.968	0.798	1.170	1.029	-0.318	20	42	0.361	0.378	-0.329	1.446	27.933	11.053	16.334	21.109	12.577	5.052	7.525	0	2.191	
30-01-2022	5	285	30	16.1	97.976	0.065	0.117	0.077	3.361	0.948	2.155	1.035	1.120	1.029	-0.314	20	42	0.361	0.378	-0.324	1.448	28.060	11.068	18.297	21.205	14.089	5.566	8.523	0	2.306	
31-01-2022	5	285	31	15.9	97.976	0.065	0.115	0.102	3.130	1.002	2.066	0.634	1.432	1.028	-0.309	20	42	0.361	0.378	-0.319	1.450	28.188	11.082	18.875	21.302	14.533	6.658	7.876	0	2.191	
01-02-2022	5	285	32	20.4	97.976	0.065	0.148	0.333	4.442	1.228	2.835	0.846	1.989	1.028	-0.304	20	42	0.361	0.378	-0.314	1.452	28.319	11.097	18.818	21.400	14.490	6.488	8.002	0	2.791	
02-02-2022	5	285	33	20	97.976	0.065	0.145	0.128	4.493	1.148	2.820	0.959	1.862	1.028	-0.300	20	42	0.361	0.378	-0.309	1.454	28.451	11.112	18.762	21.500	14.447	6.137	8.310	0	2.531	
03-02-2022	5	285	34	21.1	97.976	0.065	0.154	0.102	4.544	1.313	2.928	0.917	2.011	1.028	-0.295	20	42	0.361	0.378	-0.304	1.456	28.585	11.128	18.706	21.602	14.404	6.243	8.160	0	2.499	18.777
04-02-2022	5	285	35	22.65	97.976	0.065	0.167	1.407	4.596	1.588	3.092	1.179	1.913	1.027	-0.290	20	42	0.361	0.378	-0.298	1.458	28.721	11.143	18.779	21.704	14.460	5.804	8.656	0	4.268	
05-02-2022	6	285	36	16	97.976	0.065	0.116	0.486	3.361	0.935	2.148	0.651	1.497	1.027	-0.285	20	42	0.361	0.378	-0.293	1.460	28.858	11.159	18.205	21.808	14.018	6.090	7.929	0	2.725	
06-02-2022	6	285	37	18	97.976	0.065	0.130	0.179	3.824	1.058	2.441	0.960	1.481	1.027	-0.280	20	42	0.361	0.378	-0.287	1.462	28.997	11.175	18.537	21.913	14.273	5.702	8.571	0	2.550	
07-02-2022	6	285	38	19.7	97.976	0.065	0.142	0.333	4.195	1.195	2.695	1.006	1.689	1.026	-0.275	20	42	0.361	0.378	-0.282	1.464	29.137	11.191	18.610	22.019	14.330	5.735	8.595	0	2.847	
08-02-2022	6	285	39	21.15	97.976	0.065	0.154	0.205	4.442	1.357	2.899	1.051	1.848	1.026	-0.269	20	42	0.361	0.378	-0.276	1.466	29.279	11.208	18.684	22.126	14.387	5.746	8.641	0	2.764	
09-02-2022	6	285	40	21.9	97.976	0.065	0.160	0.435	4.974	1.313	3.143	1.247	1.896	1.025	-0.264	20	42	0.361	0.378	-0.270	1.469	29.422	11.224	17.186	22.235	13.233	4.771	8.462	0	3.051	
10-02-2022	6	285	41	20.6	97.976	0.065	0.150	0.767	4.243	1.330	2.787	0.904	1.882	1.025	-0.259	20	42	0.361	0.378	-0.265	1.471	29.567	11.241	17.781	22.344	13.691	5.504	8.187	0	3.401	20.539
11-02-2022	6	285	42	19.75	97.976	0.065	0.143	0.537	4.493	1.110	2.801	1.062	1.739	1.025	-0.253	20	42	0.361	0.378	-0.259	1.473	29.712	11.258	18.645	22.454	14.356	5.494	8.863	0	3.200	

12-02-2022	7	285	43	18.6	97.976	0.065	0.134	0.358	3.780	1.164	2.472	0.835	1.637	1.024	-0.248	20	42	0.361	0.378	-0.253	1.475	29.859	11.275	19.779	22.564	15.230	6.318	8.911	0	2.922	
13-02-2022	7	285	44	18.6	97.976	0.065	0.134	0.435	4.052	1.073	2.562	1.072	1.490	1.024	-0.242	20	42	0.361	0.378	-0.247	1.477	30.007	11.293	19.459	22.676	14.983	5.647	9.337	0	3.070	
14-02-2022	7	285	45	20.3	97.976	0.065	0.147	0.230	4.006	1.366	2.686	1.095	1.591	1.024	-0.236	20	42	0.361	0.378	-0.241	1.480	30.155	11.310	19.137	22.788	14.735	5.543	9.192	0	2.875	
15-02-2022	7	285	46	23.1	97.976	0.065	0.171	0.384	4.493	1.727	3.110	1.237	1.873	1.023	-0.230	20	42	0.361	0.378	-0.235	1.482	30.304	11.328	18.277	22.901	14.073	5.085	8.988	0	3.145	
16-02-2022	7	285	47	21.6	97.976	0.065	0.158	0.358	4.292	1.498	2.895	1.054	1.841	1.023	-0.225	20	42	0.361	0.378	-0.228	1.484	30.454	11.346	18.216	23.014	14.026	5.246	8.781	0	3.017	
17-02-2022	7	285	48	24.7	97.976	0.065	0.186	0.384	4.755	1.987	3.371	1.430	1.941	1.022	-0.219	20	42	0.361	0.378	-0.222	1.487	30.605	11.364	19.232	23.128	14.809	5.164	9.644	0	3.383	22.140
18-02-2022	7	285	49	22.6	97.976	0.065	0.166	1.433	4.147	1.772	2.960	1.553	1.407	1.022	-0.213	20	42	0.361	0.378	-0.216	1.489	30.756	11.382	15.661	23.243	12.059	3.487	8.572	0	3.728	
19-02-2022	8	285	50	24.4	97.976	0.065	0.183	0.665	4.544	2.013	3.278	1.560	1.718	1.022	-0.207	20	42	0.361	0.378	-0.210	1.492	30.908	11.400	15.725	23.357	12.108	3.559	8.550	0	3.285	
20-02-2022	8	285	51	25.25	97.976	0.065	0.191	0.281	5.030	2.000	3.515	1.580	1.935	1.021	-0.201	20	42	0.361	0.378	-0.203	1.494	31.060	11.419	15.789	23.472	12.158	3.574	8.584	0	2.958	
21-02-2022	8	285	52	21.8	97.976	0.065	0.159	0.819	4.918	1.313	3.116	1.114	2.002	1.021	-0.194	20	42	0.361	0.378	-0.197	1.496	31.213	11.437	20.357	23.587	15.675	5.863	9.812	0	3.973	
22-02-2022	8	285	53	21.6	97.976	0.065	0.158	0.333	4.974	1.261	3.118	0.777	2.341	1.020	-0.188	20	42	0.361	0.378	-0.190	1.499	31.365	11.456	20.299	23.703	15.630	6.518	9.112	0	3.220	
23-02-2022	8	285	54	24.5	97.976	0.065	0.184	0.384	5.623	1.599	3.611	1.086	2.525	1.020	-0.182	20	42	0.361	0.378	-0.184	1.501	31.518	11.475	20.652	23.818	15.902	6.177	9.725	0	3.575	
24-02-2022	8	285	55	26.95	97.976	0.065	0.209	0.563	6.073	2.000	4.036	1.308	2.729	1.019	-0.176	20	42	0.361	0.378	-0.177	1.504	31.671	11.494	20.042	23.934	15.432	5.618	9.814	0	3.967	24.930
25-02-2022	8	285	56	24.45	97.976	0.065	0.183	0.640	5.748	1.547	3.648	1.046	2.602	1.019	-0.169	20	42	0.361	0.378	-0.171	1.506	31.824	11.513	19.980	24.049	15.385	5.889	9.496	0	3.953	
26-02-2022	9	285	57	24.95	97.976	0.065	0.188	0.537	5.202	1.853	3.528	0.943	2.585	1.018	-0.163	20	42	0.361	0.378	-0.164	1.509	31.976	11.532	20.334	24.165	15.657	6.243	9.414	0	3.756	
27-02-2022	9	285	58	26.1	97.976	0.065	0.200	1.100	5.876	1.865	3.871	1.281	2.590	1.018	-0.156	20	42	0.361	0.378	-0.158	1.511	32.129	11.551	19.158	24.280	14.752	5.139	9.613	0	4.639	
28-02-2022	9	285	59	25.25	97.976	0.065	0.191	0.588	5.623	1.761	3.692	1.309	2.383	1.017	-0.150	20	42	0.361	0.378	-0.151	1.514	32.281	11.570	19.509	24.395	15.022	5.134	9.888	0	3.887	
01-03-2022	9	285	60	26.1	97.976	0.065	0.200	0.384	5.685	1.938	3.811	1.381	2.430	1.017	-0.143	20	42	0.361	0.378	-0.144	1.516	32.433	11.590	19.022	24.510	14.647	4.841	9.806	0	3.592	
02-03-2022	9	285	61	25.7	97.976	0.065	0.196	0.512	5.685	1.842	3.763	1.149	2.615	1.016	-0.137	20	42	0.361	0.378	-0.137	1.519	32.585	11.609	18.391	24.624	14.161	4.921	9.240	0	3.676	
03-03-2022	9	285	62	27.2	97.976	0.065	0.211	0.665	5.876	2.143	4.010	1.228	2.782	1.016	-0.130	20	42	0.361	0.378	-0.131	1.521	32.736	11.629	18.881	24.738	14.538	5.044	9.494	0	4.052	27.064
04-03-2022	9	285	63	25.6	97.976	0.065	0.195	0.614	5.623	1.842	3.732	1.358	2.375	1.015	-0.123	20	42	0.361	0.378	-0.124	1.524	32.886	11.648	14.997	24.852	11.548	3.230	8.318	0	3.463	
05-03-2022	10	285	64	26.15	97.976	0.065	0.200	0.281	5.812	1.901	3.857	1.324	2.532	1.015	-0.117	20	42	0.361	0.378	-0.117	1.527	33.036	11.668	19.867	24.965	15.298	5.129	10.168	0	3.573	
06-03-2022	10	285	65	26.35	97.976	0.065	0.202	0.358	5.685	2.000	3.843	1.539	2.303	1.014	-0.110	20	42	0.361	0.378	-0.110	1.529	33.185	11.688	19.085	25.078	14.696	4.469	10.227	0	3.652	
07-03-2022	10	285	66	26.5	97.976	0.065	0.204	0.588	5.623	2.064	3.843	1.700	2.143	1.014	-0.103	20	42	0.361	0.378	-0.103	1.532	33.333	11.708	19.579	25.190	15.076	4.374	10.702	0	4.031	
08-03-2022	10	285	67	27.9	97.976	0.065	0.219	0.716	5.685	2.427	4.056	1.645	2.411	1.013	-0.096	20	42	0.361	0.378	-0.096	1.534	33.480	11.728	18.647	25.301	14.359	4.183	10.176	0	4.152	
09-03-2022	10	285	68	25.2	97.976	0.065	0.191	0.640	5.144	1.938	3.541	1.704	1.837	1.013	-0.089	20	42	0.361	0.378	-0.090	1.537	33.627	11.748	16.421	25.412	12.645	3.206	9.438	0	3.575	
10-03-2022	10	285	69	21.75	97.976	0.065	0.159	0.793	4.052	1.630	2.841	1.028	1.813	1.012	-0.082	20	42	0.361	0.378	-0.083	1.540	33.772	11.768	9.878	25.522	7.606	1.272	6.334	0	2.883	25.235
11-03-2022	10	285	70	25.75	97.976	0.065	0.196	0.153	5.623	1.877	3.750	1.491	2.259	1.012	-0.075	20	42	0.361	0.378	-0.076	1.542	33.917	11.788	18.981	25.631	14.616	4.324	10.292	0	3.369	
12-03-2022	11	285	71	26.4	97.976	0.065	0.203	0.333	5.812	1.962	3.887	1.082	2.805	1.011	-0.069	20	42	0.361	0.378	-0.069	1.545	34.060	11.808	20.197	25.739	15.552	5.474	10.078	0	3.692	
13-03-2022	11	285	72	25.35	97.976	0.065	0.192	0.358	6.007	1.651	3.829	1.158	2.671	1.011	-0.062	20	42	0.361	0.378	-0.062	1.547	34.202	11.828	21.273	25.846	16.381	5.655	10.726	0	3.879	28.430
14-03-2022	11	285	73	24.1	97.976	0.065	0.180	0.281	5.319	1.619	3.469	0.734	2.735	1.010	-0.055	20	42	0.361	0.378	-0.055	1.550	34.342	11.848	21.629	25.953	16.654	6.572	10.082	0	3.550	
15-03-2022	11	285	74	26	97.976	0.065	0.199	0.230	6.448	1.651	4.049	1.367	2.682	1.010	-0.048	20	42	0.361	0.378	-0.048	1.553	34.482	11.868	20.242	26.058	15.586	4.880	10.706	0	3.677	
16-03-2022	11	285	75	26.3	97.976	0.065	0.202	0.230	6.139	1.818	3.979	1.257	2.722	1.009	-0.041	20	42	0.361	0.378	-0.041	1.555	34.620	11.889	21.905	26.162	16.867	5.671	11.195	0	3.839	
17-03-2022	11	285	76	29.9	97.976	0.065	0.242	0.640	7.696	2.197	4.947	1.297	3.650	1.009	-0.034	20	42	0.361	0.378	-0.034	1.558	34.756	11.909	21.968	26.265	16.916	5.864	11.052	0	4.802	
18-03-2022	11	285	77	30.05	97.976	0.065	0.244	0.691	8.028	2.130	5.079	1.273	3.806	1.008	-0.027	20	42	0.361	0.378	-0.027	1.561	34.891	11.929	22.324	26.367	17.189	6.034	11.155	0	4.990	

ANNEXURE III

Water demand of rabi chickpea in Akola (2021-22)

MET. Week	Month	Dates	Weeks past sowing	Weekly ETo (mm)	PM Kc	VI (NDWI)	Kc derived	ETc (mm)	Crop Acreage (ha)	Water demand	
										m^3	Mm^3
47	Nov.	19-25	1	18.68	0.85	0.0888	0.84	15.73	95576	15031513.76	15.03151
48		26-2	2	16.46	0.84	0.0957	0.88	14.49	95576	13847217.39	13.84722
49	Dec.	3-9	3	12.73	0.88	0.1036	0.92	11.75	95576	11234030.54	11.23403
50		10-16	4	15.81	0.95	0.1088	0.95	15.06	95576	14390202.16	14.3902
51		27-23	5	13.35	1.04	0.1333	1.09	14.53	95576	13883616.78	13.88362
52		24-31	6	15.56	1.12	0.1424	1.14	17.72	95576	16933585.11	16.93359
1	Jan.	1-7	7	13.96	1.18	0.1426	1.14	15.91	95576	15209930.64	15.20993
2		8-14	8	13.56	1.21	0.1647	1.26	17.11	95576	16349113.88	16.34911
3		15-21	9	15.80	1.20	0.1544	1.20	19.03	95576	18188150.51	18.18815
4		22-28	10	18.20	1.15	0.1510	1.19	21.59	95576	20634401.21	20.6344
5		29-4	11	18.78	1.05	0.1076	0.95	17.76	95576	16973140.75	16.97314
6	Feb.	5-11	12	20.54	0.91	0.0811	0.80	16.41	95576	15686947.02	15.68695
7		12-18	13	22.14	0.75	0.0623	0.70	15.40	95576	14716444.17	14.71644
8		19-5	14	24.93	0.57	0.0150	0.43	10.81	95576	10335462.75	10.33546
9		26-4	15	27.06	0.38	0.0081	0.40	10.70	95576	10225798.86	10.2258
10	Mar.	5-11	16	25.24	0.23	0.0066	0.39	9.77	95576	9338478	9.338478
11		12-18	17	28.43	0.12	-0.0350	0.16	4.47	95576	4272037.242	4.272037
TOTAL								**248.23**		**237250070.8**	**237.2501**

VITA

1	Name of student	:	Moncy S Akkara
2	Date of birth	:	28 June 1997
3	Name of the College	:	Department of Irrigation and Drainage Engineering, Post Graduate Institute, Dr. PDKV, Akola
4	Residential Address along with phone no.	:	Akkara House, P O Ollur, Thrissur Kerala 680306 Mobile: 8289860250 Email: moncyuw28@gmail.com
5	Academic Qualification	:	

Sr. No	Name of Degrees awarded	Year in which obtained	Division/Class	Name of awarding university	Subject
1	B. Tech.	2020	8.42/10	KAU, Thrissur	Agricultural Engineering
2	Certificate in Remote Sensing and Digital Image Analysis	2022	A Grade	IIRS, Dehradun	Remote Sensing

6	Research papers published (if any)	:	01
7	Field of Interest (in which you desire to work)	:	Remote Sensing Applications in Natural Resources Management, Research & Development, Teaching, Social Impact sectors

Place: Akola

Date: **Signature of Student**